Titre: Title:	Blackbox Optimization for Loss Minimization in Power Distribution Networks Using Feeder Reconfiguration
Auteur: Author:	Christina Soldati
Date:	2025
Type:	Mémoire ou thèse / Dissertation or Thesis
Référence: Citation:	Soldati, C. (2025). Blackbox Optimization for Loss Minimization in Power Distribution Networks Using Feeder Reconfiguration [Mémoire de maîtrise, Polytechnique Montréal]. PolyPublie. https://publications.polymtl.ca/67855/

URL de PolyPublie: PolyPublie URL:	https://publications.polymtl.ca/67855/
Directeurs de recherche: Advisors:	Antoine Lesage-Landry, Sébastien Le Digabel, & Octavio Ramos
Programme: Program:	Génie électrique

POLYTECHNIQUE MONTRÉAL
affiliée à l'Université de Montréal

Blackbox Optimization for Loss Minimization in Power Distribution Networks using Feeder Reconfiguration

CHRISTINA SOLDATI
Département de génie électrique

Mémoire présenté en vue de l'obtention du diplôme de *Maîtrise ès sciences appliquées*
Génie électrique

Août 2025

POLYTECHNIQUE MONTRÉAL
affiliée à l'Université de Montréal

Ce mémoire intitulé :

Blackbox Optimization for Loss Minimization in Power Distribution Networks using Feeder Reconfiguration

présenté par **Christina SOLDATI**
en vue de l'obtention du diplôme de *Maîtrise ès sciences appliquées*
a été dûment accepté par le jury d'examen constitué de :

Antoine LEGRAIN, président
Antoine LESAGE-LANDRY, membre et directeur de recherche
Sébastien LE DIGABEL, membre et codirecteur de recherche
Octavio RAMOS, membre et codirecteur de recherche
Ilhan KOCAR, membre

DEDICATION

À mes parents Nancy et Simone qui sont toujours là pour m'encourager, à mon frère Antoine qui est fier de moi même s'il dit que ça sert à rien les études supérieures, à mon amoureux Félix qui a dû subir bien des séances d'explications de ma recherche qu'il ne comprenait pas toujours, à mes amis Étienne, ensembles dans le même bateau depuis BAC 1er année, et Samuel, mon pote de bureau, à mes autres amis du lab, Julien, Olivier, Abraham, Nohaila, Matthias, Loreley, Xavier, William, Victor, etc, dsl si j'ai pas mis votre nom c'est pas que je vous aime pas mais je peux pas mettre la liste au complet, à mes amis Raphaël, Lambert et Andrés que j'ai rencontré en Écosse où j'ai commencé à rédiger ce mémoire, avec qui j'ai eu ben du fun et qui ont su être une oreille attentive quand j'en avais besoin...

« Un magicien n'est jamais en retard, Frodon Sacquet. Ni en avance d'ailleurs. Il arrive précisément à l'heure prévue. »

– J.R.R. Tolkien, Le Seigneur des Anneaux : La Communauté de l'Anneau (adaptation cinématographique réalisée par Peter Jackson, 2001)

ACKNOWLEDGEMENTS

I would like to start by thanking my research director Pr. Antoine Lesage-Landry and my research co-director Pr. Sébastien Le Digabel for guiding and supporting me during my master. Your passion and motivation are contagious and inspired me to pursue a PhD. I'm eager to see what we'll achieve together in the future. Next, I would also like to thank Pr. Miguel F. Anjos, who supervised me during my research stay at The University of Edinburgh. I hope we'll have more opportunities to brainstorm research ideas together in the future.

I would also like to thank Dr. Octavio Ramos from the Hydro-Québec Research Center for providing advice throughout the project. Also a huge thank to Edoh and Pierre from GERAD for their help and support related to all the technical informatics challenges.

Finally, I would like to give my thanks to the president and the member of the study committee of this Master's Thesis, Pr. Antoine Legrain and Pr. Ilhan Kocar, for taking the time to read and evaluate this work.

This work is supported by the Natural Sciences and Engineering Research Council of Canada (NSERC), the Fonds de recherche du Québec - Nature et technologies (FRQNT) [1], and the NSERC Alliance-Mitacs Accelerate grant ALLRP 571311-21 ("Optimization of future energy systems") in collaboration with Hydro-Québec.

A conference paper based on this work has been accepted for the CIGRE 2025 International Symposium.

RÉSUMÉ

Les réseaux de distribution électrique modernes intègrent un nombre croissant de technologies associées aux réseaux de distribution actifs, tels que les ressources énergétiques distribuées et les interrupteurs contrôlables à distance. Naturellement débalancés en raison des fluctuations et de la nature multi-phasée de la demande, ces réseaux voient leur débalancement de phases amplifié par les ressources énergétiques distribuées, lesquelles peuvent induire un écoulement de puissance bidirectionnel. Ce débalancement peut impacter significativement la gestion du réseau, affectant ainsi l'efficacité, entre autres au niveau des pertes de puissance active. Cela peut aussi nuire à la fiabilité et la résilience du réseau, notamment au niveau des profils de tension anormaux et en induisant un stress supplémentaire sur l'infrastructure du réseau tel les transformateurs de distribution. À terme, ceci peut conduire à une augmentation des coûts d'opération et une réduction de la fiabilité du réseau. Pour mitiger ces impacts, les réseaux de distribution tentent généralement de minimiser les pertes de puissance, soit par balancement de phases ou de charges, ou par la reconfiguration de la topologie du réseau. La reconfiguration de la topologie est un problème de type optimisation non-linéaire à variables mixtes, classifié en tant que $\mathcal{NP}$-difficile et irréalisable à résoudre efficacement. Il combine les équations non-linéaires et non-convexes du modèle d'écoulement de puissance, avec le problème combinatoire associé aux états des interrupteurs. Ce problème est typiquement résolu soit par des méthodes heuristiques soit en le simplifiant grâce à des relaxations convexes ou à des approximations linéaires. Cependant, ces méthodes ne permettent pas de garantir la réalisabilité de la solution, ce qui est crucial pour un opérateur de réseau. Ainsi l'approche proposée, basée sur l'optimisation de boîtes noires (*Blackbox Optimization*, BBO), est une méthode de reconfiguration de la topologie du réseau utilisant des commutateurs bidirectionnels et des sectionneurs afin de minimiser les pertes de puissance. L'approche considère un réseau de distribution triphasé, débalancé, radial et équipé de ressources énergétiques distribuées. Ainsi, cela permet une intégration efficace des ressources énergétiques distribuées tout en limitant les écarts par rapport aux contraintes opérationnelles du réseau par reconfiguration de la topologie. La réalisabilité de la solution est facilitée par un simulateur d'écoulement de puissance à haute précision et la formulation du problème en tant que BBO. Afin de contourner la charge computationnelle de la BBO, des algorithmes inspirés de l'optimisation combinatoire sont adaptés au contexte des réseaux de distribution, soit la méthode méta-heuristique de recherche en voisinages variables (*Variable Neighbourhood Search*, VNS) et l'algorithme de séparation et évaluation (*Branch-and-Bound*, B&B). Le VNS intègre des composants aléatoires, pouvant potentiellement conduire à une progression plus rapide vers

une “bonne” solution. La méthode de B&B approxime les mécanismes de la méthode exacte de séparation et évaluation utilisée sur des problèmes de type combinatoire. De plus, sa performance est très sensible au choix du point initial. Quatre méthodes consistant en diverses séquences de BBO indépendante, d'un VNS et d'un B&B sont implémentées. Les méthodes servant de point de départ à la suivante induisent une amélioration continue de la qualité de la solution. Les méthodes sont testées sur les réseaux IEEE 34-bus, 136-bus, et IEEE 8500-bus, tous intégrant des ressources énergétiques distribuées. Les résultats démontrent l'impact direct issu de la combinaison de la production locale avec la reconfiguration de réseau pour l'amélioration de l'efficacité du réseau de distribution. Notamment, la solution résulte typiquement en une topologie différente de la topologie radiale originale, avec une contribution significative des ressources énergétiques distribuées sur le réseau. En effet, elles contribuent à un minimum de 64% et un à maximum de 87% de la production totale observée, et ce pour l'ensemble des réseaux de test. De plus, les ressources énergétiques distribuées contribuent à satisfaire au moins 77% de la demande totale pour l'ensemble des réseaux de test. Ensuite, les pertes de puissance sont considérablement réduites dans tous les cas, avec une diminution d'au moins 37% pour le problème comportant le plus de variables décisionnelles, le 136-bus, et 7% pour le cas du réseau IEEE 8500-bus. Finalement, les résultats permettent l'identification des méthodes les mieux adaptées à une application pratique, en fonction des priorités visées. Si le temps de calcul est le critère premier, alors BBO-VNS est le meilleur choix. Si une moindre variabilité dans la qualité de la solution et la réduction des pertes de puissance est préférée, BBO-B&B-VNS ou BBO-VNS-B&B sont plus adaptées, la dernière démontrant une meilleure efficacité pour les problèmes à haute dimension, tel que souligné par le cas du 136-bus.

ABSTRACT

Modern Distribution Networks (DNs) increasingly incorporate active distribution network technologies, such as Distributed Energy Resources (DERs) and remotely activated switches. As DNs are naturally unbalanced due to a multi-phase and highly fluctuating demand, DERs, which can lead to bidirectional power flows, can further exacerbates the phase imbalances. Unbalanced phases can significantly impact network operations, affecting efficiency, i.e., power losses, and compromising network reliability and resilience, i.e., voltage levels and additional stress on the network components such as the distribution transformers. Ultimately, these all may lead to an increase in operational costs and reduced reliability. To mitigate these impacts, DNs commonly seek to minimize power losses, either through phase or load balancing, or by topology reconfiguration. Topology reconfiguration is a mixed-integer nonlinear programming problem classified as $\mathcal{NP}$-hard and is impractical to solve. It combines the nonlinear, nonconvex equations of the power flow, with the combinatorial problem related to the switch statuses. It is typically solved either with heuristics methods or by simplifying the problem using convex relaxations or linear approximations, hence not guaranteeing the feasibility of the solution. However, feasibility is crucial for DN operators. As such, the proposed approach, based on Blackbox Optimization (BBO), is a network topology reconfiguration method utilizing tie and sectionalizing switches to minimize power losses in a three-phase, unbalanced, radial DN equipped with DERs. This approach enables efficient DER integration while mitigating network operational constraints using topology reconfiguration. Feasibility of the solution is enhanced through a high-accuracy load-flow simulator and a BBO formulation. To circumvent the computational burden of BBO, combinatorial optimization-inspired algorithms are adapted to the DN context, namely the Variable Neighbourhood Search (VNS) meta-heuristic and the Branch-and-Bound (B&B) framework. VNS incorporates a random component, thus potentially leading to faster progress toward a "good" solution. B&B approximates the mechanisms underlying the exact Branch-and-Bound method used in combinatorial problems, though its performance remains highly sensitive to the choice of initial point. Four methods using various sequences of a stand-alone BBO optimization, a VNS, and a B&B, are devised. Each optimization technique being the warm start for the next induces constant improvement on the solution quality. The methods are tested on the IEEE 34-bus, 136-bus, and IEEE 8500-bus systems, all integrating DERs. The results demonstrate the direct impact of combining local generation with network reconfiguration to improve DN efficiency. Notably, the solution typically results in a topology different from the original one, with DERs contributing significantly to the total network generation, with a minimum

of 64% and a maximum of 87%, and participating in satisfying at least 77% of the total demand, across all test systems. Moreover, power losses are considerably reduced across all test cases, with a decrease of at least 37% for the largest problem in terms of decision variables, the 136-bus, and 7% for the practical IEEE 8500-bus case. Finally, these results permit to identify the most suitable methods for practical deployments based on prioritized requirements. If the computational time is the primary concern, BBO-VNS is the better choice. For greater stability in the solution and the reduction of power losses, BBO-B&B-VNS or BBO-VNS-B&B are preferred, with BBO-VNS-B&B demonstrating improved efficiency in higher-dimensional problems, as seen in the 136-bus system case.

CONDENSÉ EN FRANÇAIS

Les réseaux de distribution électrique modernes intègrent un nombre croissant de technologies associées aux réseaux de distribution actifs, tels que les ressources énergétiques distribuées et les interrupteurs contrôlables à distance. Traditionnellement passifs du point de vue du réseau de transport, où tout changement sur le réseau est prévu d'avance ou basé sur des scénarios programmés, les réseaux de distribution actifs permettent une gestion plus flexible et dynamique du réseau. Cela favorise entre autre l'ajout de ressources énergétiques distribuées, tels que les systèmes photovoltaïques, les systèmes de stockage, et autres, qui ont un comportement fortement stochastique nécessitant une meilleure capacité d'adaptation du réseau. Les ressources énergétiques distribuées introduisent de la génération locale sur le réseau et permettent la diversification et la décentralisation de la production. Ceci tend à mitiger les contraintes de réseaux, tels les profils de tensions et les pertes de puissance, et à augmenter la résilience et la fiabilité du service. Cependant, si l'intégration de telles technologies et leur utilisation sont improprement gérées, cela peut générer des impacts négatifs. En effet, l'écoulement de puissance bidirectionnel potentiellement engendré par de telles technologies et leur présence même en temps que "charge négative" sur le réseau, tendent à causer des sur/sous-tension et des déséquilibres au niveau des fréquences et des phases. De plus, cela peut entraîner des distorsions de signal, créer des surcharges dans les lignes et générer une augmentation des pertes en puissance. Naturellement débalancés en raison des fluctuations et de la nature multi-phasée de la demande, les réseaux de distribution peuvent donc voir leur débalancement de phases encore plus amplifié par les ressources énergétiques distribuées. Ce débalancement tend à impacter significativement la gestion du réseau. Notamment en affectant son efficacité, entre autres par l'augmentation des pertes de puissance. De plus, cela peut nuire à la fiabilité et la résilience du réseau, notamment en induisant des profils de tension anormaux et un stress supplémentaire sur l'infrastructure, en particulier sur les transformateurs de distribution. À terme, ceci peut conduire à une augmentation des coûts d'opération et une réduction de la fiabilité du réseau.

Les approches dominantes en littérature cherchent généralement à mitiger ces impacts par la minimisation des pertes de puissance, soit par balancement de phases ou charges, ou par la reconfiguration de la topologie du réseau. La reconfiguration de la topologie est un problème complexe de type optimisation non-linéaire à variables mixtes, classifié en tant que $\mathcal{NP}$-difficile et impossible à résoudre efficacement. Il est constitué à la fois des équations non-linéaires, non-convexes du modèle d'écoulement de puissance optimal en courant alternatif, le modèle mathématique le plus complet pour un réseau électrique, et du problème combinatoire

associé aux états des interrupteurs. Ce problème est typiquement résolu soit par des méthodes heuristiques soit en le simplifiant grâce à des relaxations convexes ou à des approximations linéaires. Les méthodes heuristiques ont l'avantage d'être relativement simples à implémenter, pouvant s'appliquer directement au problème d'optimisation non-linéaire à variables mixtes, et génèrent rapidement des solutions réalisables. Cependant, elles n'ont par définition aucune garantie de convergence. D'une part, les méthodes basées sur l'optimisation mathématique, notamment dans ce contexte les relaxations convexes coniques, quadratiques et les approximations linéaires, sont déterministes et peuvent offir une garantie de convergence. Cependant, celles-ci sont fondées sur un modèle relaxé ou approximé, et donc ne garantissent en aucun cas la réalisabilité de la solution lorsque appliquée au problème original. Les approches en apprentissage machine sont aussi utilisées, en particulier pour les applications dynamiques et en temps réel, en raison de leur capacité à retourner rapidement une topologie une fois entraînées. Néanmoins, elles manquent de garantie au niveau de la réalisabilité de la solution. Enfin, les méthodes basées sur l'optimisation de boîtes noires (*Blackbox Optimization*, BBO), d'une autre part, ont peu d'applications en réseaux électriques, encore moins en reconfiguration de réseau. Cependant, ces méthodes permettent de modéliser avec haute précision les contraintes du problème dans une boîte noire dédiée, typiquement une simulation numérique, garantissant une forte réalisabilité du modèle et facilitant l'atteinte d'une solution réalisable. Dans ce cas-ci, la boîte noire simule un écoulement de puissance. La réalisabilité est cruciale pour un opérateur de réseau, ainsi l'approche proposée est basée sur la BBO. De plus, les algorithmes de BBO, tel que *Mesh Adaptive Direct Search* (MADS), possèdent des propriétés de convergence démontrables sous certaines conditions. Toutefois, la BBO peut nécessiter un grand nombre d'évaluations de la boîte noire pour converger vers une "bonne" solution. Ceci peut être exacerbé par la taille du problème, menant à des temps de calcul potentiellement élevés.

L'approche proposée dans ce mémoire est une méthode de reconfiguration de la topologie du réseau utilisant des commutateurs bidirectionnels et des sectionneurs afin de minimiser les pertes de puissance dans un réseau de distribution triphasé, débalancé, radial et équipé de ressources énergétiques distribuées. Les contraintes opérationnelles de réseau, notamment les profils de tension, le balancement des phases et l'écoulement de puissance dans les lignes, sont fortement inter-reliées. Ainsi, minimiser les pertes de puissance tant à les atténuer aussi. Enfin, l'approche BBO permet de combiner l'utilisation d'un simulateur d'écoulement de puissance à haute précision avec une méthode de prise de décision, facilitant ainsi l'obtention d'une solution réalisable. Ceci est en contraste aux approches plus conventionnelles favorisant l'optimalité avant la réalisabilité, comme les méthodes heuristiques, les méthodes mathématiques et les méthodes d'apprentissage machine. Ainsi, cette approche permet une intégration

efficace des ressources énergétiques distribuées tout en assurant le respect des contraintes opérationnelles du réseau par reconfiguration de la topologie. Par conséquent, les variables de décisions du problème d'optimisation incluent à la fois les états binaires des interrupteurs et les puissances active et réactive, des variables continues, injectées par les ressources énergétiques distribuées dans le réseau. Ces dernières sont déterministes, mais libres au cours du processus d'optimisation, en faisant partie à part entière et évoluant de façon interdépendante avec la recherche de la topologie du réseau. Ceci est différent des approches connues de BBO pour résoudre ce type de problème, celles-ci optimisant uniquement sur la topologie du réseau et considérant les ressources énergétiques distribuées comme fixes. Tout aspect considérant la stochasticité des ressources énergétiques distribuées et/ou de la demande, ainsi que la possibilité de former des micro-réseaux par îlotage grâce aux ressources énergétiques distribuées, sont laissés à de futurs travaux. C'est aussi le cas pour le contrôle des composants de réseaux, ceux-ci supposés complètement automatisés, ainsi que pour tout aspect en lien avec le réseau de communication et les notions économiques.

La réalisabilité de la solution est facilitée par un simulateur d'écoulement de puissance à haute précision, ici `EMTP`, et la formulation du problème en tant que BBO, grâce au solveur `NOMAD` implémentant MADS. Le problème BBO cherche à minimiser la génération totale observée sur le réseau, étant équivalent à minimiser les pertes dans un réseau radial. Les contraintes, gérées à l'aide de la technique de la barrière progressive, sont : bornes inférieure et supérieure sur l'amplitude des tensions à chaque bus, ampacité des lignes, limites maximum et minimum de génération provenant du réseau de transport et des ressources énergétiques distribuées. De plus, la topologie finale doit être radiale et connectée, c'est-à-dire aucune portion n'est isolée du réseau principal. Afin de contourner la charge computationnelle de la BBO, et sachant que l'optimisation est plus efficace avec un budget d'évaluation limité si les variables du problèmes sont continues, le problème de type variables mixtes initial est scindé en une formulation continue et une formulation binaire. La formulation continue, résolue par BBO, consiste à trouver une solution pour les ressources énergétiques distribuées alors que la topologie est fixe. La formulation binaire, résolue par des algorithmes inspirés de l'optimisation combinatoire, consiste à trouver une solution pour la topologie alors que les ressources énergétiques distribuées sont fixes. Ce processus itératif combine l'optimisation combinatoire pour la recherche d'une "bonne" topologie avec la BBO pour la recherche de valeurs pour les ressources énergétiques distribuées qui satisfont à toutes les contraintes du réseau. Des algorithmes de l'optimisation combinatoire sont adaptés au contexte des réseaux de distribution, soit la méthode méta-heuristique de recherche en voisinages variables (*Variable Neighbourhood Search*, VNS) et l'algorithme de séparation et d'évaluation (*Branch-and-Bound*, B&B). Le VNS effectue une recherche locale dans le voisinage d'une solution initiale et intègre des

composants aléatoires, pouvant potentiellement conduire à une progression plus rapide vers une “bonne” solution. La procédure sélectionne une nouvelle topologie à évaluer en permutant aléatoirement un certain nombre d'éléments dans les voisinages de la solution initiale. Ensuite, BBO est appliqué pour un nombre limité d'évaluations afin de trouver une solution pour les ressources énergétiques distribuées, tout en gardant la nouvelle topologie fixe au cours du processus. Le voisinage est incrémenté à la prochaine itération si l'optimisation résulte en une solution pire que la meilleure connue. Le processus continue tant qu'un critère d'arrêt global, soit un nombre maximal d'évaluations, n'est pas atteint. La méthode du B&B approxime les mécanismes de la méthode exacte de séparation et évaluation utilisée sur des problèmes de type combinatoire, et sa performance est très sensible au choix du point initial. Le B&B partitionne le problème initial en sous-problèmes, soit des nœuds de l'arbre de branchement. L'arbre est exploré avec la stratégie de *cyclic best-first search* et en effectuant un branchement binaire sur les nœuds, consistant à poser l'état d'un nouvel interrupteur à chaque niveau de l'arbre. En d'autres mots, à chaque niveau de l'arbre, un nouveau branchement consiste à produire deux sous-problèmes où un possède une variable binaire fixée à 0 et l'autre à 1, la variable binaire en question étant choisie à l'aide d'une heuristique. Ensuite, chaque nœud est résolu avec BBO pour un nombre limité d'évaluations sur le reste des variables binaires, lesquelles sont temporairement relaxées à continues, et les variables continues associées aux ressources énergétiques distribuées. Le processus se poursuit tant qu'il y a des sous-problèmes à évaluer, ceux-ci étant élagués si BBO a échoué (irréalisable, aucune solution) ou si la solution est pire que la meilleure connue.

Enfin, les méthodes proposées combinent BBO, facilitant la réalisabilité de la solution, et des méthodes d'optimisation combinatoire pour augmenter l'efficacité de résolution, considérant un budget d'évaluation et des délais raisonnables. Quatre méthodes consistant en diverses séquences d'une BBO indépendante, d'un VNS et d'un B&B sont implémentées. Puisque les algorithmes VNS et B&B sont sensibles aux conditions initiales, une BBO avec un petit budget est utilisée pour les initialiser avec une solution partiellement optimisée. De plus, des séquences combinant les algorithmes, chacun servant de point de départ au suivant et favorisant une amélioration continue de la qualité de la solution, sont proposées. Cela résulte donc en quatre méthodes de résolutions distinctes : BBO-VNS, BBO-B&B, BBO-VNS-B&B et BBO-B&B-VNS. Le budget d'évaluation pour BBO, spécifique à chaque algorithme, méthode proposée et problème, soit le réseau de distribution étudié, est défini préalablement dans une phase de paramétrage. De plus, les méthodes sont comparées en tout temps à une méthode de base, consistant en une BBO effectuée seule pour un nombre d'évaluations suffisant. Le VNS est une méthode méta-heuristique, alors que le B&B est une approximation de la méthode exacte. Aussi, toutes les étapes de BBO sont résolues pour un budget limité.

Ainsi, les méthodes ne peuvent pas offrir de garantie de convergence, mais fournissent en pratique une “bonne” solution qui tend à être réalisable, et on espère, localement optimale.

Les méthodes sont testées sur les réseaux IEEE 34-bus, 136-bus, et IEEE 8500-bus, tous modifiés pour intégrer un certain nombre d'interrupteurs et de ressources énergétiques distribuées. Les réseaux sont modélisés dans le logiciel `EMTP` et contrôlés via l'interface `MATLAB-EMTP API`. Les méthodes sont programmées dans `MATLAB`, où le solveur d'optimisation de boîtes noires, `NOMAD`, est appelé directement via son API dédiée. Enfin, les méthodes sont testées sur un total de 40 divers profils de charges et points initiaux, et les résultats sont présentés sous forme de profils de données et de tableaux récapitulatifs des résultats numériques. Tous les points initiaux sont réalisables au regard des contraintes de réseau. Les profils de données permettent de comparer l'efficacité et la robustesse, c'est-à-dire le nombre de problèmes résolus à un certain niveau de précision, des différentes méthodes. Dans le cas plus pratique du IEEE 8500-bus, les tests sont effectués une seule fois, et ce, avec le même paramétrage que pour le réseau de test possédant le plus de variables décisionnelles, le 136-bus.

Le IEEE 34-bus est un réseau triphasé et débalancé qui consiste en un problème de 15 variables de décisions, où 6 sont continues, soit 2 variables par ressource énergétique distribuée, les puissances active et réactives injectées ou consommées, et 9 sont binaires, soit les états des interrupteurs. Les profils de données démontrent que les méthodes sont généralement plus efficaces que la méthode de base, soit BBO uniquement. BBO-VNS se démarque particulièrement pour sa rapidité et sa consistance. Elle est suivi de proche par BBO-B&B-VNS, plus demandante computationnellement en raison du B&B, mais qui se démarque après un certain nombre d'évaluations. Les résultats numériques comparent les méthodes à la solution de base pour le cas spécifique du profil de charge de base. La solution de base n'inclut aucune optimisation et consiste en la topologie radiale originale pour des valeurs de ressources énergétiques distribuées qui permettent le respect des contraintes de réseau. Les résultats montrent une réduction de pertes importante allant de 78.06% pour BBO-B&B à 80.14% pour BBO-VNS. Aussi, les ressources énergétiques distribuées contribuent en moyenne à 72.26% de la génération totale alors que la solution de base est de 38.03%, et participent à l'alimentation de 72.87% de la demande totale, soit 1769 kW pour le 34-bus, alors que la solution de base est de 39.57%. De plus, la topologie finale est typiquement différente de la topologie radiale originale. Enfin, afin de comparer les méthodes proposées à ce qui est fait dans la littérature, une méthode d'optimisation mathématique a été implémentée pour résoudre le même problème. Cette implémentation consiste en une relaxation convexe conique du second ordre pour les problèmes à variables mixtes basée sur le modèle `DistFlow`. Le modèle de réseau y est simplifié, ignorant entre autres certains composants comme les transformateurs et simplifiant le modèle des lignes en ignorant l'aspect capacitif. La solution

obtenue est appliquée au réseau modélisé dans le simulateur afin de permettre la comparaison entre les différentes méthodes. La réduction des pertes observée est de 53.38%, et ce pour une contribution des ressources énergétiques distribuées à la génération et l'alimentation de la demande, respectivement, de 92.11% et 94.10%. Les pertes sont considérablement moins réduites que ce qui est obtenu avec les méthodes proposées dans ce mémoire, et ce, malgré une plus grande contribution des ressources énergétiques distribuées. Il semble donc valable de poser l'hypothèse que les simplifications sur le modèle de réseau et la relaxation du problème ont impacté grandement la qualité de la solution. Ensuite, le 136-bus consiste en 4 instances du 34-bus, celles-ci considérées maintenant comme des lignes de distribution. Le problème résultant possède 40 variables, soit 24 variables continues et 16 variables binaires, ce qui est un problème d'optimisation beaucoup plus grand que le précédent. Il est observé que les méthodes sont généralement moins efficace que la méthode de base BBO, comparativement à ce qui est remarqué pour le 34-bus. Cela laisse supposer que la grande taille du problème pose un défi non négligeable, surtout en ce qui concerne le problème combinatoire. En effet, il s'agit dorénavant de la méthode BBO-B&B-VNS, suivie de la méthode BBO-VNS-B&B, qui se démarque au détriment de BBO-VNS. Le processus plus guidé de l'arbre de branchement du B&B semble lui donner un avantage comparativement au processus aléatoire du VNS. Enfin, la topologie finale est encore typiquement différente de la topologie radiale originale. De plus, une réduction de pertes importante allant de 36.94% pour BBO-B&B à 60.90% pour BBO-VNS est observée. Ensuite, les ressources énergétiques distribuées contribuent en moyenne à 79.89% de la génération totale alors que la solution de base est de 60.93%, et participent à alimenter en moyenne 80.75% de la demande totale, soit 7076 kW pour le 136-bus, alors que la solution de base est de 62.18%. Finalement, les méthodes sont appliquées au cas du IEEE 8500-bus, un problème de 18 variables, soit 10 continues et 8 binaires. Il s'agit d'un problème d'optimisation beaucoup plus petit que le 136-bus, mais un réseau plus réaliste qui capture des aspects clés d'un réseau de distribution, soit une taille plus réaliste, des niveaux de tension variables, des charges débalancées et différents types de branchements de phases. Le réseau original, avant modifications, ne respecte pas de nombreuses contraintes, affichant des problèmes de sous-tension à plusieurs bus, ainsi que des dépassements des capacités de courant pouvant circuler dans les lignes. Afin de permettre plus de liberté au processus d'optimisation, les bornes des contraintes de tensions sont relaxées, passant de $\overline{v} = 1.05$ p.u à $\overline{v} = 1.10$ p.u et $\underline{v} = 0.95$ p.u à $\underline{v} = 0.90$ p.u. BBO-VNS s'avère ici le plus efficace, avec 32.52% de réduction de pertes, suivi par BBO-VNS-B&B, avec 29.85% de réduction. Ce sont aussi les deux seules méthodes qui ont généré une topologie différente de la solution initiale. De plus, les ressources énergétiques distribuées contribuent à 82.19% de la génération totale pour BBO-VNS et 87.44% pour BBO-B&B-VNS, alors que la solution de base est de 59.67%.

Enfin, elles participent à alimenter en moyenne 78.52% de la demande totale, soit 10.77 MW pour le 8500-bus, alors que la solution de base est de 63.14%.

Les méthodes proposées considèrent un modèle complexe et réaliste du réseau de distribution, c'est-à-dire en facilitant l'atteinte d'une topologie et d'injections pour les ressources énergétiques distribuées satisfaisant toutes les conditions opérationnelles et les contraintes de réseau. Les résultats démontrent l'impact direct issu de la combinaison de la production locale avec la reconfiguration de réseau pour l'amélioration de l'efficacité du réseau de distribution et la minimisation des pertes. Notamment, la solution résulte typiquement en une topologie différente de la topologie radiale originale, avec une contribution significative des ressources énergétiques distribuées sur le réseau, soit un minimum de 64.32% et un maximum de 87.44% sur la production totale observée. De plus, les ressources énergétiques distribuées participent à satisfaire au moins 77% de la demande totale, et ce, pour l'ensemble des réseaux de test. Enfin, les pertes de puissance sont considérablement réduites dans tous les cas, avec une diminution d'au moins 36.94% pour le 136-bus, 78.06% pour le 136-bus et 7.34% pour le cas pratique du réseau IEEE 8500-bus. Finalement, les résultats permettent l'identification des méthodes les mieux adaptées à une application pratique, en fonction des priorités visées. Si le temps de calcul est le critère premier, alors BBO-VNS est le meilleur choix. Si une plus faible variabilité de la qualité de la solution et de la réduction des pertes de puissance est préférée, BBO-B&B-VNS ou BBO-VNS-B&B sont plus adaptées, la dernière démontrant une meilleure efficacité pour les problèmes à haute dimension, tel que soulevé par le cas du 136-bus.

Une baisse notable de performance est observée pour l'ensemble des méthodes entre les résultats du 34-bus et du 136-bus, ce dernier représentant un problème d'optimisation beaucoup plus complexe en terme de nombre de variables. L'hypothèse principale est que la dimension du problème constitue un défi de taille, particulièrement en ce qui concerne l'aspect combinatoire, comme suggéré par la forte baisse de performance de BBO-VNS entre les résultats du 34-bus et du 136-bus. En revanche, les méthodes intégrant une étape de B&B pour résoudre le problème combinatoire semblent plus flexibles face aux problèmes de différentes tailles, soit BBO-B&B-VNS et BBO-VNS-B&B. Ensuite, comme mentionné précédemment, les méthodes sont limitées en terme d'optimalité car elles n'offrent pas de garantie de convergence, leur force étant au niveau de la réalisabilité. De plus, par choix d'implémentation, les aspects de stochasticité au niveau de la demande et des ressources énergétiques distribuées, ce qui se rapproche beaucoup plus de leur comportement réel, ne sont pas pris en compte par le modèle. Aussi, l'optimisation de boîtes noires, et par ce fait le solveur `NOMAD`, sont utilisés en tant que simples outils pratiques, sans développement théorique, ce qui limite leur application et efficacité. Des travaux sont déjà en cours afin de proposer des méthodes

ayant une plus grande capacité de mise à l'échelle, notamment en considérant un espace de solution binaire différent. L'espace de solution est donc constitué de topologies complètes et non, comme actuellement, d'interrupteurs individuels qui forment une topologie lorsque regroupés. Améliorer l'efficacité des méthodes de résolution permettra d'explorer une approche considérant l'incertitude des ressources énergétiques distribuées et de la demande, tel qu'en programmation par scénarios. Cela peut aussi ouvrir la voie à une approche permettant la formation des micro-réseaux grâce à la présence de ressources énergétiques distribuées. Aussi, il est prévu de réaliser une étude de cas plus approfondie sur le IEEE 8500-bus. Le but étant de mieux évaluer la performance respective des différentes méthodes et l'impact de la résolution d'un tel problème de reconfiguration combiné à l'intégration des ressources énergétiques distribuées sur ce réseau complexe. Afin d'obtenir des garanties théoriques sur les méthodes, il serait pertinent d'explorer la convergence théorique de celles-ci, ainsi que leur capacité à fournir des solutions réalisables lorsque les conditions initiales sont fortement irréalisables au niveau des contraintes du réseau. Une autre piste de recherche serait aussi d'explorer des développements méthodologiques propres à l'optimisation de boîtes noires afin d'en maximiser le potentiel.

TABLE OF CONTENTS

LIST OF TABLES

LIST OF FIGURES

LIST OF SYMBOLS AND ABBREVIATIONS

ADNs	Active Distribution Networks
AC-OPF	Alternative Current Optimal Power Flow
ANN	Artificial Neural Network
B&B	Branch-and-Bound
BBO	Blackbox Optimization
BFS	Best-First Search
BrFS	Breadth-First Search
CBFS	Cyclic Best-First Search
DERs	Distributed Energy Resources
DGs	Distributed Generators
DFS	Depth-First Search
DN	Distribution Network
DNR	Distribution Network Reconfiguration
DNN	Deep Neural Networks
GNN	Graph Neural Networks
MADS	Mesh Adaptive Direct Search
MDP	Markov Decision Process
MICQP	Mixed-Integer Convex Quadratic Programming
MILP	Mixed-Integer Linear Programming
MINLP	Mixed-Integer Nonlinear Programming
MISDP	Mixed-Integer Semi-definite Programming
MISOCP	Mixed-Integer Second-order Cone Programming
SMILP	Stochastic Mixed-integer Linear Programming
VND	Variable Neighbourhood Descent
VNS	Variable Neighbourhood Search

LIST OF APPENDICES

CHAPTER 1 INTRODUCTION AND LITERATURE REVIEW

A main aspect of the energy transition is the diversification of energy resources. It consists mainly in the integration of low- and medium-voltage Distributed Energy Resources (DERs) on the transmission network, such as wind farms or storage systems, and on the distribution network, such as Distributed Generators (DGs) that are utility-owned by consumers. Efficient integration of such technologies raises the need for a flexible network infrastructure, defined as Active Distribution Networks (ADNs) and typically composed of remotely controlled components such as switches, capacitors, voltage regulators, among others.

This chapter introduces the research context and problem, as well as an overview of the literature and the main approaches used to solve this type of problems. This leads to the identification of the main literature gaps and the research objective.

1.1 Research context and problem

The Power Distribution Network (DN) is a three-phase system, usually operated in a radial topology. While it is often meshed to facilitate network reconfiguration, network operators prefer radial operation as it enables efficient coordination of protection systems and reduction in fault current magnitudes [2]. A network is considered radial when its graph has a spanning tree structure with unidirectional power flows, no cycles, and all buses or nodes connected by a path to the substation or root node. The phases are typically unbalanced because of the multi-phase loads and variation in the demand. Unbalanced phases impact power losses, network reliability and voltage levels, and impose additional stress on the network infrastructure [3]. Modern DNs are becoming more than just a passive load connected to the transmission network, for example, with the development of ADNs. ADNs are defined by a high integration of DERs to diversify and decentralize power production, combined with a flexible network topology using remotely controlled switching components, such as normally open tie switches and normally closed sectionalizing switches [4]. Tie switches are normally open devices that allow alternative power flows either between feeders, a feeder being a power line originating from a substation, or between laterals within the same feeder. Sectionalizing switches are normally closed devices that connect sections of a feeder, enabling operations such as fault isolation and the preservation of a radial topology during topology reconfiguration [5], [6]. This infrastructure enables a dynamic response of the network to demand and renewable generation fluctuations during nominal operations, enhancing energy efficiency and mitigating constraints violations such as abnormal voltage profiles and equip-

ment overloading [7]. However, this may also results in bidirectional power flows that tend to increase further phase imbalances and power losses, as both are closely related to each other [3], [8]. Such impacts are critical for network operators, as they influence efficiency, network reliability and resilience, and operational costs [8].

One of the main strategy to mitigate these constraints and integrate efficiently DERs in the network is to minimize power losses. In the literature, this is done either by phase or load balancing [3], or topology reconfiguration [5], [6]. Distribution Network Reconfiguration (DNR) aims to find the radial topology that minimizes power losses by opening and closing tie and sectionalizing switches. The resulting problem combines the nonlinearity and nonconvexity of the Alternative Current Optimal Power Flow (AC-OPF) to the combinatorial nature of switch statuses, yielding a Mixed-Integer Nonlinear Programming (MINLP) problem. Due to the MINLP complexity, most methodologies rely on linear approximations or convex relaxations, or solve it using heuristics. The aim of this Master's Thesis is to propose methods to tackle the complex DNR problem, while considering DER integration.

1.1.1 Distributed Energy Resources

In [8], DERs are referred to as all local technologies on the network that "can generate, store and control electricity", and they are predominantly utilized in the low voltage regions, but also in the medium voltage regions of the DN. They can be any type of storage systems, vehicle-to-grid, or DGs, as addressed in this Master's Thesis. Some examples of DGs are photovoltaic systems, geothermal heating and bio-energy, among others. Thus, they create a new category of presumers that induce bidirectional power flows on the DN, a network that was originally designed for power consumption only. Their integration allows a diversification and decentralization of the power sources, reducing the dependency towards the transmission grid and large non-renewable power sources, such as fossil fuels that are based on conventional generators.

As described in [3], [7], [8], DERs can have a significant positive impact, but also a negative one if poorly integrated and managed. Such positive impacts, among others, are an increased network reliability and resilience as DERs can support the network during peak phases and emergency situations [8]. It can also contribute to the mitigation of the network constraints, like voltage and frequency profiles, equipment overloading and power losses [8]. However, ineffective integration or management can result in negative impacts. The most predominant issues include voltage imbalance across phases, frequency instability and signal distortion (power quality). These are also all related to phase imbalances and overloading of lines that tend to increase power losses. In an already highly unbalanced network such as the DN,

these impacts tend to be more important.

In load-flow analyses [8], [9], DERs are modelled either as deterministic or stochastic components. The deterministic formulation fixes the active and reactive power values during the load-flow calculation, while the probabilistic formulation accounts for the uncertainty of the DERs over the course of the day or the seasons, among others, typically modelling it as a probability density function such as a Markov Decision Process (MDP).

1.1.2 Active Distribution Networks

Traditionally, DNs operate as passive networks where reconfiguration, protection, voltage management, generation scheduling, among others, are planned in advance. In most cases, if changes are to be made on the network, such as during a power outage, a service restoration process, planned maintenance, any other emergency situation, or simply during nominal operation to increase the system reliability, they are carried out based on pre-set scenarios [7].

Modernization of DNs takes into account an increasing integration of DER technologies, such as vehicle-to-grid systems, photovoltaic systems, storage systems, and small wind farms, all directly connected to DNs. As mentioned beforehand, DERs allow for a more flexible and dynamic control of power flows and mitigation of the network operational constraints, such as voltage profiles and equipment overloading. However, they also induce bidirectional power flows, which may impact network constraints and lead to overloading of lines, over-voltages throughout the network, and phase imbalances. ADNs contribute to the high integration of DERs by efficiently managing these technologies and dynamically reconfiguring the network to adapt to fluctuating load and generation conditions, ensuring safe and reliable operations. In this work, ADNs cannot operate in islanded mode, i.e., independently of the main grid like a micro-grid would. This could be enabled by integrating DERs with grid-forming technologies, a predominant research focus in recent years [10].

1.1.3 Blackbox Optimization

State-of-the-art load-flow solver and Blackbox Optimization (BBO) can be combined for DNR. This process has scarcely been used in the context of electrical power systems optimization in general, with only a few applications in reconfiguration problems. An optimization algorithm based on a *blackbox*, typically a numerical simulation, is most reliable in terms of feasibility because it models the desired system with a high level of details, leading to a very accurate representation of the DN constraints. However, BBO may require a large number of evaluations in order to converge, one evaluation being a single iteration

of the blackbox, therefore leading to long computation times to achieve a "good" solution. This limitation is exacerbated when the problem dimension grows. BBO algorithms like the Mesh Adaptive Direct Search (MADS) [11] yield provable local convergence properties, under mild assumptions, while enhancing the feasibility of the solution with respect to a detailed load-flow solution, which is crucial for network operators.

1.2 Literature review

The literature related to DNR is now surveyed, presenting the different methodologies used to solved this type of problem. The main approaches to minimize power losses in DNs are phase or load balancing [3] and topology reconfiguration [5], [6]. Due to the problem complexity, most methodologies simplify the problem using approximations or relaxations, or solve it using heuristics. The DNR problem itself to minimize power losses was first introduced in [12], where the Branch-and-Bound (B&B) algorithm was used to search for the minimum-loss spanning tree. Today, the prevalent approaches in the literature are heuristics, convex relaxations, linear approximations, and machine learning methods [13], [14]. These approaches are now reviewed.

1.2.1 Heuristics

Heuristics are used for DNR as they can provide fast solutions, are fairly simple to implement, and can be applied directly to MINLPs [13], [15]. However, they often lack convergence properties. Prior work on DNR include approaches based on the branch exchange method [5], [6], the minimum spanning tree [16], tabu search, simulated annealing, and population-based optimization such as genetic algorithms and particle swarm optimization [17].

The first heuristic methods to use DNR to minimize power losses are the Distribution Network Optimization (DISTOP) [18] and the branch exchange method [5], [6]. The approach in [18] uses a technique similar to that of [12], opening the switch with the minimum current value, starting from the fully connected network. To determine these current values, an optimal flow pattern is produced, treating closed switches as flexible current sources that act as adaptable variables in the load-flow solution. The main drawback, as noted in [13], is that the solution may not be optimal due to the possible mutuality between loops in the network. The branch exchange method [5], [6], starting from a "base radial configuration", consists in obtaining a new spanning tree by performing one or multiple branch exchanges between pairs of switches. A branch exchange involves analysing two cases, where one switch is always closed, and the other always open, and comparing which scenario results in greater power loss reduction while

meeting the network constraints. The main drawback, as highlighted in [13], is that the final solution may depend heavily on the initial point, i.e., a base radial configuration, because every branch exchange is initiated from it. Also, the method can become computationally intensive as the network size increases.

Finding a minimum spanning tree minimizing power loss is a recurrent approach or/and intuition when faced with a DNR problem, and is much used in the literature. In [16], the minimum spanning tree algorithm is employed to offer a warm start for mathematical optimization approaches. The authors use the Prim algorithm to construct the spanning tree, considering the negative of current magnitudes in the lines as the weights, prioritizing the lines with the highest current magnitudes. A local search based on a sensitivity analysis and the line outage distribution factors is also conducted to assess if it is better to open another line in series.

As noted in [13]–[15], meta-heuristics like tabu search, simulated annealing, and population-based algorithms are often preferred over heuristics in DNR due to their greater adaptability to various problem contexts. Being general algorithms, they are more versatile compared to specific heuristic methods, provided their hyperparameters are well-tuned. In [17], the network is partitioned into subnetworks, and an equivalent network is constructed to account for the boundary edges. The reconfiguration problem is solved in two stages using particle swarm optimization: the first stage addresses the subproblems, while the second stage solves the equivalent network with the subproblems solution fixed through the process. Furthermore, the implementation considers hourly scenarios to account for load and DER uncertainty, and allows both grid-connected and micro-grid operations.

1.2.2 Mathematical Optimization

Mathematical optimization for DNR [13], [14] is slower and complex to implement as it entails a dedicated model of the system, but it provides a guarantee of convergence to a solution given some optimality conditions. These methods, commonly based on linear approximations and/or convex relaxations of the MINLP, provide globally optimal solutions with respect to the approximated or relaxed problem but may lead to infeasibility and/or sub-optimality when applied to the original problem. Mixed-Integer Linear Programming (MILP) use linear approximations of the power flow like LinDistFlow [4], or other formulations like linearized trigonometric terms and disjunctive constraints in [19]. Convex relaxations including Mixed-Integer Convex Quadratic Programming (MICQP) [20] and Mixed-Integer Second-order Cone Programming (MISOCP) [21] are also common because they allow a more accurate modelling of the problem then linear approximations, without losing much solving efficiency.

The LinDistFlow model is a linearization of the DistFlow or branch flow model. It is the most used linear approximation to mathematically model the DN as it represents the network based on simplifications possible because of the radial structure. Notably, it focuses on the power flowing through the line and neglects the quadratic terms associated with the losses, as well as large voltage angle variations [22]. The authors of [4] proposes a two-stage unit commitment method that incorporates a DNR problem, modelled as a MILP, in order to minimize the total grid operation cost. At all times during the process, the alternative current power flow constraints set is formulated with the linearized equations of LinDistFlow. In [19], a Stochastic Mixed-integer Linear Programming (SMILP) model is formulated to solve the DNR problem combined with flexible DER integration. Linear equations of the original AC-OPF are used to model the power flow in the lines, incorporating linearized trigonometric terms and disjunctive constraints formulation. This model considers different types of DERs as well as their uncertainty using 24-hour period stochastic scenarios, each with the same level of probability. Finally, the model is evaluated across different cases including both DNR and DER integration, as well as cases including each alone or neither. In [4], the unit commitment with network reconfiguration problem is decomposed in two subroblems: an operation scheduling problem, represented as a MILP using the LinDistFlow model (unit commitment and dispatch problem), and a network reconfiguration problem. This approach is applied to a 24-hour ahead scheduling, accounting for DER fluctuations and enabling both grid-connected and micro-grid operations.

Convex relaxations are often preferred over the faster linear approximations as they allow a more accurate modelling of the power flows [14]. As surveyed in [22], the main convex relaxations are the semi-definite, second-order cone programming relaxations and their variations, including the convex quadratic programming relaxation. For alternative current power systems, they are applied generally either using the DistFlow model (branch flow), focusing on the power flowing through the lines, or the bus injection model, focusing on the values at each bus, or even on a combined version of the two [19]. MISOCP [21], [23] is typically favoured over Mixed-Integer Semi-definite Programming (MISDP) [2], despite providing looser bounds, due to its greater computational tractability.

In [21], a MISOCP formulation derived from the DistFlow equations is first proposed. In [23], MISOCP is applied to model power flow constraints within a multi-objective dynamic reconfiguration model. This model is embedded in a stochastic programming framework to account for DER and load uncertainty, using fuzzy C-means clustering to divide time periods and enhance computational efficiency. It is further combined with a binary particle swarm optimization integrated with `Cplex` [24] to solve the MISOCP for large-scale DN problems. In [20], the authors introduce a new MICQP that offers tighter bounds than MISOCP while

being also more scalable than MISDP, thus offering a compromise between the two. Finally, [2] introduces, for the first time, a chordal relaxation of the MISDP model for DNR and the optimal operation of DERs, as well as other network components such as voltage regulators. The chordal relaxation significantly enhances the computational efficiency of the MISDP model, itself solved using B&B.

1.2.3 Machine Learning

Machine Learning techniques like reinforcement learning [25] and Artificial Neural Network (ANN) have also been applied to DNR, as surveyed in [13]. In particular, physics-informed Graph Neural Networks (GNN) can deal with reconfiguration problems while considering physical constraints, such as load-flow constraints [26]–[28]. Machine learning-based DNR approaches can provide fast solutions well-suited for online applications. However, these techniques, especially when incorporating end-to-end learning architectures, often lacks the feasibility guarantee for practical deployments and the transparency related to the process [29].

As machine learning techniques can efficiently provide fast solutions, they permit reconfiguration in near real-time. In [30], a DNR method is proposed based on an ANN, combined with a fuzzy C-means clustering technique to improve the performance of the training set by reducing the size complexity of the problem. In [25], an online, real-time DNR problem is proposed, formulated as a MDP to account for DER and load uncertainty. It is solved using a deep reinforcement learning actor-critic algorithm incorporating two Deep Neural Networks (DNN). The actor DNN determines the binary decisions for the switches, DERs, and loads based on the network's current state. These decisions are fixed, and an optimal power flow, formulated as a second-order cone problem, is solved to compute the continuous variables required to satisfy the network constraints. Meanwhile, the critic DNN computes the relative function value based on the network state, enabling the evaluation and improvement of the policy predicted by the actor DNN. This process quickly generates solutions but may still produce solutions that violate the network constraints, which is dealt with in real-time through multiple forward propagations until feasibility is achieved. In [28], the DNR problem is also formulated as a MDP to account for DER and load uncertainty in real-time decision-making. An on-policy reinforcement learning algorithm with a capsule-based GNN is used to determine the binary decisions for the switches based on the network state. The GNN is a specialized type of neural network designed to process graph-structured data by considering local information, such as neighbouring bus data, and the global structure of the graph, or network in this case. More recent approaches that use physics-informed GNNs are

presented in [26], [27]. The GNN in [27] encapsulates the physical properties of the network, including bus information such as voltage, impedance, generation, and demand, within the graph structure itself. A certain percentage of the predicted binary decisions for the switches are fixed and given as an input to a MISOCP solver, which then produces the final topology while ensuring that the network constraints are satisfied. The feasibility of the final solution is closely tied to the percentage of predicted binary decisions passed to the MISOCP solver, as a larger percentage may lead to a higher chance of infeasibility. In [26], an online, dynamic DNR using a physics-informed DNN is also proposed. Unlike [27], where power flow constraints are indirectly incorporated, this approach applies the power flow constraints, formulated with LinDistFlow, in the final layer of the neural network, guaranteeing that these constraints are never violated. Additionally, the loss function aims to minimize power losses and violation of both the generation and the network connectivity constraints. However, the final predicted solution may still violate some of these constraints, including the voltage bounds.

Finally, the approach to solving DNR in [31], although not strictly a machine learning method, is a relevant online dynamic submodular optimization approach. One of their proposed method called online submodular greedy algorithm (OSGA) can be applied to obtain an online, real-time reconfiguration of the network. Firstly, based on the demand from the previous iteration, Newton-Raphson algorithm is used to solve the power flow on a weakly-meshed network, i.e., with some loops. This weakly-meshed network is obtained by allowing a relaxation of the radiality constraints. Then, Prim's minimum spanning tree algorithm is applied on the weakly-meshed network power flow solution to obtain a "good" radial topology. This results in a sub-optimal solution because of the power flow calculation on the weakly-meshed network and reliance on the demand from the previous iteration. However, the overall process still ensures that the regret vanishes after a sufficient number of iterations.

1.2.4 Blackbox Optimization

Alternatively, BBO [32] performs the optimization on a problem modelled as a *blackbox*, typically represented by a numerical simulation that returns an output for a given input. With only few applications in electrical power systems, such as the determination of bus connection capacity considering DER integration [33], this optimization framework does not have an extensive body of literature related to this Master's Thesis topic. To the best of the current knowledge, only two studies have specifically applied BBO in DNR problems. These two approaches are reviewed below.

In [34], a reconfiguration method based on MADS [11] and the `NOMAD` software [35] is proposed.

The approach integrates DERs and tests both integer and binary decision variables for the switch statuses. It also considers, without any simplification, a highly detailed three-phase, unbalanced DN modelled with the open-source simulator `OpenDSS` [36]. The implementation is tested on a single medium-sized feeder (IEEE 123-bus) with a limited number of switches and the DERs are treated as constant components. Reference [9] proposes a multi-objective reconfiguration problem for DNR with constant DERs and also uses MADS. The authors do not use a simulator to model the AC-OPF, but a mathematical optimization formulation using polar coordinates. Also, the DN is approximated as an equivalent topology using graph theory mapping rules to reduce the problem dimension. Performance evaluation is done on the balanced IEEE 33-bus test feeder.

Both references consider the reconfiguration problem and treat the DERs as constant component that are not part of the optimization process. However, the topology can have a significant impact on the DER behaviour and vice-versa [7]. Also, both test their methods on relatively small-sized networks, thus not fully addressing the inherent challenge of DNR related to scalability. Furthermore, the second reference [9] considers a simplified, balanced model of a DN.

1.3 Research objective

The objective of this Master's Thesis is to develop a DNR method to minimize power losses and efficiently integrate DERs in the network, while ensuring that the network constraints are satisfied. While the focus is on loss minimization considering satisfaction of current and voltage limits, constraints like phases imbalances, equipment overloading, among others, are tightly interconnected. Thus, minimizing the losses inherently mitigates the other network constraints [3]. To meet this objective, BBO-based methods are proposed because they allow for the use of a highly accurate load-flow simulation for decision-making that prioritize feasibility over optimality. This contrasts with traditional approach pursuing optimality over feasibility as with mathematical optimization, heuristics, and machine learning, which can limit their practical deployments. Moreover, BBO-based methods offer a level of transparency that often lacks in machine learning approaches. Thus, despite their high effectiveness, they are not as trustworthy as BBO. For improved performance, the approach is focused on both the combinatorial aspect of DNR and the integration of DERs, examining the interactions and impacts they may have on one another as well as on the overall DN operation. DNR is performed assuming the network is designed as a meshed grid but operated radially, as in most practical cases. Therefore, any micro-grid or islanded behaviour is left for future work. Also, as opposed to [9], [34], the DERs are not treated as fixed components, but rather as

variable parts of the optimization process, thus evolving through it. Additionally, the DERs and loads are represented using their deterministic formulation, without yet accounting for scenario-based optimization aspects, such as hourly predictions that consider fluctuations throughout the day. Moreover, this work focuses on the decision-making process to improve operational constraints and therefore, assumes a fully automated DN. Aspects related to communication, infrastructure management, and any economic or cost considerations are left for future work.

1.4 Contributions to the literature

From January 2025 to May 2025, a research stay aimed at improving the proposed approaches was carried out at the School of Mathematics, University of Edinburgh, United Kingdom, with Pr. Miguel F. Anjos.

Below are listed the main scientific contributions that were made as part of this Master's Thesis.

Conference Papers

- C. G. Soldati, S. Le Digabel, and A. Lesage-Landry, "Blackbox optimization for loss minimization in power distribution networks using feeder reconfiguration", in *Proceedings of the CIGRE 2025 International Symposium*, Accepted, CIGRE, Palais des Congrès de Montréal, Canada, Sep. 29–Oct. 3, 2025.

Presentations

- C. G. Soldati, *Blackbox optimization for loss minimization in power distribution networks using feeder reconfiguration*, Presented at *JOPT 2025: Journées de l'Optimisation* conference, HEC Montréal, Canada, May 12–14, 2025.
- C. G. Soldati, *Blackbox optimization for loss minimization in power distribution networks using feeder reconfiguration*, Presented at fORum: Discussion group and junior seminar for PhD students of Optimization and Operational Research (OOR), School of Mathematics, The University of Edinburgh, United Kingdom, Feb. 25, 2025.

Posters

- C. G. Soldati, *Méthode d'optimisation de boîte noire pour la minimisation des pertes en puissance des réseaux de distribution électrique par reconfiguration*, Presented at

the conference *"Repenser la gestion énergétique via l'innovation et son implantation"*, organized by the Energy Modelling Hub and Volt-Age Concordia, Concordia University, Montréal, Canada, Nov. 12, 2024.

1.5 Master's Thesis outline

In Chapter 1, an introduction to the research context and problem is presented, as well as the literature review. In Chapter 2, key concepts used in this research are introduced and explained in detail. Next, Chapter 3 discusses the dedicated BBO model for DNR and the various resolution methods. Computational results are presented and discussed in Chapter 4 for the three test systems. Finally, Chapter 5 summarizes this Master's Thesis contributions, while outlining its limitations and the future research opportunities.

CHAPTER 2 BACKGROUND CONCEPTS

This chapter introduces in more detail the motivations and objectives of the research. It then presents the DNR model, the BBO framework and its integration within this problem.

2.1 Distribution Network Reconfiguration

DNs are highly dependant to consumer behaviour, as loads can vary much during the day. DN hosts three main types of loads: residential and commercial loads that are mostly single-phased, and three-phased industrial loads. Load variations, combined with their multi-phase nature, can result in a highly unbalanced network in terms of phase loading. Moreover, integrating DERs such as solar photovoltaic and storage systems can, on the one hand, mitigate the network's equipment overloading, and abnormal voltage profiles. On the other hand, DERs can induce bidirectional power flows, which may exacerbates phase imbalances, power losses and impact the voltage profile [8]. Integrated DNR and DER optimization can thus play a crucial role in ensuring efficient and safe DN operations [7].

A three-phase power distribution network is represented as a graph $(\mathcal{N}, \mathcal{L})$ with of a set of vertices, i.e., buses, $i \in \mathcal{N} \subset \mathbb{N}$ and a set of edges, i.e., lines, $(i,j) \in \mathcal{L}$. Let the superscript $\phi \in \{a,b,c\}$ denote the phase. Let $\mathcal{G} \subset \mathcal{N}$ be the set of generation buses where $\mathcal{N}^{\mathrm{r}} \subseteq \mathcal{G}$ is the set of substations, $\mathcal{N}^{\mathrm{DER}} \subseteq \mathcal{G}$ is the set of buses equipped with DERs, and $\mathcal{L}^{\mathrm{s}} \subset \mathcal{L}$ be the set of lines equipped with switches. Let $Y_{ij} \in \mathbb{C}^{3\times 3}$ be the three-phase admittance of a line $(i,j) \in \mathcal{L}$. Let $P_{ij} \in \mathbb{R}^3$ and $Q_{ij} \in \mathbb{R}^3$ be the active and reactive three-phase power flowing through a line $(i,j) \in \mathcal{L}$. Let $\overline{S}_{ij} \in \mathbb{R}^3$ be the maximum apparent power (thermal limit) that can flow through line $(i,j) \in \mathcal{L}$ for each phase. Let $\tau_{ij} \in \mathbb{R}^3$ and $\rho_{ij} \in \mathbb{R}^3$ be auxiliary variables representing the active and reactive three-phase power for lines equipped with switches $(i,j) \in \mathcal{L}^{\mathrm{s}}$. Let $p_i \in \mathbb{R}^3$, $q_i \in \mathbb{R}^3$, $p_{d,i} \in \mathbb{R}^3$, $q_{d,i} \in \mathbb{R}^3$, $p_{g,i} \in \mathbb{R}^3$, $q_{g,i} \in \mathbb{R}^3$, and $v_i \in \mathbb{C}^3$ denote the active and reactive power, the active and reactive demand, the active and reactive generation and voltage at bus $i \in \mathcal{N}$ on all phases, respectively. For example, the first element of the vector $p_i \in \mathbb{R}^3$ is associated with the phase $\phi = a$ and is written as p_i^a. Therefore, in the following model, p_i^ϕ denotes a specific element of the vector corresponding to a particular phase. Let $p_{\mathrm{DER},i} \in \mathbb{R}^3$, $q_{\mathrm{DER},i} \in \mathbb{R}^3$ be the generated or consumed active and reactive power for the DERs on all phases, and $\overline{s}_{\mathrm{DER}} \in \mathbb{R}$ denote the cumulative maximum apparent power over all phases at bus $i \in \mathcal{N}^{\mathrm{DER}}$. Let $Z_{ij} \in \mathbb{R}$ indicate the power flow direction between buses i and j on line $(i,j) \in \mathcal{L}$, and $X_{ij} \in \{0,1\}$ represent the state of the switch on line $(i,j) \in \mathcal{L}^{\mathrm{s}}$. Finally, let $\mathcal{M} \gg 0$ be a large constant. DNR can be effectively

visualized using the AC-OPF three-phased equations and disjunctive constraints, leading to the AC-OPF-DNR model expressed as follows:

$$\min_{P,Q,p,q,\tau,\rho,p_{\text{DER}},q_{\text{DER}},v,Z,X} \quad \sum_{(i,j)\in\mathcal{L}}\sum_{\phi\in\{a,b,c\}} P_{ij}^{\phi}+P_{ji}^{\phi} \tag{2.1a}$$

s.t.

$$P_{ij}+\jmath Q_{ij}=v_i(v_i^*-v_j^*)Y_{ij}^* \qquad (i,j)\in\mathcal{L}\backslash\mathcal{L}^{\text{s}}, \tag{2.1b}$$

$$\tau_{ij}+\jmath\rho_{ij}=v_i(v_i^*-v_j^*)Y_{ij}^* \qquad (i,j)\in\mathcal{L}^{\text{s}}, \tag{2.1c}$$

$$p_i^{\phi}=\sum_{(i,j)\in\mathcal{L}} P_{ij}^{\phi},\quad q_i^{\phi}=\sum_{(i,j)\in\mathcal{L}} Q_{ij}^{\phi} \qquad i\in\mathcal{N},\ \phi\in\{a,b,c\}, \tag{2.1d}$$

$$(P_{ij}^{\phi})^2+(Q_{ij}^{\phi})^2\le(\overline{S}_{ij}^{\phi})^2 \qquad (i,j)\in\mathcal{L},\ \phi\in\{a,b,c\}, \tag{2.1e}$$

$$\underline{v}\le|v_i^{\phi}|\le\overline{v} \qquad i\in\mathcal{N},\ \phi\in\{a,b,c\}, \tag{2.1f}$$

$$\underline{p}_i\le p_i^{\phi}\le\overline{p}_i,\quad \underline{q}_i\le q_i^{\phi}\le\overline{q}_i \qquad i\in\mathcal{N},\ \phi\in\{a,b,c\}, \tag{2.1g}$$

$$\underline{p}_{\text{g},i}\le\sum_{\phi\in\{a,b,c\}} p_{\text{g},i}^{\phi}\le\overline{p}_{\text{g},i},\quad \underline{q}_{\text{g},i}\le\sum_{\phi\in\{a,b,c\}} q_{\text{g},i}^{\phi}\le\overline{q}_{\text{g},i} \qquad i\in\mathcal{N}^{\text{r}}, \tag{2.1h}$$

$$p_i^{\phi}=p_{\text{g},i}^{\phi}-p_{\text{d},i}^{\phi},\ q_i^{\phi}=q_{\text{g},i}^{\phi}-q_{\text{d},i}^{\phi} \qquad i\in\mathcal{G},\ \phi\in\{a,b,c\}, \tag{2.1i}$$

$$p_i^{\phi}=-p_{d,i}^{\phi},\ q_i^{\phi}=-q_{d,i}^{\phi} \qquad i\in\mathcal{N}\backslash\mathcal{G},\ \phi\in\{a,b,c\}, \tag{2.1j}$$

$$\left(\sum_{\phi\in\{a,b,c\}} p_{\text{DER},i}^{\phi}\right)^2+\left(\sum_{\phi\in\{a,b,c\}} q_{\text{DER},i}^{\phi}\right)^2\le(\overline{s}_{\text{DER},i})^2 \qquad i\in\mathcal{N}^{\text{DER}}, \tag{2.1k}$$

$$|P_{ij}^{\phi}|\le\mathcal{M}X_{ij},\quad |Q_{ij}^{\phi}|\le\mathcal{M}X_{ij} \qquad (i,j)\in\mathcal{L}^{\text{s}},\ \phi\in\{a,b,c\}, \tag{2.1l}$$

$$|P_{ij}^{\phi}-\tau_{ij}^{\phi}|\le\mathcal{M}(1-X_{ij}),\quad |Q_{ij}^{\phi}-\rho_{ij}^{\phi}|\le\mathcal{M}(1-X_{ij}) \quad (i,j)\in\mathcal{L}^{\text{s}},\ \phi\in\{a,b,c\}, \tag{2.1m}$$

$$Z_{ij}\ge 0 \qquad (i,j)\in\mathcal{L}, \tag{2.1n}$$

$$\sum_{i\in\mathcal{N}} Z_{ij}=0 \qquad j\in\mathcal{N}^{\text{r}}, \tag{2.1o}$$

$$Z_{ij}+Z_{ji}=X_{ij} \qquad (i,j)\in\mathcal{L}^{\text{s}}, \tag{2.1p}$$

$$Z_{ij}+Z_{ji}=1 \qquad (i,j)\in\mathcal{L}, \tag{2.1q}$$

$$\sum_{j\in\mathcal{N}} Z_{ji}=1 \qquad i\in\mathcal{N}\backslash\mathcal{N}^{\text{r}}, \tag{2.1r}$$

$$X_{ij}\in\{0,1\} \qquad (i,j)\in\mathcal{L}^{\text{s}}, \tag{2.1s}$$

where (2.1a) represents active power losses, (2.1b) and (2.1c) are the power flow constraints for the lines with and without switches, respectively, (2.1d) are the nodal power balances, (2.1e) is the thermal line limits, (2.1f) is the voltage magnitude limits, (2.1g)−(2.1j) are the power limits at each bus, (2.1h) and (2.1i) being the case specifically for buses with generation, and (2.1j) being the case specifically for buses without generation, (2.1k) is the power limit

of the DERs, (2.1l) and (2.1m) are disjunctive constraints indicating if power flows or not in the lines with switches, and (2.1n)−(2.1r) are the radiality constraints. These last constraints are inspired by [41] and enforce a radial and connected topology. Specifically, (2.1n) ensures that the variable Z_{ij} is positive, (2.1o) guarantees that power flows originate from a substation rather than flowing toward it, (2.1p)−(2.1q) impose an unidirectional power flow between buses i and j, (2.1q) being specifically the case for lines with switches, allowing no power flows when a switch is open, and (2.1r) enforces that power can flow from a single predecessor bus, thus preventing loops in the network graph. Moreover, disjunctive constraints with constant $\mathcal{M} \gg 0$, (2.1l)−(2.1m), are common in discrete optimization as they enable modelling of binary switching actions while preserving the feasibility of the power flow equations. When $X_{ij} = 0$, no power flows through line (i, j), resulting in $P_{ij} = Q_{ij} = 0$ in (2.1b), and leaving $\tau_{ij},\ \rho_{ij}$ unconstrained. This causes voltage values at the corresponding buses to become unconstrained due to (2.1c). When $X_{ij} = 1$, power flows through line (i, j). This enforces $P_{ij} = \tau_{ij},\ Q_{ij} = \rho_{ij}$ and ensures both (2.1b) and (2.1c) are equal, thus resulting in a valid power flow. Constraints (2.1b), (2.1c), and (2.1f) are nonconvex, while constraints (2.1l), (2.1m), (2.1p), and (2.1s) are mixed-integer. This problem is shown as such, because if a relaxed or approximated formulation of AC-OPF-DNR is employed, it reduces to a mixed-integer convex form akin to those used in the literature review presented in Chapter 1. The MINLP (2.1) is $\mathcal{NP}$-hard and is impractical to solve, especially at the scale of a full DN. For example, the 9500-bus in [7] is composed of 15 DERs and 109 switches, while the 100k-bus in [42], composed of 12 instances of the 8500-bus equipped with 44 switches, has a total of 520 switches. Moreover, such mathematical model lacks details of practical implementations, such as precise network components and their behaviour, that load-flow simulators can provide.

In this work, a reconfiguration method that prioritizes feasibility and practicality of the solution over optimality or speed is proposed. For this purpose, the DN is considered with all its specificity, without any relaxation or approximation of the power flow and the network components, and is optimized with BBO tools.

2.2 Blackbox Optimization

BBO [32] considers problem of the form

$$\min_{\mathbf{x} \in \mathcal{X} \subseteq \mathbb{R}^n} \quad f(\mathbf{x}) \tag{2.2a}$$

$$\text{s.t.} \qquad g_i(\mathbf{x}) \leq 0 \qquad i = 1, 2, \ldots, m, \tag{2.2b}$$

where $f : \mathcal{X} \subseteq \mathbb{R}^n \to \mathbb{R} \cup \{\infty\}$ is the objective function and $g_i : \mathcal{X} \subseteq \mathbb{R}^n \to \mathbb{R} \cup \{\infty\}$, for $i = 1, 2, \ldots, m$, are constraint functions. The f and g_i functions are the outputs of a *blackbox*, most commonly a computer simulation, namely a load-flow simulation in this case. The set $\mathcal{X}$ is the domain of these functions and may include bound constraints. These functions are set to ∞ at the points where the blackbox fails to provide an output. Contrarily to classical mathematical optimization, where the gradients of f and g_i can be exploited, in BBO, no derivative information is available, and so-called *derivative-free methods* must be considered. In addition, querying the functions relying on the blackbox can be resource and time intensive. In this context, BBO allows to accurately model DNs with all the complexities using a dedicated load-flow simulator, instead of variations of the AC-OPF. In the engineering community, these problems are often solved with heuristics due to their relative simplicity of implementation. However, they do not have convergence properties, unlike derivative-free algorithms, such as the Mesh Adaptive Direct Search (MADS). For a comprehensive overview of BBO applications, see [43]. In the following, MADS is employed because it can handle multiple types of variables, including continuous and integers, and is publicly available through the `NOMAD` software package [35]. Sustained research and development in power engineering led to several highly accurate simulators capable of modelling and testing multiples settings and components. The methods proposed in this Master's Thesis leverage highly accurate load-flow solvers that ensure feasibility of the model, thereby also enhancing feasibility in the decision-making process. Some notable examples are `CYMDIST` [44], `OpenDSS` [36], `EMTP` [45], `PSCAD` [46], and `MATLAB/Simulink` [47].

2.3 Combinatorial Optimization

Combinatorial optimization seeks to solve problems with discrete variables, or in this case binary variables. The space of variables itself is finite but can be very large, e.g., for a combinatorial problem with N variables, it can contain up to 2^N solutions. This is why such problems are often subject to high dimensionality issues and are complex to solve. Typical approaches use either heuristics methods or exact methods such as the B&B algorithm.

2.3.1 Branch-and-Bound

The exact B&B algorithm [48] is a combinatorial optimization method that consists in the exploration of a tree until convergence to a global optimal solution. By relaxing variables, it partitions the initial binary problem in subproblems, where each of them is a different node of the tree. This algorithm is defined by three main aspects that are highly problem specific: the search strategy, the branching strategy, and the pruning rules.

The search strategy determines how the tree is explored. As reviewed in [48], some typical search strategies include the Depth-First Search (DFS), the Breadth-First Search (BrFS), the Best-First Search (BFS), and the Cyclic Best-First Search (CBFS). These strategies are illustrated in Figure 2.1, incorporating pruning rules for the search strategies presented in a similar figure in [48]. Each subproblem is defined by two numbers: a number inside the subproblem showing its lower bound and a number outside denoting its exploration order. The grey-filled nodes represent subproblems that are pruned during the exploration of the tree. The optimal solution is indicated by the dashed subproblem and the B&B starts with an incumbent value of 10. In this example, the lower bound, supposing it is known for each subproblem, is the pruning rule as well as the the measure-of-best function used for BFS and CBFS. A measure-of-best function is an heuristic that assigns a numerical "score" to a subproblem, guiding the algorithm to prioritize subproblems with the lowest value [48]. A common one is a lower bound on the subproblem, as used in Figure 2.1, where the subproblem is pruned if its lower bound is worse than the value of the incumbent solution. Initially, the incumbent solution has a value of 10, but it is eventually replaced by the optimal solution with a value of 9, allowing the pruning of an increasing number of nodes. As illustrated in Figure 2.1, due to the problem structure in [48], BFS ends up pruning the same nodes as CBFS. However, the former follows a much different search strategy than the latter, as seen in the exploration order.

The DFS operates as first-in first-out, trying to go to the closest and fastest it can to the bottom of the tree towards a complete solution. A complete solution consists of DER values combined with a radial, fully connected topology in which all variables are binary, meaning none are relaxed. The BrFS explores the tree level by level and requires much more memory than DFS. Thus, it is more robust as it considers the problem as whole and not just some specific regions at a time. However, it can become highly inefficient. This is the case especially for large problems, as complete solutions that are usually located at the bottom of the tree take a longer time to reach. The BFS ranks each unexplored subproblem of the tree using an heuristic measure-of-best function and evaluates nodes based on this order. It better exploits the structure of the problem than DFS, while being a more effective strategy than BrFS. In fact, it selects promising regions rather than going through all of them sequentially. The CBFS strategy [49] is the most recently developed one and combines aspects from both DFS and BFS. First, this strategy classify the subproblems in categories called contours based on some characteristics, such as depth in the tree, as illustrated in Figure 2.1. A contour represents, in other words, a region of the tree based on some characteristics specific to the application or the implementation of the algorithm. Hence, it groups together "similar" subproblems. Next, in the contours themselves, the subproblems are again ordered

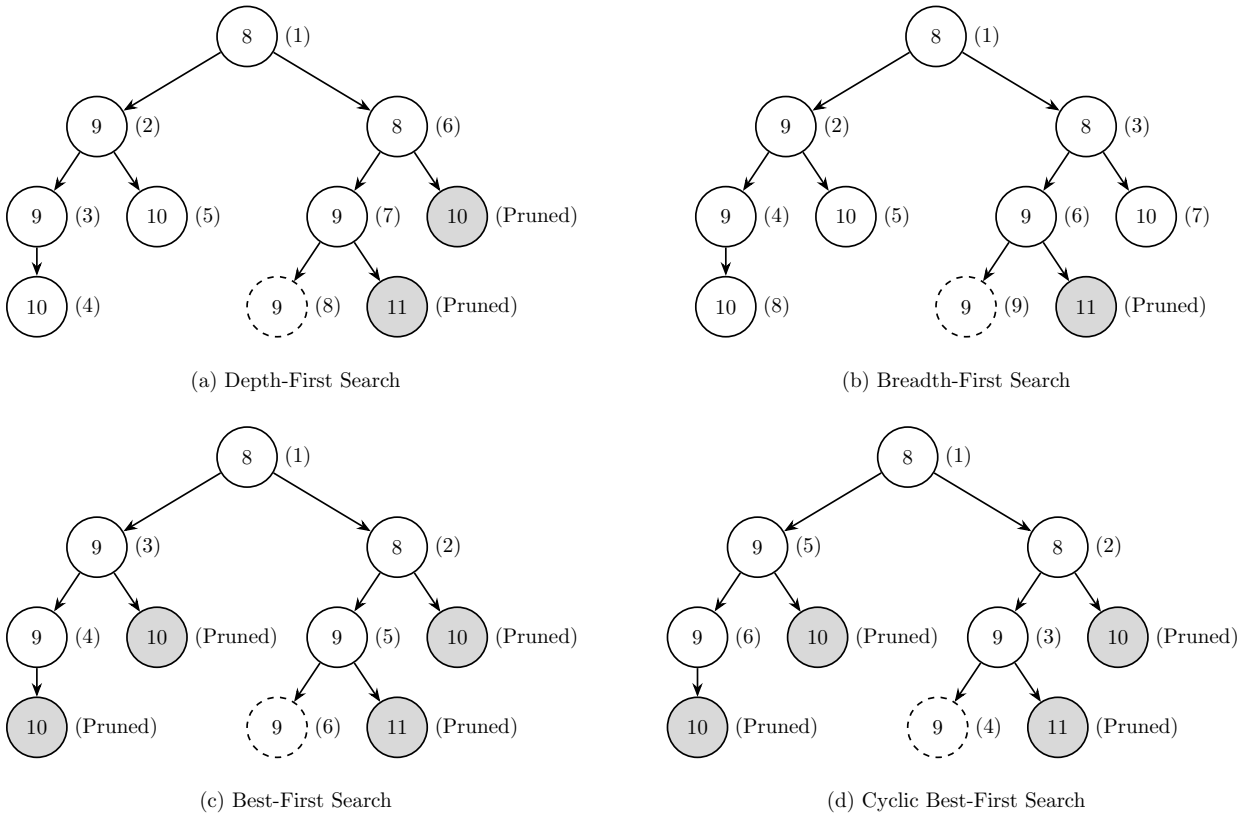

(a) Depth-First Search

(b) Breadth-First Search

(c) Best-First Search

(d) Cyclic Best-First Search

Figure 2.1 Search strategies for the B&B algorithm inspired by [48].

with a heuristic measure-of-best function, as in BFS. CBFS searches the tree by iterating, or cycling, through the contours and evaluating subproblems based on this ordering. By regularly exploring different regions of the tree, it fully exploits the structure of the problem and may accelerate the obtention of a complete solution.

The branching strategy establishes how branching is conducted on a subproblem. As described in [48], the main techniques are binary branching, which partitions the subproblem into two new subproblems, and wide branching, which partitions the subproblem in more than two new subproblems. In integer programming specifically, binary branching generally consists in choosing a variable using an heuristic and then branching on it by imposing bounds on its value. As for wide branching, the same principle is applied but for more then one variable at the same time, based on some rule or heuristic specific to the problem.

The pruning rules are most important as they allow to limit the B&B computational complexity by reducing the tree that is explored. A wide range of rules have been applied in the literature. Because they are highly application-oriented, they will be presented in a general manner. One notable example is the lower bound on the objective value of a subproblem.

This rule permits to discard a subproblem if its lower bound on the objective function is worse than that of the incumbent solution. There are also the dominance relations that involve pruning a subproblem if it is dominated by another. This means that at least one complete solution derived from the dominating subproblem performs equally well or better than any subproblems derived from the dominated one. Finally, there are variations of the original B&B that prune subproblems using cutting planes, i.e., Branch-and-Cut, and column generation, i.e., Branch-and-Price [48].

In the exact B&B algorithm, convergence properties to a global optimal solution are guaranteed using two bounds on the problem [48]. The upper bound indicates that the objective value of any relaxed subproblem in the tree must not exceed that of the current incumbent solution, otherwise the subproblem is pruned. Next, by definition of the relaxation, the lower bound indicates that the objective value of any complete binary solution must be greater or equal to that of its relaxed counterpart. A global optimum occurs when these bounds, assumed to be exact in the convergence proof, converge to the same value and that all subproblems that cannot be pruned have been evaluated [48]. In cases where the problem is neither linear or convex, the bounds may not be exact but can still be tight enough to yield a local optimum. Otherwise, the B&B algorithm acts as an heuristic without any convergence properties. For the MINLP in particular, an ϵ-global solution can be reached by convexifying the nonconvex functions and/or tightening the bounds of the variables and constraints, thereby obtaining and underestimation of the original problem [50]. However, this is theoretically based on the asymptotic tightening of the B&B bounds, thus enabling the use of a ϵ-optimality gap in practice.

2.3.2 Variable Neighbourhood Search

Variable Neighbourhood Search (VNS) is a general meta-heuristic framework used in combinatorial optimization [51] that performs a local search in the neighbourhood of an initial solution. It is typically composed of three steps that are reproduced at each iteration until a stopping criteria is reached: the shaking procedure, the improvement procedure, and the neighbourhood change [52]. The stopping criteria is generally a maximum number of iteration of these steps or a maximum computation time.

The simplest shaking procedure consists in selecting a new random point from the neighbourhood of the initial solution. The main objective being to disturb the VNS search in order to avoid getting stuck in a local optimum. The neighbourhood change guides how the search will continue in the next iteration, based on the result of the current one. The most commonly used techniques are the `Sequential neighbourhood change step`,

the `Cyclic neighbourhood change step`, the `Pipe neighbourhood change step`, and the `Skewed neighbourhood change step` [53]. The `Sequential neighbourhood change step` proceeds to the next neighbourhood if there is no improvement compared to the incumbent solution, otherwise, the neighbourhood is reset to the first one. The `Cyclic neighbourhood change step` proceeds to the next neighbourhood in all cases, regardless of whether there is an improvement or not. The `Pipe neighbourhood change step` stays on the current neighbourhood if there is an improvement compared to the incumbent solution, otherwise, it proceeds to the next neighbourhood. The `Skewed neighbourhood change step` considers that an improvement is not only based on whether the objective function of the solution improves compared to the incumbent solution, but also by how far it is from the incumbent solution. This encourages the exploration of regions farther from the incumbent solution, aiming for a more global search, and is combined with a neighbourhood change strategy such as those described earlier.

Next, the improvement procedure refers to an optional step which objective is to improve the current solution at each iteration. The two main approaches are the local search and the Variable Neighbourhood Descent (VND) [53]. The local search involves seeking a better solution within the neighbourhood of the current solution. A prevalent strategy is the *first improvement*, which stops as soon as an improving solution is found. Another one is the *best improvement*, that selects the best solution among all the improving ones. Apart from these main ones, various meta-heuristics techniques can also be used depending on the problem context. The VND itself may be used as a local search strategy. It consists in the exploration of multiple neighbourhoods, rather than just the current one. Thus aiming for a more global solution.

Apart from the improvement step which may guarantee a local optimum with respect to the current neighbourhood, VNS does not provide any convergence properties as it is a meta-heuristic. It can only ensure the obtention of a “good” solution, with the advantages of being a relatively fast process and fairly simple to implement.

CHAPTER 3 SOLUTION DETAILS

This chapter introduces the dedicated BBO model and the proposed resolution methods.

3.1 Optimization model

Model (2.1) is reformulated as a BBO problem. The DN is considered as a three-phase unbalanced system that is radially operated and equipped with DERs. In order to fully consider the impact of the ADN technologies, the decision variables are both the switch statuses and the power injections and absorptions (active power p, reactive power q) of DERs. As described in [8], [9], DERs are typically modelled either with a deterministic formulation, i.e., constant, viewed as a "negative load", or with a probabilistic formulation, i.e., viewed as a probability density function. For both, the power factor is usually considered constant, thus overlooking the impact of the DN structure (topology, loads, capacitors, etc.). In the proposed model, the DERs are considered as deterministic PQ-controlled components, with a constant power factor. However, as p and q are considered as decision variables, it is possible to study how DERs behave best based on the network's topology and equipments, thus assessing the impacts on the DN itself. This differs from [9], [34] that considers constant DER outputs, optimizing only on the switches' state.

The optimization workflow is detailed in Figure 3.1. A more detailed version illustrating the inner workings of the blackbox is provided in Appendix A. An evaluation of `NOMAD` represents one cycle of this workflow. Let the input of decision vector $\mathbf{x}$ be:

$$\mathbf{x} = \left(\left[\sum_{\phi \in \{a,b,c\}} p^{\phi}_{\mathrm{DER},i} \right]_{i \in \mathcal{N}^{\mathrm{DER}}}, \left[\sum_{\phi \in \{a,b,c\}} q^{\phi}_{\mathrm{DER},i} \right]_{i \in \mathcal{N}^{\mathrm{DER}}}, [X_{ij}]_{(i,j) \in \mathcal{L}^{\mathrm{s}}} \right).$$

The objective is to minimize the DN power losses. Let $I_{ij} \in \mathbb{C}^3$ and $r_{ij} \in \mathbb{R}^3$ be the three-phase current phasor and resistance of line $(i,j) \in \mathcal{L}$, respectively. In a radial system, minimizing total generation is equivalent to minimizing power losses:

$$\begin{aligned} \arg\min \sum_{(i,j) \in \mathcal{L}} \sum_{\phi \in \{a,b,c\}} r^{\phi}_{ij} |I^{\phi}_{ij}|^2 &= \arg\min \sum_{(i,j) \in \mathcal{L}} \sum_{\phi \in \{a,b,c\}} P^{\phi}_{ij} + P^{\phi}_{ji} \\ &= \arg\min \sum_{i \in \mathcal{N}} \sum_{\phi \in \{a,b,c\}} p^{\phi}_{g,i} - p^{\phi}_{d,i} \\ &= \arg\min \sum_{i \in \mathcal{G}} \sum_{\phi \in \{a,b,c\}} p^{\phi}_{g,i} \ . \end{aligned}$$

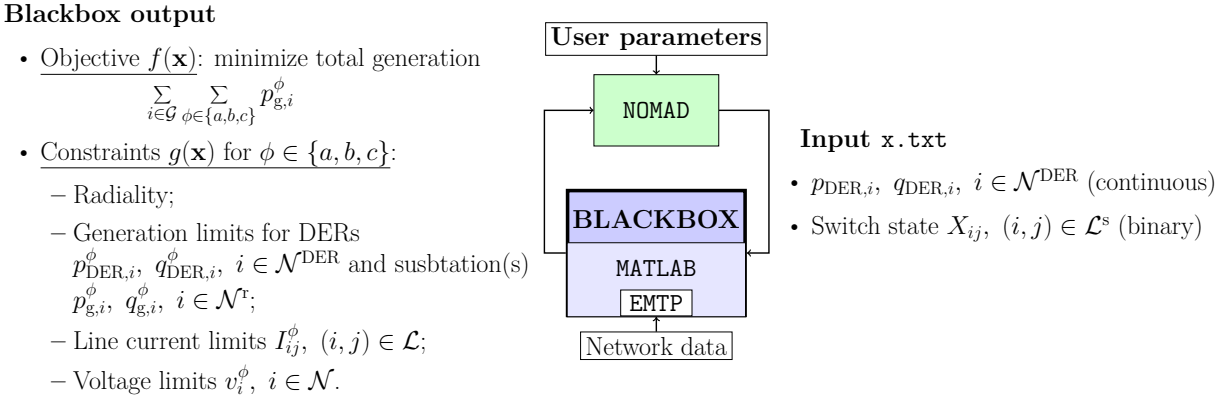

Figure 3.1 DNR blackbox optimization workflow.

Next, the DNR constraints are adapted to the BBO settings by incorporating typical power system requirements, namely, voltage magnitude at each bus, generated power, including DERs, and line current flows, as defined by

$$|v_i^{\phi}| - \overline{v} \leq 0,\ \underline{v} - |v_i^{\phi}| \leq 0 \qquad i\in\mathcal{N},\ \phi\in\{a,b,c\} \tag{3.1a}$$

$$\left(\sum_{\phi\in\{a,b,c\}} p^{\phi}_{\mathrm{DER},i}\right)^2 + \left(\sum_{\phi\in\{a,b,c\}} q^{\phi}_{\mathrm{DER},i}\right)^2 - (\overline{s}_{\mathrm{DER},i})^2 \leq 0 \qquad i\in\mathcal{N}^{\mathrm{DER}} \tag{3.1b}$$

$$|I_{ij}^{\phi}| - \overline{I}_{ij}^{\phi} \leq 0 \qquad (i,j)\in\mathcal{L},\ \phi\in\{a,b,c\} \tag{3.1c}$$

$$\underline{p}_{\mathrm{g},i} - \left(\sum_{\phi\in\{a,b,c\}} p^{\phi}_{\mathrm{g},i}\right) \leq 0,\ \left(\sum_{\phi\in\{a,b,c\}} p^{\phi}_{\mathrm{g},i}\right) - \overline{p}_{\mathrm{g},i} \leq 0 \qquad i\in\mathcal{N}^{\mathrm{r}} \tag{3.1d}$$

$$\underline{q}_{\mathrm{g},i} - \left(\sum_{\phi\in\{a,b,c\}} q^{\phi}_{\mathrm{g},i}\right) \leq 0,\ \left(\sum_{\phi\in\{a,b,c\}} q^{\phi}_{\mathrm{g},i}\right) - \overline{q}_{\mathrm{g},i} \leq 0 \qquad i\in\mathcal{N}^{\mathrm{r}}, \tag{3.1e}$$

where (3.1a) represents the voltage limits in p.u., (3.1c) enforces the line ampacity limit $\overline{I}_{ij}$, and (3.1d)−(3.1e) are the active and reactive power limits of the substation(s). Finally, (3.1b) represents the apparent power limit of the DERs. The voltage magnitude limit, upper and lower bounds are, respectively, set to $\overline{v} = 1.05$ p.u and $\underline{v} = 0.95$ p.u.

The set (3.1) is enforced continuously throughout the optimization process. This ensures that the resulting solution is feasible, provided that all network constraints in (3.1) are satisfied, which is enhanced by the use of a highly accurate load-flow solver. The number of constraints composing (3.1) is linked to the network size, which can lead to dimensionality issues. To simplify the constraint set in the BBO solver, `NOMAD`, the constraints (3.1) are aggregated

using a formulation inspired by the constraints violation function [32]:

$$g_i(\mathbf{x}) = \sum_{j \in \mathcal{J}} \max\{c_j(\mathbf{x}), 0\}^2 \leq 0 \quad \mathcal{J} = \{1, 2, \ldots, m\},\ i = 1, 2, \ldots, 8, \tag{3.2}$$

where $g_i(\mathbf{x})$ represents constraints (3.1a)−(3.1e), and $c_j(\mathbf{x})$ represents a single instance of the constraint for a given bus, line and phase. For example, $i = 1$ for (3.1a), $j = 3$ for bus 3, phase a, yields $c_3(\mathbf{x}) = v_3^a - \overline{v} \leq 0$. At each iteration of the BBO workflow shown in Figure 3.1, the load-flow solver, modelled in `EMTP`, is used to evaluate the network's electrical values given $\mathbf{x}$, i.e., a topology and DER settings. Preceding the load-flow, the radiality and connectivity of $\mathbf{x}$ are verified through graph theory functions, thereby defining a feasible topology as a spanning tree. Because micro-grids are not considered in this work, each bus of the network must be connected to the substation. Thus, a feasible topology is a radial and fully connected DN. Islanding of the network is left for future work. Finally, the BBO-DNR reconfiguration problem is

$$\min_{\mathbf{x}} \quad \sum_{i \in \mathcal{G}} \sum_{\phi \in \{a,b,c\}} p_{\mathrm{g},i}^{\phi} \tag{3.3a}$$

$$\text{s.t.} \quad g_i(\mathbf{x}) \leq 0 \qquad i = 1, 2, \ldots, 8, \tag{3.3b}$$

$$[X_{ij}]_{(i,j) \in \mathcal{L}^{\mathrm{s}}} \in \mathbf{x} \text{ represents a radial and connected network,} \tag{3.3c}$$

where $g_i(\mathbf{x})$, $i = 1, 2, \ldots, 8$ are calculated based on the load-flow results and the input vector $\mathbf{x}$, and treated by the BBO solver `NOMAD` using the progressive barrier (PB) method [32] for the constraints.

3.2 Resolution methods

The proposed methods thrive to reduce the resolution time of the BBO-DNR problem (3.3). The BBO solver usually performs better given a limited budget when only considering continuous variables. Thus, the mixed-integer problem is separated into a continuous formulation solved by BBO (DER optimization, fixed topology) and a binary formulation (topology optimization, fixed DER injections) solved using combinatorial optimization-inspired algorithms. This results in an iterative process, with combinatorial optimization seeking a "good" binary topology, followed by continuous optimization on the DER variables, as illustrated in Figure 3.2. The continuous optimization step, conducted as a BBO, is directly invoked within the main combinatorial optimization process using a simple function defined in Appendix B.

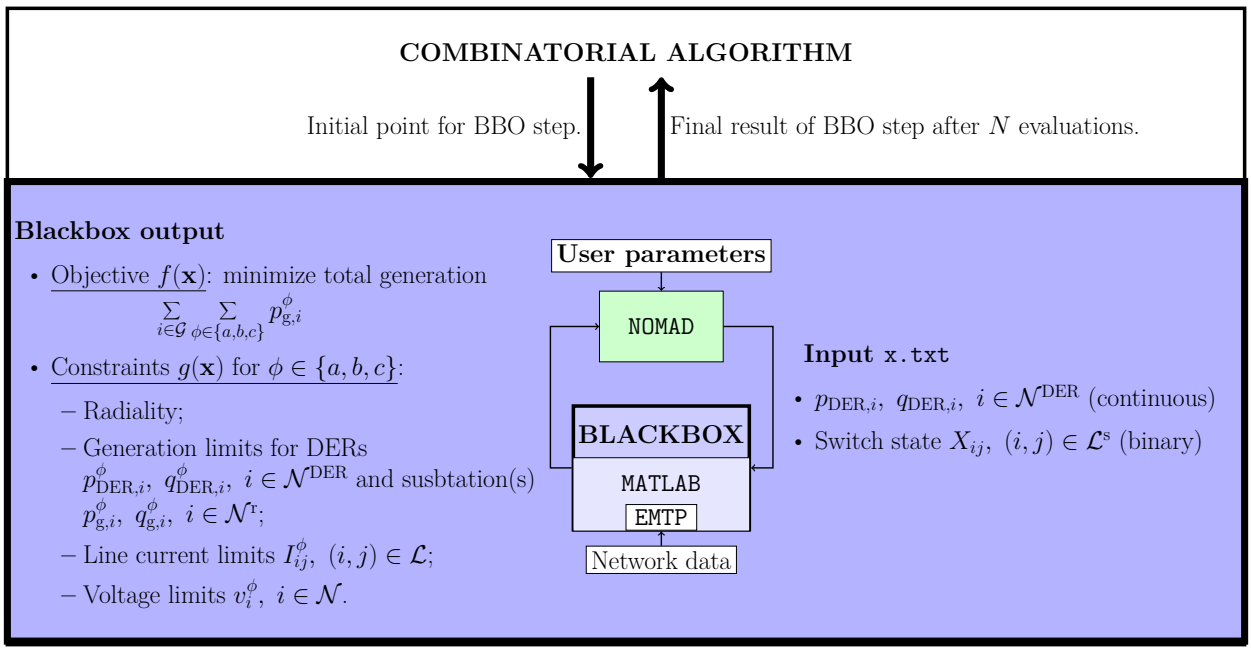

Figure 3.2 Optimization workflow with the combinatorial algorithm implementation.

3.2.1 Branch-and-Bound

The B&B algorithm [48] is a combinatorial optimization method consisting in the exploration of a tree until convergence to a solution. The B&B algorithm partitions the mixed-integer problem into subproblems, each of them being a different node of the tree. At each level of the tree, a new binary variable of the topology is fixed using an heuristic until a complete binary solution is obtained. Convergence occurs when no more nodes are left to evaluate. In this case, each node of the tree is evaluated with the BBO solver given a limited evaluation budget. The BBO solver `NOMAD` optimization parameters are detailed in Appendix B.1. The binary variables that are not already fixed are relaxed to continuous variables, meaning that BBO only considers continuous variables, i.e., DER injections and relaxed switches. Relaxing the switch statuses is done in the simulator by modifying the line components, namely the resistance, the inductance and the capacitance, thus affecting the power that can flow through this line. While having no physical meaning, this temporary relaxation allows for a more efficient use of the BBO solver. In typical B&B algorithms, exact upper and lower bounds are used to guarantee convergence to a solution. In B&B applied to MINLP as described in Section 2.3.1, an ϵ-global solution can be guaranteed by modifying the problem formulation. However, the only guarantee in this implementation is that an approximation of these bounds is available given that the problem is not solved to optimality when provided with a limited evaluation budget. In theory, under some conditions, an asymptotic result guaranteeing a

local solution could be reached if an infinite evaluation budget was permitted at each step.

The tree is explored using binary branching combined with a technique inspired by the CBFS strategy. The binary branching involves fixing a binary variable to 0 in one of the subproblems and to 1 in the other, thereby testing both of the switch's statuses. The strategy to select which variable to fix and branch on is outlined in Algorithm 1. The branching itself is done by the function `branch_CBFS.m` and detailed in Appendix B.1. With BBO as the subproblem solver, ranking unexplored subproblems with a measure-of-best function is not possible, as no prior information about them is available. Consequently, each pair of subproblems resulting from a binary branching are evaluated and stored in a contour, defined in Section 2.3.1, based on their objective function values. If both subproblems yield feasible optimization solutions with objective function values smaller than that of the incumbent solution, the one with the better objective function remains in the current contour, while the other is moved to the next contour. This is guided by a pruning rule that uses a lower bound on the subproblem's objective, which is compared to the incumbent's objective. The contours, numbered as $0, 1, 2, \ldots$, represent regions of the tree with similar objective function values. The subproblems within a contour are processed in a first-in, first-out order, prioritizing newly generated subproblems when working within the current contour, following a pattern similar as DFS. A contour must be fully processed before proceeding to the next one. In Algorithm 1, which presents B&B as pseudocode, the primary queue for storing unevaluated nodes is structured by contour, with each of them consisting of a set of nodes represented as structures. All nodes of the tree are defined as a structure, which is detailed in Appendix B.1.

Algorithm 1 B&B

Input: $\mathbf{x}_0$, the initial solution, N_{local}, the evaluation budget for each node at the beginning (root and first tree level), and $N_{\text{local\_next}}$, the budget for the rest of the tree nodes.

$N \leftarrow N_{\text{local}}$.
Starting from $\mathbf{x}_0$, **optimize with BBO** for N evaluations, while relaxing all binary variables to continuous values.
Branching strategy: Sort in ascending order the section of the obtained solution corresponding to the relaxed variables and select the first fractional value. If there is no fractional value, take the first in the sorting order. The selected topology variable is the next branching *bval*.
$node_{\text{r}}$ is the root node of the tree with ID $\leftarrow 0$ and initialized with $\mathbf{x}_0$.
$nodes_{\text{t}} \leftarrow node_{\text{r}}$. ▷ Dataset of structures.
$nodes_{\text{q}} \leftarrow node_{\text{r}}$. ▷ Dataset of structures sort by contours.
$Best \leftarrow node_{\text{r}}$. ▷ Incumbent solution.
$nodes_{\text{d}} \leftarrow \emptyset$, $branch_{\text{f}} \leftarrow \emptyset$. ▷ Datasets of structures.
$contour_{\text{c}} = 1$. ▷ Contour of the subproblem the algorithm is currently evaluating, initialized at 1 for the root node.
$it \leftarrow 0$.
Branch with `branch_CBFS.m` at $node_{\text{r}}$ on the previously chosen topology variable *bval*.
while $nodes_{\text{q}} \neq \emptyset$ **do** ▷ Main algorithm loop.
    $contour_{\text{c}} \leftarrow nodes_{\text{q}}[1][1]$.contour. ▷ Current contour.
    $it \leftarrow it + 1$.
    $node_{\text{c}} \leftarrow nodes_{\text{q}}[1][it]$. ▷ Current node to optimize.
    Optimize with BBO on $node_{\text{c}}$ for N evaluations, while relaxing all binary unfixed variables, and taking as initial values for the DERss the values from the node with the best objective function among all previously evaluated nodes, stored in $nodes_{\text{t}}$.
    if $node_{\text{c}}$.obj $<$ $Best$.obj **and** $node_{\text{c}}$ is feasible **then** ▷ Analysis of result.
        if All topology decision variables are binary **then** ▷ Success, a leaf of the tree.
            $Best \leftarrow node_{\text{c}}$.
            $node_{\text{c}}$.status $\leftarrow 2$.
            $nodes_{\text{q}}[1][it] \leftarrow node_{\text{c}}$.
        else ▷ Success, but not yet a leaf.
            Use the branching strategy described in **Step 3** to select the next topology variable *bval* to branch on among the unfixed variables. The only difference from **Step 3** is that a non fractional value may be chosen only when branching on the last remaining unfixed variable.
            $node_{\text{c}}$.branching $\leftarrow$ *bval*.
            Add *bval* to $node_{\text{c}}$.branching_vec.
            $node_{\text{c}}$.status $\leftarrow 0$.
            $nodes_{\text{q}}[1][it] \leftarrow node_{\text{c}}$.
        end if
        Add $node_{\text{c}}$ to $nodes_{\text{t}}$. ▷ Successful branching, store the node.

30: **else** ▷ Failure, prune the node.
31: $node_{\mathrm{c}}$.status $\leftarrow 1$.
32: $nodes_{\mathrm{q}}[1][it] \leftarrow node_{\mathrm{c}}$.
33: **end if**
34: **if** $it = 2$ **then** ▷ Finished evaluating a pair of child nodes.
35: **if** Both child nodes are feasible, such that status $= 0$ **then**
36: Increment the contour for the node with the worst objective function value.
37: **end if**
38: ID $= [nodes_{\mathrm{q}}[1][1].\mathrm{ID} \quad nodes_{\mathrm{q}}[1][2].\mathrm{ID}]$.
39: **for** $i \leftarrow 1$ to 2 **do**
40: $index \leftarrow \mathrm{Find}(nodes_{\mathrm{q}}[1].\mathrm{ID} = \mathrm{ID}[i])$.
41: **if** $nodes_{\mathrm{q}}[1][index]$.status $= 1$ **then** ▷ Failure, prune the node.
42: Add $nodes_{\mathrm{q}}[1][index]$ to $nodes_{\mathrm{d}}$.
43: Remove $nodes_{\mathrm{q}}[1][index]$ from $nodes_{\mathrm{q}}$.
44: **else if** $nodes_{\mathrm{q}}[1][index]$.status $= 2$ **then**. ▷ Success, leaf.
45: Add $nodes_{\mathrm{q}}[1][index]$ to $branch_{\mathrm{f}}$.
46: Remove $nodes_{\mathrm{q}}[1][index]$ from $nodes_{\mathrm{q}}$.
47: **else if** $nodes_{\mathrm{q}}[1][index]$.status $= 0$ **then** ▷ Success, branch on the node.
48: **Branch** with `branch_CBFS.m` at $nodes_{\mathrm{q}}[1][index]$ on the previously chosen topology variable for this node *bval*.
49: **end if**
50: **end for**
51: $it \leftarrow 0$.
52: **end if**
53: **for** $i \leftarrow |nodes_{\mathrm{q}}|$ **downto** 1 **do** ▷ Remove a contour if it is empty.
54: **if** $nodes_{\mathrm{q}}[i] = \emptyset$ **then**
55: Remove $nodes_{\mathrm{q}}[i]$ from $nodes_{\mathrm{q}}$.
56: **end if**
57: **end for**
58: **end while**

3.2.2 Variable Neighbourhood Search

VNS [51] is a meta-heuristic designed for various type of problems, including combinatorial optimization. It performs a local search in the neighbourhood of an initial solution. The procedure selects a new random feasible topology from the neighbourhood of the initial solution. BBO is then carried out for this fixed topology given a limited evaluation budget, and solely focused on continuous variables, i.e., DER injections. The BBO solver parameters are detailed in Appendix B.2. The neighbourhood is incremented, e.g., from two to three switch changes, if there is no improvement compared to the incumbent solution. The stopping criteria is based on a global evaluation budget. As a meta-heuristic method, VNS does not provide formal convergence properties.

This implementation of VNS consists in a shaking procedure that selects a new random feasible topology by permuting N_{bin} elements in the initial solution, where N_{bin} represents the neighbourhood and is minimally 2 for a permutation operation. Thus, each topology at a new iteration is derived from the initial solution. For the starting solution at a new iteration, the DER injections correspond to those of the current incumbent solution, which may differ from the initial solution as the algorithm progresses. The neighbourhood change procedure, as described previously, follows the `Sequential neighbourhood change step`, and no formal improvement procedure is included in the process. However, applying BBO to optimize the DER injections for a fixed topology, obtained using the shaking procedure, closely resembles an improvement procedure. Still, this does not enhance convergence properties, as the BBO step has a limited number of evaluations. Algorithm 2 presents the pseudocode of VNS.

Algorithm 2 VNS

Input: $\mathbf{x}_0$, the initial solution, N_{local}, the initial budget for each iteration, and N_{global}, the global budget.

$N_{\text{bin}} \leftarrow 2$.
$\mathcal{X}_{\text{conf}} \leftarrow \mathbf{x}_0$.conf. ▷ Extract the binary variables from the initial solution.
$\mathcal{X}_{\text{vec}} \leftarrow \mathcal{X}_{\text{conf}}$. ▷ $\mathcal{X}_{\text{vec}}$ is a dataset of vectors to track the topologies that are evaluated.
$Best \leftarrow \mathbf{x}_0$.
$flag\_\text{reset} \leftarrow 0$.
$nbEval \leftarrow 0$.
$N \leftarrow N_{\text{local}}$.
$budget \leftarrow N_{\text{global}}$.
while true **do** ▷ Main algorithm loop.
    if $flag\_\text{reset} == 1$ **then** ▷ Update procedure in case of success.
        $N_{\text{bin}} \leftarrow 2$.
        $N \leftarrow 2N$.
        $flag\_\text{reset} \leftarrow 0$.
    end if
    if $nbEval + N > budget$ **and** $nbEval \neq budget$ **then** ▷ Check stopping criteria.
        $N \leftarrow budget - nbEval$.
    else if $nbEval == budget$ **then**
        Exit. ▷ Exit the while loop.
    end if
    if $N_{\text{bin}} > |\mathcal{X}_{\text{conf}}|$ **then** ▷ Check stopping criteria.
        Exit. ▷ Exit the while loop.
    end if
    $\mathcal{X}_{\text{new}} \leftarrow \mathcal{X}_{\text{conf}}$.
    while $X_{\text{new}} \in X_{\text{vec}}$ **or** (not radial **or** not connected) **do** ▷ Shaking procedure
        Generate new topology by swapping N_{bin} elements in $\mathcal{X}_{\text{new}}$.
    end while
    Add $\mathcal{X}_{\text{new}}$ to $\mathcal{X}_{\text{vec}}$.

$\mathcal{X}_{\text{BBO}} \leftarrow [Best.\text{DER} \quad \mathcal{X}_{\text{new}}]$. ▷ Construct the starting optimization point.
Starting from $\mathcal{X}_{\text{BBO}}$, **optimize with BBO** for N evaluations to obtain *Solution*, while fixing $\mathcal{X}_{\text{new}}$ throughout the process.
$nbEval \leftarrow nbEval + N$.
if *Solution*.obj $\neq 0$ **then** ▷ Analysis of result and update procedure.
  if *Solution*.obj $<$ *Best*.obj **and** *Solution* is feasible **then** ▷ Success
    $Best \leftarrow Solution$.
    $flag\_\text{reset} \leftarrow 1$.
  else ▷ Failure, worst then incumbent or infeasible.
    $N_{\text{bin}} \leftarrow N_{\text{bin}} + 1$.
  end if
else ▷ Failure, no solution.
  $N_{\text{bin}} \leftarrow N_{\text{bin}} + 1$.
end if
end while

3.2.3 Combined methods

The methods of VNS and B&B combine the speed-up of combinatorial-inspired optimization methods and the feasibility strength of BBO to obtain "good" topologies result in a reasonable time and a limited budget. As both algorithms performance is sensitive to the initial conditions, BBO is used both as part of these algorithms and as a warm start. The tested resolution methods are sequences of BBO, VNS, and B&B. First, BBO-VNS and BBO-B&B are implemented. Second, two longer sequences, BBO-VNS-B&B and BBO-B&B-VNS, are tested to investigate if there is an advantage to combine both algorithms, i.e., if the second can improve the first's solution when used as a warm start. The evaluation budget for BBO, which is the global budget for the VNS, as well as the local budget specific to a VNS iteration or a B&B node, is constrained and defined in a tuning phase. This tuning is specific to the considered DN, and may also vary between sequences. These four resolutions methods are compared to a baseline method in which BBO is utilized alone with a sufficiently large evaluation budget. The baseline method is purely a blackbox optimization, for which the theory is well known in the literature. This Master's Thesis goes farther and combine blackbox optimization with combinatorial optimization to develop methods that are specific to DNR and DER integration in power systems. The B&B adapted to the problem is an approximation of the exact Branch-and-Bound algorithm while the VNS is a meta-heuristic. Hence, both do not have any convergence guarantee, but the methods used in this work can lead to a "good" solution, and hopefully a local optimum. The proposed solution will, however, tend to be feasible with respect to the network constraints due to the embedded BBO steps and the highly accurate network model, thus enhancing the practicality of the approach.

CHAPTER 4 RESULTS AND DISCUSSION

This chapter introduces the case studies and presents the results and discussion for each.

4.1 Case studies

The performance of the methods is evaluated on three different DN benchmarks: the IEEE 34-bus test system, a 136-bus made of four 34-bus test systems, and the IEEE 8500-bus system. All networks are modified to integrate a number of DERs, and tie and sectionalizing switches. The test cases are modelled and simulated using a state-of-the-art commercial load-flow solver, `EMTP`, and connected to the numerical implementation of the methods in `MATLAB` via the dedicated `MATLAB-EMTP API`. The DERs are modelled as PQ-controlled load-flow components and the substation as a slack source. All switches are modelled as ideal switching components. The methods are designed to be independent of the load-flow simulator, allowing the use of any software, as long as the output/input formatting is the same as described in Figure 3.1. Below are the software versions utilized to acquire the results, all running on Windows 11:

- `NOMAD` 4.4.0 [54];
- `MATLAB` 2023b, and 2024b [47];
- `EMTP` 4.6 [55];
- `MATLAB-EMTP API` 2.0.5 [56].

4.1.1 IEEE 34-bus

The IEEE 34-bus test feeder [57] is a 24.9 kV multi-phase network with unbalanced loads, consisting of primary three-phase buses and secondary single-phase buses on the laterals. The network includes two voltage regulators between buses 814-850 and buses 852-832, and a transformer (24.9 kV to 4.16 kV) between buses 832-888. To model the distributed loads, intermediate buses labelled as buses 0 to 18 are added, splitting in half the concerned lines along with their respective impedance within the original network. The total demand across all network phases amounts to 1769 kW of active power and to 1044 kVAr of reactive power. The DERs, located at buses 890, 848, and 822, are positioned in critical under-voltage regions, as seen on the base model, which is coherent with [58]. As for the switches, they are placed to facilitate network reconfiguration while ensuring radiality and connectivity, based on [28], [58]. The modified network is illustrated in Figure 4.1, where solid green and dashed red

lines are sectionalizing and tie switches, respectively, and Table 4.1 and Table 4.2 summarize the switches positions, the DER positions and power limits in the network. There are a total of three DERs, five sectionalizing switches, and four tie switches, resulting in 15 decision variables in the optimization problem, of which 6 are continuous, i.e., 2 variables per DERs, and 9 are binary. Further details on the model modifications and constraint bounds can be found in Appendix C.1. Also, the evaluation budget for all methods is detailed in Table 4.3.

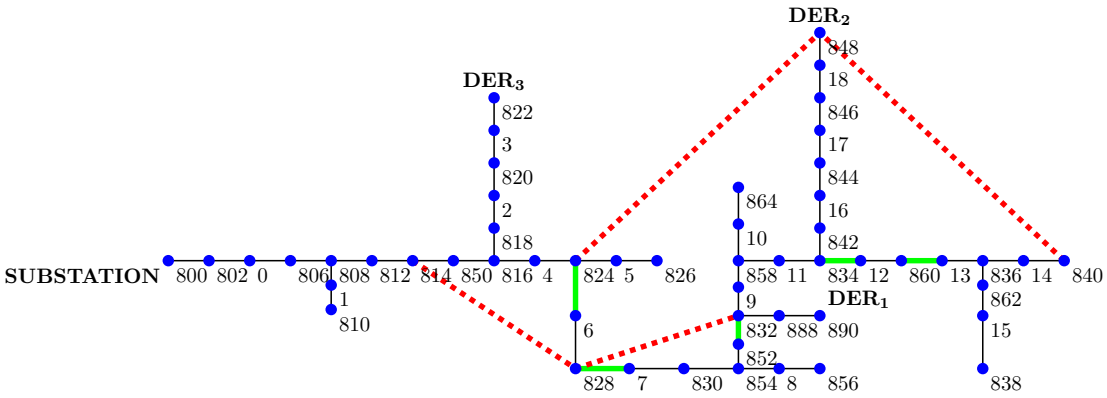

Figure 4.1 IEEE 34-bus network *(solid green line: sectionalizing switch; dashed red line: tie switch)*.

Table 4.1 Position of the switches in Figure 4.1.

Line Data	**Sectionalizing switch**					**Tie switch**			
	SW_1	SW_2	SW_3	SW_4	SW_5	SW_6	SW_7	SW_8	SW_9
From Bus	824	828	852	834	860	814	824	848	828
To Bus	6	7	832	12	13	828	848	840	832

Table 4.2 Position and specifications of the DERs in Figure 4.1.

Data	**Slack source**	**DER_1**	**DER_2**	**DER_3**
Bus	800	890	848	822
P_{max} (kW)	3300	900	800	200
P_{min} (kW)	0	200	200	20
Q_{max} (kVAr)	550	300	200	550
Q_{min} (kVAr)	−190	−300	−200	−190
S_{max} (kVA)	3345.519	948.683	824.621	206.155

Table 4.3 Budget of blackbox evaluations allowed for each method with the IEEE 34-bus.

BBO	**BBO-VNS**			**BBO-B&B**			**BBO-VNS-B&B**					**BBO-B&B-VNS**				
	BBO	VNS		BBO	B&B		BBO	VNS		B&B		BBO	B&B		VNS	
		N_{local}	N_{global}		N_{local}	N_{local_next}		N_{local}	N_{global}	N_{local}	N_{local_next}		N_{local}	N_{local_next}	N_{local}	N_{global}
1000	100	20	1000	100	50	35	100	20	200	50	35	100	50	35	20	500

Figure 4.2 presents data profiles for the 34-bus system. Date profiles [32], [59] compare the efficiency and the robustness of optimization algorithms. To obtain the profiles, each algorithm is run on the same set of 40 problems, with random variations in load profiles and in initial points to test robustness. All the initial points are feasible solutions with respect to the network constraints. Data profiles present the proportion of problems solved within a certain tolerance $\tau > 0$ compared to others, given a certain number of evaluations. The tolerance indicates how close the solution is to the best result obtained among all algorithms for the same problem. A small tolerance means a high level of precision, while a larger one indicates a less strict level of precision.

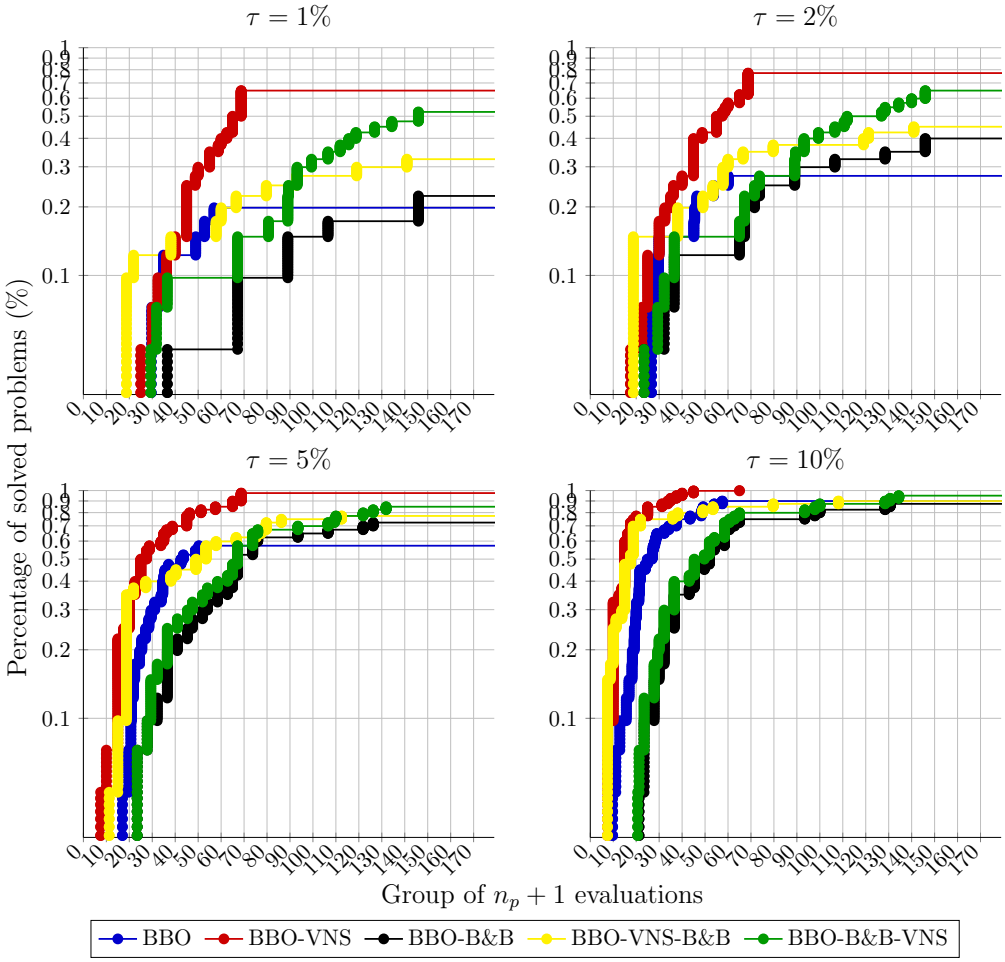

Figure 4.2 Results for the 34-bus network for tolerances τ of 1, 2, 5, and 10 %.

As shown in Figure 4.2, the best-performing method is BBO-VNS, followed by BBO-B&B-VNS, where adding a VNS step after B&B significantly improves performance. As seen with BBO-B&B-VNS, B&B is more computationally demanding but competes with VNS and BBO after enough evaluations. VNS, as anticipated for a meta-heuristic, is the fastest

and appears to be the most consistent in reducing losses. All methods are generally more consistent in minimizing the power losses than the baseline method BBO. Table 4.12 shows the mean power loss reduction and the corresponding standard deviation achieved by each method, compared to the baseline solution. These results correspond specifically to the subset of the 40 problems that use the base load profile. The baseline solution consists of the original topology (opened tie switches and closed sectionalizing switches) with DER injections ensuring network constraints are satisfied, as without DERs the baseline solution is unfeasible. No optimization is involved in the baseline solution. The results illustrate that loss reduction is important and ranges from 78.06% for BBO-B&B to 80.14% for BBO-VNS. Moreover, solution for all problems across all algorithms typically differs from the original topology. Table 4.13 shows the DER contribution to the total generation on the network, considering only the subset of the 40 problems that use the base load profile. The results illustrate that DERs contribute, on average, to 72.26% of the total generation, in comparison to the baseline solution at 38.03%. Table 4.14 presents the DER penetration level and the corresponding standard deviation, calculated by dividing the total active power generated by the DERs in the network by the total demand, 1769 kW for the 34-bus. Again, these results consider only the subset of the 40 problems that use the base load profile. This metric is similar to the one used in Table 4.13, but it provides an even clearer measure of how DERs contribute to the network as it explicitly illustrates the percentage of demand powered by these sources. It shows that DERs contribute to supply, on average, 72.87% of the total demand, in comparison to the baseline solution that is 39.57%. When deployed, the choice of the resolution method depends mostly on the practical requirements. If computational time is the primary concern, BBO-VNS is the best choice. However, BBO-B&B-VNS may be preferred when greater stability in the quality of the solution and the reduction of power losses is desired, and a larger budget is allowed.

A mathematical optimization model based on MISOCP, given in Appendix C, is solved for this test feeder by relaxing the original `DistFlow` equations and using the same objective function as the BBO-DNR problem (3.3). This results in a three-phase MISOCP based on these similar implementations [23], [41], [60] and on the single-phase implementation from [61]. This implementation optimizes both the network topology and the DER injections, and considers a simplified version of the network as modelled in the simulator. Transformers and voltage regulators are not incorporated in the implementation, and the lines are modelled as RL components, discarding the capacitive components. To enable a comparison between the results of the methods and the solution of this implementation, the relaxed solution is applied to the `EMTP` model. The total generation and power loss obtained are, respectively, 1807.14 kW and 38.14 kW, yielding a power loss reduction of 53.38% compared to the baseline

solution. Additionally, DER contribution to the total generation and the supply of the demand are, respectively, 92.11% and 94.10%. The loss reduction is much smaller than what is obtained with the proposed methods, despite the important DER contribution. This suggests that the simplifications to the model and the relaxation of the constraints may have impacted the solution quality, particularly in the combinatorial problem.

Finally, to compare the results and demonstrate the relevance of the methods, the simplest optimization technique is employed: the brute force approach. At first, all spanning trees, corresponding to radial and fully connected topologies, are computed from the fully connected graph of the network using graph theory functions. In order to pinpoint the most promising solutions, BBO is conducted for each fixed topology given a budget of 60 evaluations, and solely focused on the continuous variables of the DERs. All topologies that result in a feasible solution or exhibit only minor constraint violations are retained, while the rest is discarded. On these remaining topologies, BBO is conducted again, but with a larger budget of 1000 evaluations. The solution of the brute force is the one with the best result in terms of objective function. Table 4.4 compares the brute force with the best result obtained for each method, including the topology and the budget of evaluations. Brute force secures the largest power loss reduction, and the same topology as the baseline method BBO. However, it is done after a considerably large number of 39340 evaluations and is therefore not practical nor scalable. These results correspond specifically to the best result for each method, but only within the subset of the 40 problems that use the base load profile, and not the entire set. This may explain the slight differences with the more global results observed in Figure 4.2, which uses the entire set.

Table 4.4 Best solution obtained for each method on the IEEE 34-bus compared to the baseline solution, with initially 0.0714 MW of power losses, and the brute force technique.

Method	**Number of evaluations**	**Topology**	**Loss reduction (%)**	**DER contribution (%)**	**DER penetration level (%)**
Base solution	0	1,1,1,1,1,0,0,0,0	0	38.03	39.57
Brute force	39340	1,1,0,1,0,0,0,1,1	83.00	73.35	73.86
BBO	1000	1,1,0,1,0,0,0,1,1	82.66	74.38	74.90
BBO-VNS	1100	1,1,0,1,1,0,0,0,1	82.10	72.51	73.03
BBO-B&B	2300	1,1,0,1,1,0,0,0,1	81.51	71.99	72.53
BBO-VNS-B&B	1730	0,1,0,1,0,1,1,1,0	81.76	72.95	73.49
BBO-B&B-VNS	2460	1,1,0,1,1,0,0,0,1	81.51	71.99	72.53

4.1.2 136-bus

The 136-bus is an arrangement of four instances of the IEEE 34-bus, resulting in a four feeder configuration. The resulting demand across all network phases amounts to 7076 kW of active power and to 4176 kVAr of reactive power. The baseline solution for this network also considers DER injections, otherwise the network constraints are not satisfied. As described

previously, three DERs are added at buses 890, 848 and 822, for each feeder. Four tie switches, as seen in Figure 4.3 as dashed red lines, enables connection between pairs of feeders, and Table 4.5 summarizes the switches positions in the network. To ensure radiality and connectivity, three sectionalizing switches are placed on each feeder and are illustrated by solid green lines in Figure 4.3. The DER positions and power limits for each feeder are identical to the IEEE 34-bus, as is described in Table 4.2. As for the slack source generation power limits, they are increased to accommodate the larger loading as seen in Table 4.6. There are a total of 12 DERs, 12 sectionalizing switches, and four tie switches, which results in 40 decisions variables, of which 24 are continuous, and 16 are binary. This is a much larger problem instance when compared to the IEEE 34-bus and, therefore, is more challenging to solve. Further details on the model modifications and constraint bounds can be found in Appendix C.2. Lastly, the evaluation budget for every method is detailed in Table 4.7.

Table 4.5 Position of the switches in Figure 4.3 (*FX refers to Feeder X*).

Line Data	**Sectionalizing switch**				**Tie switch**			
	SW_1	SW_4	SW_{10}	SW_{11}	SW_{12}	SW_{13}	SW_{14}	SW_{15}
From Bus	824	834	858	816	854 (F1)	840 (F1)	854 (F3)	840 (F3)
To Bus	6	12	11	4	824 (F2)	840 (F2)	824 (F4)	840 (F4)

Table 4.6 Position and specifications of the slack source in Figure 4.3.

Data	**Slack source**
Bus	800 (F1, F2, F3, F4)
$P_{\max}$ (kW)	6600
$P_{\min}$ (kW)	0
$Q_{\max}$ (kVAr)	1100
$Q_{\min}$ (kVAr)	−760
$S_{\max}$ (kVA)	6691.039

Table 4.7 Budget of blackbox evaluations allowed for each method with the 136-bus.

BBO	**BBO-VNS**			**BBO-B&B**			**BBO-VNS-B&B**					**BBO-B&B-VNS**				
	BBO	VNS		BBO	B&B		BBO	VNS		B&B		BBO	B&B		VNS	
		N_{local}	N_{global}		N_{local}	$N_{\text{local\_next}}$		N_{local}	N_{global}	N_{local}	$N_{\text{local\_next}}$		N_{local}	$N_{\text{local\_next}}$	N_{local}	N_{global}
1000	100	75	2000	100	75	60	100	75	500	75	60	100	75	60	75	450

Figure 4.4 provides the data profiles for the 136-bus system. On average, across the different load profiles, both BBO-B&B-VNS and BBO-VNS-B&B are more consistent than BBO-VNS, achieving overall lower losses with a sufficient evaluation budget. In particular, the VNS step in BBO-VNS-B&B provides an efficient warm start, allowing it to outperform quickly the other methods. As seen on the data profiles, a fewer number of problems are solved by

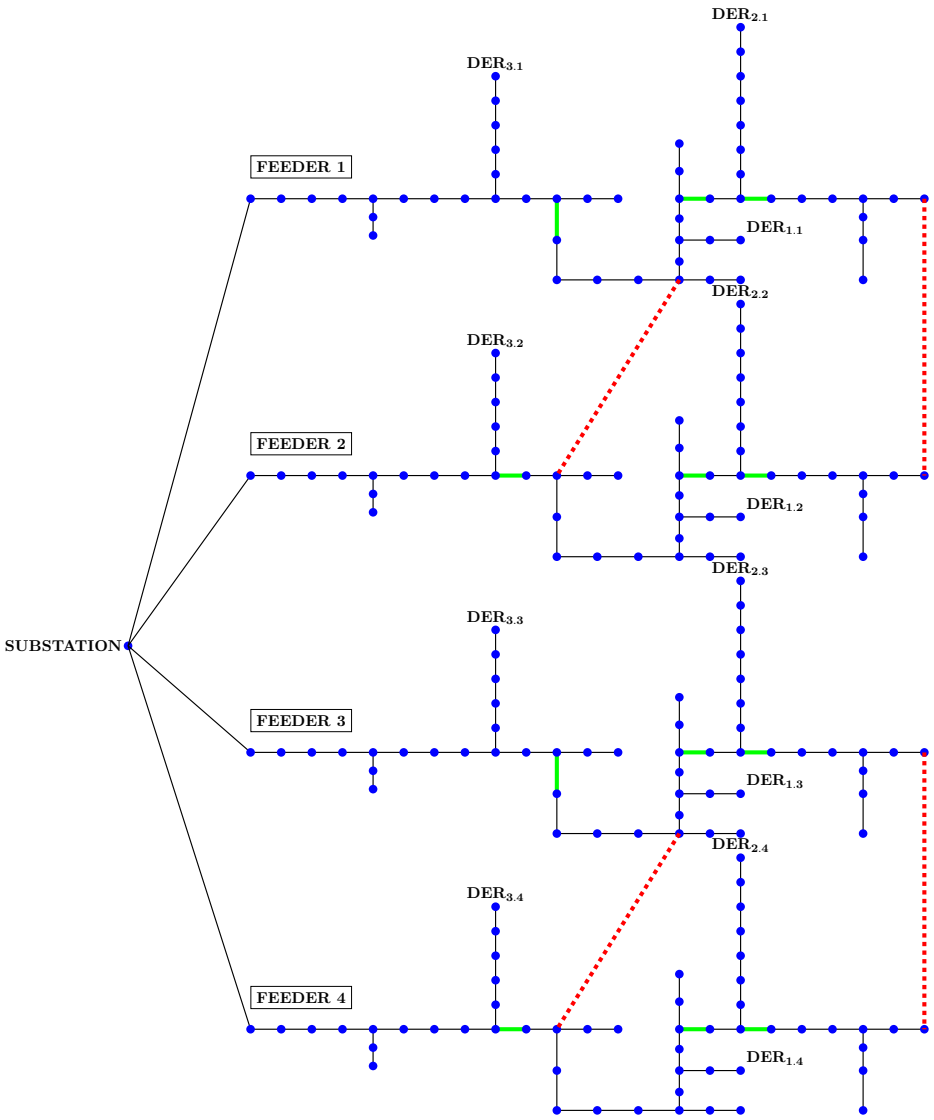

Figure 4.3 136-bus network *(solid green line: sectionalizing switch; dashed red line: tie switch).*

the methods, suggesting that the high dimension poses significant challenges. Specifically, for BBO-VNS, it is necessary to double the global evaluation budget used with the 34-bus to avoid under-performance compared to the other methods. This suggests that the reconfiguration problem is challenging and prone to dimensionality issues. Moreover, the more guided process of B&B appears to have an advantage over the random VNS process due to these difficulties. Similarly, it is also clearly shown that the baseline method BBO performs efficiently under a small evaluation budget compared to the proposed methods, which contrasts with what is observed on the 34-bus. As seen from Table 4.12, the loss reduction compared to the baseline solution is slightly less than for the 34-bus but still

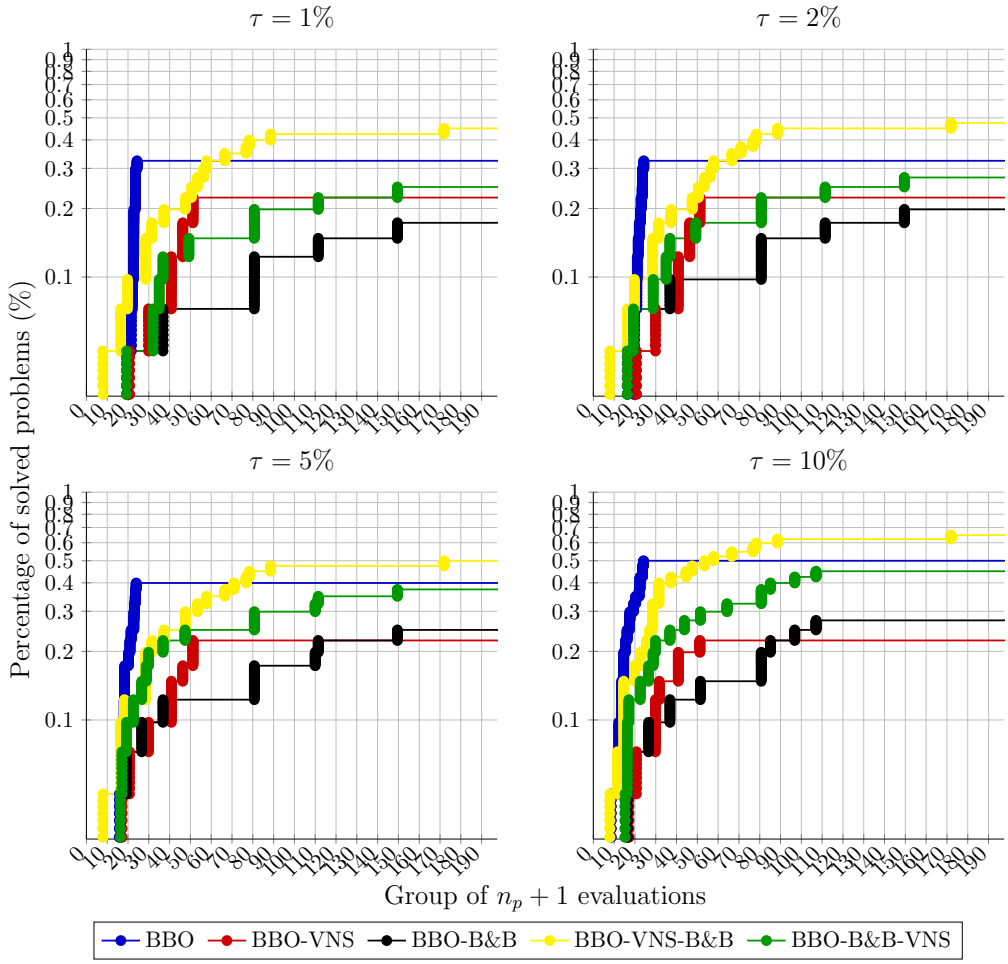

Figure 4.4 Results for the 136-bus network for tolerances τ of 1, 2, 5, and 10 %.

significant, ranging from 36.94% for BBO-B&B to 60.90% for BBO-VNS. Again, the solution for all problems across all algorithms typically differs from the original topology. The results in Table 4.13 illustrate that DERs contribute, on average, to 79.89% of the total generation, in comparison to the baseline solution that is 60.93%. Table 4.14 presents the DER penetration level for the the total demand of 7076 kW on this network. It shows that DERs contribute to supply, on average, 80.75% of the total demand, in comparison to the baseline solution that is at 62.18%. As with the 34-bus, no optimization is involved in the baseline solution, and results in Tables 4.12 to 4.14 are limited to the subset of the 40 problems that use the base load profile. Similar to the 34-bus example, the choice of resolution method for this benchmark depends on how the system operator prioritize the balance between computational time and the desire to minimize power loss consistently, regardless of the loading profile. The former would correspond to BBO-VNS, whereas the latter to BBO-VNS-B&B.

As well for this network, the brute force approach is applied to compare the results and

demonstrate the relevance of the methods. The same steps and evaluation budget as with the 34-bus are used. Table 4.8 compares the brute force with the best result obtained with each method for the base load profile, including the topology and the budget of evaluations. The brute force secures the larger power loss reduction among all, but a topology different than all methods. Also, it is done after a considerably large number of 217340 evaluations, which is again entirely not practical nor scalable. In contrast, despite a significantly smaller evaluation budget, the power loss reduction for both BBO-VNS and BBO-VNS-B&B is quite similar to the one obtained with the brute force approach.

Table 4.8 Best solution obtained for each method on the 136-bus compared to the baseline solution, with initially 0.1459 MW of power losses, and the brute force technique.

Method	**Number of evaluations**	**Topology**	**Loss reduction (%)**	**DER contribution** (%)	**DER penetration level (%)**
Base solution	0	1,1,1,1,1,1,1,1,1,1,1,0,0,0,0	0	60.93	62.18
Brute force	217340	0,1,1,1,1,1,1,1,1,1,1,1,0,0,0	75.55	83.72	84.14
BBO	1000	0,1,1,1,1,1,1,1,1,1,0,1,0,1,0	65.30	85.60	86.21
BBO-VNS	1100	1,1,1,1,1,0,0,1,1,1,1,1,1,0,0,1	74.70	83.91	84.35
BBO-B&B	2300	0,1,0,1,1,1,1,1,1,1,0,1,1,1,0	66.18	81.96	82.53
BBO-VNS-B&B	1730	1,1,1,1,1,0,1,1,1,1,1,0,1,0,0	74.49	82.80	83.24
BBO-B&B-VNS	2460	0,1,0,1,1,1,0,1,0,1,1,1,1,1,1	66.18	81.96	82.53

4.1.3 IEEE 8500-bus

The IEEE 8500-bus [62] power network is a complex, unbalanced distribution network with one feeder powered by a 115 kV high-voltage substation. It includes a primary 12.47 kV medium-voltage three-phase network and one- or two-phase laterals, which are connected to secondary 208 V low-voltage unbalanced loads through distribution transformers. The total demand across all network phases amounts to 10.77 MW of active power and to 2.70 MVAr of reactive power. Five DERs, detailed in Table 4.10, are added the network, with their positions partially inspired by [63], [64]. These are either regions at risk of under-voltage, as seen in [65], regions far from the substation or at strategic line splits. For network reconfiguration, the three tie switches are based on [42], the DER positions, and the network structure, and the five sectionalizing are placed to ensure radiality and connectivity. As seen in Figure 4.5, there are a total of five DERs, five sectionalizing switches, and three tie switches, which positions in the network are summarized in Table 4.9. This adds up to 18 decisions variables for the mixed-integer optimization problem, where 10 are continuous, and 8 are binary. This problem is larger than the IEEE 34-bus test feeder but smaller than the 136-bus in terms of optimization variables. However, the 8500-bus system effectively captures key aspects of a DN, i.e., realistic size, varying voltage levels, unbalanced loads, and different types of phase connections. For this reason, it is crucial to assess the practical performance of the methods. Further details on the model modifications and constraint bounds can be found in

Appendix C.3.

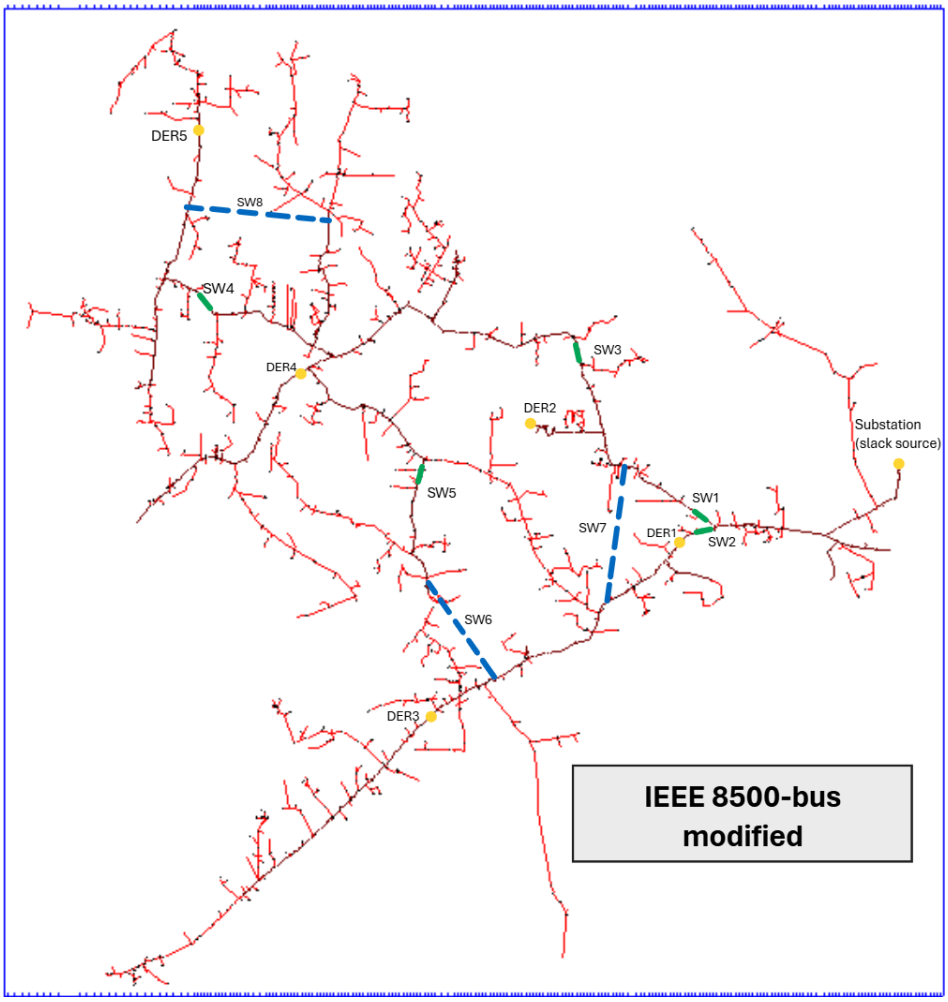

Figure 4.5 IEEE 8500-bus network *(solid green line: sectionalizing switch; dashed blue line: tie switch; yellow dot: DERs and substation).*

Table 4.9 Position of the switches in Figure 4.5.

Network component		**From Bus**	**To Bus**
Sectionalizing switch	SW_1	D5861005-2_INT	Q1301
	SW_2	D5799561-2_INT	E193509
	SW_3	D5587291-3_INT	Q14734
	SW_4	D5502543-2_INT	Q14413
	SW_5	D5956499-2_INT	Q14411
Tie switch	SW_6	M1069311	M1089131
	SW_7	L2767341	L2955081
	SW_8	R18241	M1026954

Table 4.10 Position and specifications of the DERs in Figure 4.5.

Data	**Slack source (SourceBus)**	**DER$_1$**	**DER$_2$**	**DER$_3$**	**DER$_4$**	**DER$_5$**
Bus	HVMV_Sub_connector	L2692655	M1108395	L3010556	M1047507	L2673313
$P_{\max}$ (MW)	14	3	3	3	3	3
$P_{\min}$ (MW)	0	0	0	0	0	0
$Q_{\max}$ (MVar)	4	1.5	1.5	1.5	1.5	1.5
$Q_{\min}$ (MVar)	-4	-1.5	-1.5	-1.5	-1.5	-1.5
$S_{\max}$ (MVA)	14.560	3.354	3.354	3.354	3.354	3.354

Table 4.12 shows results using the same parameters as the 136-bus example, as defined in Table 4.7, and applying the methods once for a single initial point under the base load profile. The baseline solution without DERs and reconfiguration is unfeasible due to under-voltages at some buses and line current limit violations. Given the network's complexity, finding arbitrary DER injections that renders the network feasible is difficult. Therefore, the DER injections are the first ones obtained with BBO, for the fixed original topology, that satisfy the network constraints. Thus, unlike the 34-bus and the 136-bus examples, the baseline solution here is obtained with BBO for a small evaluation budget. Additionally, voltage limits are relaxed to $\overline{v} = 1.1$ p.u and $\underline{v} = 0.9$ p.u. Tables 4.12 and 4.13 show that BBO-VNS achieves the largest power loss reduction, 32.52%, as well as, the largest DER contribution to the total generation, 82.19%. The second best method is BBO-VNS-B&B, with respectively 29.85% of power loss reduction and 87.44% of DER contribution to the total generation. This is compared to the baseline solution which consists in 59.67% of DER contribution to the total generation. Also, these two methods, combined with BBO-B&B-VNS, are the only ones that produced a different topology from the initial one. Additionally, Table 4.14 shows that DERs across all methods contribute to supply, on average, 78.52% of the total demand, 10.7 MW for the 8500-bus, in comparison to the baseline solution that is at 63.14%. It is noted that the VNS process may return different outcomes, as observed, for example, when comparing the BBO-VNS-B&B to the BBO-VNS, where the latter significantly underperformed the former despite using a VNS process at the same stage. This highlights the stochastic nature of the VNS step and its potential variability in results.

Finally, for this network as well, the brute force approach is utilized to compare the results and to demonstrate the relevance of the proposed methods. The same steps and evaluation budget as with the 34-bus and 136-bus are used. Table 4.11 compares the brute force with the best result obtained with each method for the base load profile, including the topology and the budget of evaluations. The brute force secures the largest power loss reduction, and the same topology as BBO-VNS. However, it is achieved after 7320 evaluations, almost three times more than the most computationally demanding among the proposed methods, which

here is BBO-VNS-B&B. This makes it again neither practical nor scalable.

Table 4.11 Solution obtained for each method on the IEEE 8500-bus compared to the baseline solution, with initially 0.6249 MW of power losses, and the brute force technique.

Method	**Number of evaluations**	**Topology**	**Loss reduction (%)**	**DER contribution** (%)	**DER penetration level (%)**
Base solution	0	1,1,1,1,1,0,0,0	0	59.67	63.13
Brute force	7320	1,1,0,0,1,1,0,1	33.65	92.32	95.87
BBO	1000	1,0,1,0,1,0,1,1	10.78	69.60	73.20
BBO-VNS	2100	1,0,0,0,1,1,1,1	32.52	82.19	85.41
BBO-B&B	370	1,0,1,0,1,0,1,1	7.34	64.32	67.78
BBO-VNS-B&B	2790	1,0,0,0,1,1,1,1	29.85	87.44	91.00
BBO-B&B-VNS	820	1,1,1,0,1,0,0,1	11.71	71.54	75.21

Table 4.12 Summary of the mean power loss reduction observed, along with results for the 8500-bus, both for the base load profile.

System	**Baseline solution (MW)**	**Mean power loss reduction (standard deviation) [%]**				
		BBO	BBO-VNS	BBO-B&B	BBO-VNS-B&B	BBO-B&B-VNS
34-bus	0.0714	78.74 (2.29)	80.14 (0.97)	78.06 (5.15)	78.83 (2.20)	79.96 (2.02)
136-bus	0.1459	43.99 (15.01)	60.90 (13.92)	36.94 (23.84)	48.08 (15.38)	47.86 (18.20)
8500-bus	0.6249	10.78	32.52	7.34	29.85	11.71

Table 4.13 Summary of the DER generation observed, along with results for the 8500-bus, both for the base load profile.

System	**Baseline solution (%)**	**DER contribution to the total generation (standard deviation) [%]**				
		BBO	BBO-VNS	BBO-B&B	BBO-VNS-B&B	BBO-B&B-VNS
34-bus	38.03	73.59 (0.90)	72.07 (1.28)	71.67 (2.99)	71.44 (1.34)	72.54 (2.06)
136-bus	60.93	80.33 (3.38)	81.55 (3.51)	77.81 (4.62)	79.50 (3.32)	80.24 (4.42)
8500-bus	59.67	69.60	82.19	64.32	87.44	71.54

Table 4.14 Summary of the DER penetration level observed, along with results for the 8500-bus, both for the base load profile.

System	**Baseline solution (%)**	**DER penetration level (standard deviation) [%]**				
		BBO	BBO-VNS	BBO-B&B	BBO-VNS-B&B	BBO-B&B-VNS
34-bus	39.57	74.22 (0.92)	72.65 (1.27)	72.30 (2.95)	72.05 (1.32)	73.12 (2.11)
136-bus	62.18	81.26 (3.21)	82.20 (3.36)	78.82 (4.36)	80.35 (3.17)	81.11 (4.26)
8500-bus	63.14	73.20	85.41	67.78	91.00	75.21

CHAPTER 5 CONCLUSION

This last chapter concludes the Master's Thesis by presenting a summary of the contributions, the limitations of the developed methods and the future and ongoing directions of research.

5.1 Summary

To efficiently integrate DERs in DNs, a reconfiguration method is essential to mitigate potential impacts, such as bidirectional power flows, increased phase imbalances, abnormal voltages, and power losses. The proposed resolution methods are dedicated to DNR and DER integration into DNs. They combine BBO, leveraging a high-accuracy load-flow solver that ensures model feasibility and thus enhances solution feasibility, with combinatorial optimization-inspired techniques to improve efficiency. They rely either on heuristics or on approximations. While they do not guarantee a global optimum, they instead tend to provide feasible solutions hopefully close to a local optimum. The results highlight how DERs influence the network structure and illustrate the benefits of combining them with DNR to reduce power losses and enhance constraints feasibility, namely, a voltage magnitude profile satisfying both upper and lower operational limits. This is particularly a challenge with conventional optimization techniques based on approximations and relaxations.

In all test cases, the average power loss reduction compared to the baseline solution is more than 36.94% for the 136-bus system, 78.06% for the 34-bus system, and 7.34% for the IEEE 8500-bus case. The highest loss reductions for the IEEE 8500-bus are achieved when the methods generate a topology different from the initial one, further demonstrating the efficiency of the proposed methods for DNR with DER integration. The DER contribution to the total generation is important, with a minimum of 64.32% and a maximum of 87.44%, across all test systems. From the demand perspective, DERs generally have a high penetration level, over 77% across all test systems. Both of these metrics illustrate the DER impact on the DN in terms of local production and constraints mitigation, which is even more noticeable given the evident correlation between power loss reduction and DER integration within the network. As seen in the results, all methods suffered a drop in performance when tested on the 136-bus, compared to with the 34-bus. This suggests that the scale of the optimization problem is the main challenge impacting performance, with the 136-bus involving 40 variables compared to the 34-bus with 15 variables. Specifically, the combinatorial problem complexity appears to be the biggest challenge, as hinted by the significant performance drop suffered by the BBO-VNS on the 136-bus. In contrasts, methods incorporating

the more structured combinatorial optimization step of B&B, such as BBO-VNS-B&B and BBO-B&B-VNS, show better scalability. Also, the IEEE 8500-bus achieved less loss reduction than the other networks compared to its baseline solution, but similar DER contribution to total generation and total demand, even if it is only a problem with 18 variables. The assumption is that in this specific case, the model offers a higher level of realism across all aspects, including network structure, components, and phase connections, posing a greater challenge than the one solely associated with the optimization problem dimensionality.

To summarize, the results show that analysing the impacts of both the DNR and DER integration problems together, rather than as separate problems as often done in the DNR literature, is most beneficial. Indeed, this leads to a greater active power loss reduction and a better understanding of the components interaction in ADNs. Additionally, the obtained results using a mathematical optimization approach for the IEEE 34-bus, namely MISOCP, emphasize the efficiency of the blackbox/simulation approach in terms of feasibility and reliability of the solution. In fact, when applied to the network model in the load-flow simulator, the MISOCP solution showed a significantly smaller power loss reduction of 53.38% compared to the results obtained with the proposed methods. This shows the importance of a highly accurate network model, as employed in the proposed methods due to the BBO steps. Lastly, the brute force approach is used to compare the results and demonstrate the relevance of the methods. It is employed as a global optimization technique. It is theoretically capable of achieving the global optimal solution if BBO is given an infinite evaluation budget for each topology, which is not the case in practice. This approach provides the best result among all methods, and may also provide insight into the quality of the methods' solution. However, as demonstrated by the large evaluation budget required to perform the brute force search, even with a limited number of evaluations it remains computationally intractable as a stand-alone method.

The results highlight two choice of methods for practical deployments. If computational time is the main concern, BBO-VNS is the best option. If greater consistency in performance and the reduction of power losses are desired, BBO-B&B-VNS or BBO-VNS-B&B are preferred, with BBO-VNS-B&B proving more efficient for higher-dimensional problems, as demonstrated in the 136-bus system case. Presently, DNR is typically applied in response to network perturbations, such as a line faults, or based on pre-programmed scenarios. In the context of DER integration into ADNs, it can be considered as an active strategy to mitigate and improve network constraints during nominal operation.

5.2 Limitations

The limitations of the approach may be divided into two categories: those due to design decisions, and those revealed through the analysis of the results.

VNS is a meta-heuristic that typically lacks any convergence properties, and the implemented version of B&B is an approximation of the original algorithm, losing its ability to ensure convergence to both global and even local optimum. Furthermore, the evaluation budget for BBO in all proposed methods is limited. Theoretically, supposing the problem is made of Lipschitz functions and the bounds are tight, an infinite budget, though impractical, would allow `NOMAD` to reach full convergence and guarantee a locally optimal solution in the BBO step alone. However, while the combinatorial optimization-inspired algorithms allow to solve the problem more efficiently, they would still lack a formal guarantee of convergence. This leads to limitations in terms of optimality in the proposed approaches, while their strength lies in feasibility, particularly regarding practical implementation which is the primary concern in this work. Consequently, investigating theoretical convergence and analysing the methods' behaviour in terms of feasibility when provided with a heavily infeasible initial point should be priorities for future work to establish theoretical guarantees.

Next, the focus is placed on the reconfiguration problem, intentionally disregarding considerations of the stochastic nature of load and DER generation. This is particularly important in DNs as loading fluctuates much during a day, between days, and throughout the year. Instead, they are assumed to remain constant throughout the process, while DERs are modelled as decision variables based simply on active and reactive power values. Finally, the network is considered to be operated at all times as radial and fully connected, as it is often done in practice. DERs are currently regarded as a complement to transmission grid power generation, and as a tool for mitigating network constraints when combined with DNR. However, they are not yet seen as a mean of enabling islanding or independent micro-grids separate from the original network, which would enhance overall network resilience. Additionally, in this implementation, the BBO solver, `NOMAD`, is used "out-of-the-box", as a simulation tool with basic optimization parameters. In other words, the solver is not employed to its full strength, and no blackbox optimization theory in particular is developed. Therefore, the proposed methods are limited by the solver capabilities. They could be further improved by integrating a methodology specific to the blackbox optimization itself, e.g., tailored for spanning tree structures.

As seen from the results and the discussion, one of the biggest challenges is the scale of the optimization problem. In parallel, the scale of the network itself may also be linked

to the complexity of the problem, as larger networks typically involve more switches and DERs. In this Master's Thesis, the implementation of the 8500-bus is the second largest problem in terms of decision variables, after the 136-bus. As observed, the challenges of the 8500-bus network are due primarily to the simulation time during load-flow computations and the network's inherent complexity, rather than introducing larger challenges in terms of optimization. On the other hand, the impacts of higher-dimensional optimization problem, i.e., with a large number of decision variables, are evident when comparing the results of the 34-bus and the 136-bus systems. In fact, the latter shows lower performance across all methods. Specifically, VNS suffered the most significant performance drop, being outperformed by methods using B&B in the 136-bus results. This suggests that higher dimensionality, specifically in terms of the optimization problem scale rather than the scale of the network, presents a significant challenge that limits the methods and emphasize the need for improvements. Moreover, this issue is particularly pronounced in the combinatorial problem highlighted in this case. Closely linked to this, probably a direct consequence of it, is the computational budget and time required for any of the methods. It takes between an hour or more, depending on the method used and the tested network, which might become impractical when incorporating more realistic aspects, such as stochastic parameters.

5.3 Future research

The main objective of future research opportunities is to explore techniques for scaling the algorithms to larger problems, i.e., large-scale DNs with numerous switches and DERs. This would also enable to investigate means to integrate load and DER uncertainty within the BBO formulation, as in scenario-based stochastic programming. Indeed, it has been illustrated by the numerical results that large scale optimization problems are much challenging to solve, as seen with the 136-bus, compared to the IEEE 34-bus and the IEEE 8500-bus case studies. These scalability issues were the main goal and subject of a recent research external stay at the School of Mathematics, University of Edinburgh (United Kingdom), with Pr. Miguel F. Anjos. Current work focuses on developing new methods that consider the feasible binary space as whole topologies, instead as of individual switches, hoping to reduce the computational burden and increase the optimization efficiency. The feasible set is thus consisted of a list of feasible topologies which reduce a lot the search space. Preliminary results show a promising increase in solving efficiency and power loss reduction. However, as computation of the list may not be tractable for larger-scale problems, ongoing work aims at exploring ways to navigate the binary search space without generating the list explicitly. Distinct from

this Master's Thesis, current projects at GERAD[1] focusing either on the scalability issue or on the treatment of discrete variables may also benefit future research. On top of that, a more extensive case study on the IEEE 8500-bus is planned to better assess the methods' performance on such a complex network, by incorporating, for example, more switching possibilities and DER integration. Further research opportunities also include investigating theoretical convergence and feasibility guarantee, exploring blackbox optimization theory to maximize its potential, and even considering the possibilities of islanding in the network using grid-forming technologies.

[1]Group for Research in Decision Analysis (GERAD) [66] to which this Master's Thesis is affiliated.

REFERENCES

[1] Fonds de recherche du Québec, https://doi.org/10.69777/345550, May 15, 2024–May 14, 2025.

[2] Y. Liu, J. Li, and L. Wu, "Coordinated optimal network reconfiguration and voltage regulator/DER control foruUnbalanced distribution systems", *IEEE Transactions on Smart Grid*, vol. 10, no. 3, pp. 2912–2922, May 2019.

[3] M. Dilek, R. Broadwater, J. Thompson, and R. Seqiun, "Simultaneous phase balancing at substations and switches with time-varying load patterns", *IEEE Transactions on Power Systems*, vol. 16, no. 4, pp. 922–928, Nov. 2001.

[4] H. Damgacioglu and N. Celik, "A two-stage decomposition method for integrated optimization of islanded AC grid operation scheduling and network reconfiguration", *International Journal of Electrical Power & Energy Systems*, vol. 136, p. 107 647, 2022.

[5] M. E. Baran and F. F. Wu, "Network reconfiguration in distribution systems for loss reduction and load balancing", *IEEE Power Engineering Review*, vol. 9, no. 4, pp. 101–102, Apr. 1989.

[6] S. Civanlar, J. Grainger, H. Yin, and S. Lee, "Distribution feeder reconfiguration for loss reduction", *IEEE Transactions on Power Delivery*, vol. 3, no. 3, pp. 1217–1223, Jul. 1988.

[7] A. A. Anderson, S. V. Vadari, J. L. Barr, *et al.*, "Introducing the 9500 node distribution test system to support advanced power applications", Richland, WA: Pacific Northwest National Laboratory, Tech. Rep., 2022.

[8] J. Caballero-Peña, C. Cadena-Zarate, A. Parrado-Duque, and G. Osma-Pinto, "Distributed energy resources on distribution networks: a systematic review of modelling, simulation, metrics, and impacts", *International Journal of Electrical Power & Energy Systems*, vol. 138, p. 107 900, 2022.

[9] Z. Dong, Z. Yang, J. Peng, and P. Huo, "Study on mesh adaptive direct search algorithm for distribution network reconfiguration with distribution generators", en, in *2019 IEEE 3rd International Electrical and Energy Conference (CIEEC)*, Beijing, China: IEEE, Sep. 2019, pp. 1281–1286.

[10] Q. Salem, R. Aljarrah, M. Karimi, and A. Al-Quraan, "Grid-forming inverter control for power sharing in microgrids based on P/f and Q/V droop characteristics", en, *Sustainability*, vol. 15, no. 15, p. 11 712, Jan. 2023.

[11] C. Audet and J. Dennis, Jr., "Mesh adaptive direct search algorithms for constrained optimization", *SIAM Journal on Optimization*, vol. 17, no. 1, pp. 188–217, 2006. DOI: 10.1137/040603371.

[12] A. Merlin and H. Back, "Search for a minimal-loss operating spanning tree configuration in an urban power distribution system", *Proc. 5th Power Syst. Comput. Conf.*, pp. 1–18, 1975.

[13] M. R. Behbahani, A. Jalilian, A. Bahmanyar, and D. Ernst, "Comprehensive review on static and dynamic distribution network reconfiguration methodologies", *IEEE Access*, vol. 12, pp. 9510–9525, 2024.

[14] M. Mahdavi, H. H. Alhelou, N. D. Hatziargyriou, and F. Jurado, "Reconfiguration of electric power distribution systems: comprehensive review and classification", en, *IEEE Access*, vol. 9, pp. 118 502–118 527, 2021.

[15] M. Mahdavi, H. H. Alhelou, A. Bagheri, S. Z. Djokic, and R. A. V. Ramos, "A comprehensive review of metaheuristic methods for the reconfiguration of electric power distribution systems and comparison with a novel approach based on efficient genetic algorithm", *IEEE Access*, pp. 122 872–122 906, 2021.

[16] H. Ahmadi and J. R. Martí, "Minimum-loss network reconfiguration: A minimum spanning tree problem", en, *Sustainable Energy, Grids and Networks*, vol. 1, pp. 1–9, Mar. 2015.

[17] Y. Bansal, R. Sodhi, and S. Chakrabarti, "A novel two-stage partitioning based reconfiguration method for active distribution networks", en, *IEEE Transactions on Power Delivery*, vol. 38, no. 6, pp. 4004–4016, 2023.

[18] D. Shirmohammadi and H. Hong, "Reconfiguration of electric distribution networks for resistive line losses reduction", *IEEE Transactions on Power Delivery*, vol. 4, no. 2, pp. 1492–1498, Apr. 1989.

[19] S. F. Santos, M. Gough, D. Z. Fitiwi, J. Pogeira, M. Shafie-khah, and J. P. S. Catalão, "Dynamic distribution system reconfiguration considering distributed renewable energy sources and energy storage systems", *IEEE Systems Journal*, vol. 16, no. 3, pp. 3723–3733, Sep. 2022.

[20] H. Hijazi, C. Coffrin, and P. V. Hentenryck, "Convex quadratic relaxations for mixed-integer nonlinear programs in power systems", en, *Mathematical Programming Computation*, vol. 9, no. 3, pp. 321–367, Sep. 2017.

[21] J. A. Taylor and F. S. Hover, "Convex models of distribution system reconfiguration", *IEEE Transactions on Power Systems*, vol. 27, no. 3, pp. 1407–1413, Aug. 2012.

[22] D. K. Molzahn, F. Dörfler, H. Sandberg, *et al.*, "A Survey of Distributed Optimization and Control Algorithms for Electric Power Systems", *IEEE Transactions on Smart Grid*, vol. 8, no. 6, pp. 2941–2962, Nov. 2017.

[23] H. Gao, W. Ma, Y. Xiang, *et al.*, "Multi-objective dynamic reconfiguration for urban distribution network considering multi-level switching modes", *Journal of Modern Power Systems and Clean Energy*, vol. 10, no. 5, pp. 1241–1255, Sep. 2022.

[24] IBM Corporation, *IBM ILOG CPLEX Optimization Studio*, `https://www.ibm.com/products/ilog-cplex-optimization-studio`, 2024.

[25] S. Bahrami, Y. C. Chen, and V. W. S. Wong, "Dynamic distribution network reconfiguration with generation and load uncertainty", *IEEE Transactions on Smart Grid*, vol. 15, no. 6, pp. 5472–5484, Nov. 2024.

[26] J. Authier, R. Haider, A. Annaswamy, and F. Dörfler, "Physics-informed graph neural network for dynamic reconfiguration of power systems", *Electric Power Systems Research*, vol. 235, p. 110 817, 2024.

[27] J. Qin and N. Yu, "Reconfigure distribution network with physics-informed graph neural network", in *2023 IEEE PES Innovative Smart Grid Technologies Europe (ISGT EUROPE)*, 2023, pp. 1–6.

[28] R. A. Jacob, S. Paul, W. Li, S. Chowdhury, Y. R. Gel, and J. Zhang, "Reconfiguring unbalanced distribution networks using reinforcement learning over graphs", in *2022 IEEE Texas Power and Energy Conference (TPEC)*, Feb. 2022, pp. 1–6.

[29] J. Pallage and A. Lesage-Landry, *Wasserstein distributionally robust shallow convex neural networks*, 2025. arXiv: `2407.16800 [cs.LG]`. [Online]. Available: `https://arxiv.org/abs/2407.16800`.

[30] H. Salazar, R. Gallego, and R. Romero, "Artificial neural networks and clustering techniques applied in the reconfiguration of distribution systems", *IEEE Transactions on Power Delivery*, vol. 21, no. 3, pp. 1735–1742, Jul. 2006.

[31] A. Lesage-Landry and J. Pallage, *Online dynamic submodular optimization*, 2024. arXiv: `2306.10835 [math.OC]`. [Online]. Available: `https://arxiv.org/abs/2306.10835`.

[32] C. Audet and W. Hare, *Derivative-Free and Blackbox Optimization* (Springer Series in Operations Research and Financial Engineering). Cham, Switzerland: Springer, 2017.

[33] A. Wędzik, T. Siewierski, and M. Szypowski, "The use of black-box optimization method for determination of the bus connection capacity in electric power grid", en, *Energies*, vol. 13, no. 1, p. 41, Jan. 2020.

[34] L. Tang, F. Yang, and X. Feng, "A novel method for distribution system feeder reconfiguration using black-box optimization", in *2013 IEEE Power & Energy Society General Meeting*, Jul. 2013, pp. 1–5.

[35] C. Audet, S. Le Digabel, V. Rochon Montplaisir, and C. Tribes, "Algorithm 1027: NOMAD version 4: Nonlinear optimization with the MADS algorithm", *ACM Transactions on Mathematical Software*, vol. 48, no. 3, 35:1–35:22, 2022.

[36] Electric Power Research Institute (EPRI), *OpenDSS*, 2024. [Online]. Available: `https://www.epri.com/pages/sa/opendss`.

[37] C. G. Soldati, S. Le Digabel, and A. Lesage-Landry, "Blackbox optimization for loss minimization in power distribution networks using feeder reconfiguration", in *Proceedings of the CIGRE 2025 International Symposium*, Accepted, CIGRE, Palais des Congrès de Montréal, Canada, Sep. 29–Oct. 3, 2025.

[38] C. G. Soldati, *Blackbox optimization for loss minimization in power distribution networks using feeder reconfiguration*, Presented at *JOPT 2025: Journées de l'Optimisation* conference, HEC Montréal, Canada, May 12–14, 2025.

[39] C. G. Soldati, *Blackbox optimization for loss minimization in power distribution networks using feeder reconfiguration*, Presented at fORum: Discussion group and junior seminar for PhD students of Optimization and Operational Research (OOR), School of Mathematics, The University of Edinburgh, United Kingdom, Feb. 25, 2025.

[40] C. G. Soldati, *Méthode d'optimisation de boîte noire pour la minimisation des pertes en puissance des réseaux de distribution électrique par reconfiguration*, Presented at the conference *"Repenser la gestion énergétique via l'innovation et son implantation"*, organized by the Energy Modelling Hub and Volt-Age Concordia, Concordia University, Montréal, Canada, Nov. 12, 2024.

[41] J. A. Taylor, *Convex Optimization of Power Systems*. Cambridge University Press, 2015.

[42] R. R. Nejad and W. Sun, "Enhancing active distribution systems resilience by fully distributed self-healing strategy", *IEEE Transactions on Smart Grid*, vol. 13, no. 2, pp. 1023–1034, Mar. 2022.

[43] S. Alarie, C. Audet, A. Gheribi, M. Kokkolaras, and S. Le Digabel, "Two decades of blackbox optimization applications", *EURO Journal on Computational Optimization*, vol. 9, p. 100 011, 2021.

[44] Eaton, *Distribution system analysis (CYMDIST)*, 2025. [Online]. Available: https://www.eaton.com/ca/en-gb/products/utility-grid-solutions/software-modules/distribution-system-analysis-package-CYMDIST.html.

[45] J. Mahseredjian, S. Dennetière, L. Dubé, B. Khodabakhchian, and L. Gérin-Lajoie, "On a new approach for the simulation of transients in power systems", *Electric Power Systems Research*, Selected Topics in Power System Transients - Part II, vol. 77, no. 11, pp. 1514–1520, Sep. 2007.

[46] Manitoba HVDC Research Centre, *PSCAD User's Guide v4.6*, Manitoba Hydro International Ltd., 2018. [Online]. Available: https://www.pscad.com/knowledge-base/article/160.

[47] The MathWorks, Inc., *MATLAB and Simulink*, The MathWorks, Inc., Natick, Massachusetts, United States, 2025. [Online]. Available: https://www.mathworks.com/help/?s_tid=hp_ff_l_doc.

[48] D. R. Morrison, S. H. Jacobson, J. J. Sauppe, and E. C. Sewell, "Branch-and-bound algorithms: A survey of recent advances in searching, branching, and pruning", *Discrete Optimization*, vol. 19, pp. 79–102, 2016.

[49] D. R. Morrison, J. J. Sauppe, W. Zhang, S. H. Jacobson, and E. C. Sewell, "Cyclic best first search: Using contours to guide branch-and-bound algorithms", en, *Naval Research Logistics (NRL)*, vol. 64, no. 1, pp. 64–82, Feb. 2017.

[50] C. A. Floudas and P. M. Pardalos, *Encyclopedia of optimization*, en, 2nd ed. New York: Springer, 2009.

[51] N. Mladenović and P. Hansen, "Variable neighborhood search", *Computers and Operations Research*, vol. 24, no. 11, pp. 1097–1100, 1997.

[52] J. Brimberg, S. Salhi, R. Todosijević, and D. Urošević, "Variable neighborhood search: The power of change and simplicity", *Computers & Operations Research*, vol. 155, p. 106 221, 2023.

[53] P. Hansen, N. Mladenović, R. Todosijević, and S. Hanafi, "Variable neighborhood search: basics and variants", en, *EURO Journal on Computational Optimization*, vol. 5, no. 3, pp. 423–454, Sep. 2017.

[54] C. Audet, S. Le Digabel, V. Rochon Montplaisir, and C. Tribes, *The NOMAD project*. [Online]. Available: https://www.gerad.ca/nomad/.

[55] EMTP, *EMTP*. [Online]. Available: https://emtp.com/products/emtp.

[56] EMTP, *MATLAB API*. [Online]. Available: https://emtp.com/products/modules/MATLAB-API.

[57] IEEE, *Resources – IEEE PES Test Feeder*, en-US, 1992. [Online]. Available: https://cmte.ieee.org/pes-testfeeders/resources/ (visited on 09/17/2023).

[58] P. Gangwar, S. N. Singh, and S. Chakrabarti, "Network reconfiguration for the DG-integrated unbalanced distribution system", en, *IET Generation, Transmission & Distribution*, vol. 13, no. 17, pp. 3896–3909, 2019.

[59] J. J. Moré and S. M. Wild, "Benchmarking derivative-free optimization algorithms", *SIAM Journal on Optimization*, vol. 20, no. 1, pp. 172–191, 2009.

[60] H. Hijazi and S. Thiébaux, "Optimal distribution systems reconfiguration for radial and meshed grids", en, *International Journal of Electrical Power & Energy Systems*, vol. 72, pp. 136–143, Nov. 2015.

[61] LORER, *ALLabMTL/OPF_tools*, Jan. 2024. [Online]. Available: https://github.com/LORER-MTL/OPF_Tools (visited on 04/24/2024).

[62] R. F. Arritt and R. C. Dugan, "The IEEE 8500-node test feeder", in *IEEE PES T&D 2010*, 2010, pp. 1–6.

[63] E. E. Pompodakis, G. C. Kryonidis, M. C. Alexiadis, and E. S. Karapidakis, "A three-phase sensitivity-based approach for smooth line-switching in islanded networks", *International Journal of Electrical Power & Energy Systems*, vol. 144, p. 108 515, Jan. 2023.

[64] A. Arif, S. Ma, Z. Wang, J. Wang, S. M. Ryan, and C. Chen, "Optimizing service restoration in distribution systems with uncertain repair time and demand", en, *IEEE Transactions on Power Systems*, vol. 33, no. 6, pp. 6828–6838, Nov. 2018.

[65] F. Li, I. Kocar, and A. Lesage-Landry, "A rapid method for impact analysis of grid-edge technologies on power distribution networks", *IEEE Transactions on Power Systems*, vol. 39, no. 1, pp. 1530–1542, Jan. 2024.

[66] GERAD, *GERAD: Group for Research in Decision Analysis*. [Online]. Available: https://www.gerad.ca/en/home.

[67] Southwire Company, "ACSR: Aluminum conductor. Steel reinforced. Bare.", Southwire, Tech. Rep., 2012. [Online]. Available: https://www.southwire.com/ca/en-ca/wire-cable/bare-aluminum-overhead-transmission-distribution/acsr/p/ALBARE6.

[68] A. Zhou, H. Zhai, M. Yang, and Y. Lin, "Three-phase unbalanced distribution network dynamic reconfiguration: a distributionally robust approach", en, *IEEE Transactions on Smart Grid*, vol. 13, no. 3, pp. 2063–2074, May 2022.

[69] American Wire Group - AAC, "Covered Line Wire AAC Aluminum Conductor", American Wire Group, Tech. Rep., 2025. [Online]. Available: https://www.buyawg.com/viewitems/al-covered-line-wire/covered-line-wire-aac-br-aluminum-conductor.

[70] American Wire Group - ACSR, "ACSR/AW Aluminum conductor steel reinforced", American Wire Group, Tech. Rep., 2025. [Online]. Available: https://www.buyawg.com/viewitems/bare-aluminum-acsr-aw/acsr-aw-aluminum-conductor-steel-reinforced.

[71] American Wire Group, "Item A1/0-01UD15UT100X, PowerGuard® 15kV 133% MV TR-XLPE Aluminum Collection System Cable XLPE Jacket UL MV-105/AEIC CS8-07", American Wire Group, Tech. Rep., 2025. [Online]. Available: https://www.buyawg.com/item/ion-system-cable-xlpe-jacket-ul-mv-105-aeic-cs8-07/-cable-xlpe-jacket-ul-mv-105-aeic-cs8-07-1/a1-0-01ud15ut100x.

APPENDIX A BLACKBOX

This appendix describes in details how the BBO optimization works, and how each files, code, or data interact with each other. The placeholder `XX` represents the number of buses in the network, such as in `wrapper34bus.m`, for the 34-bus system.

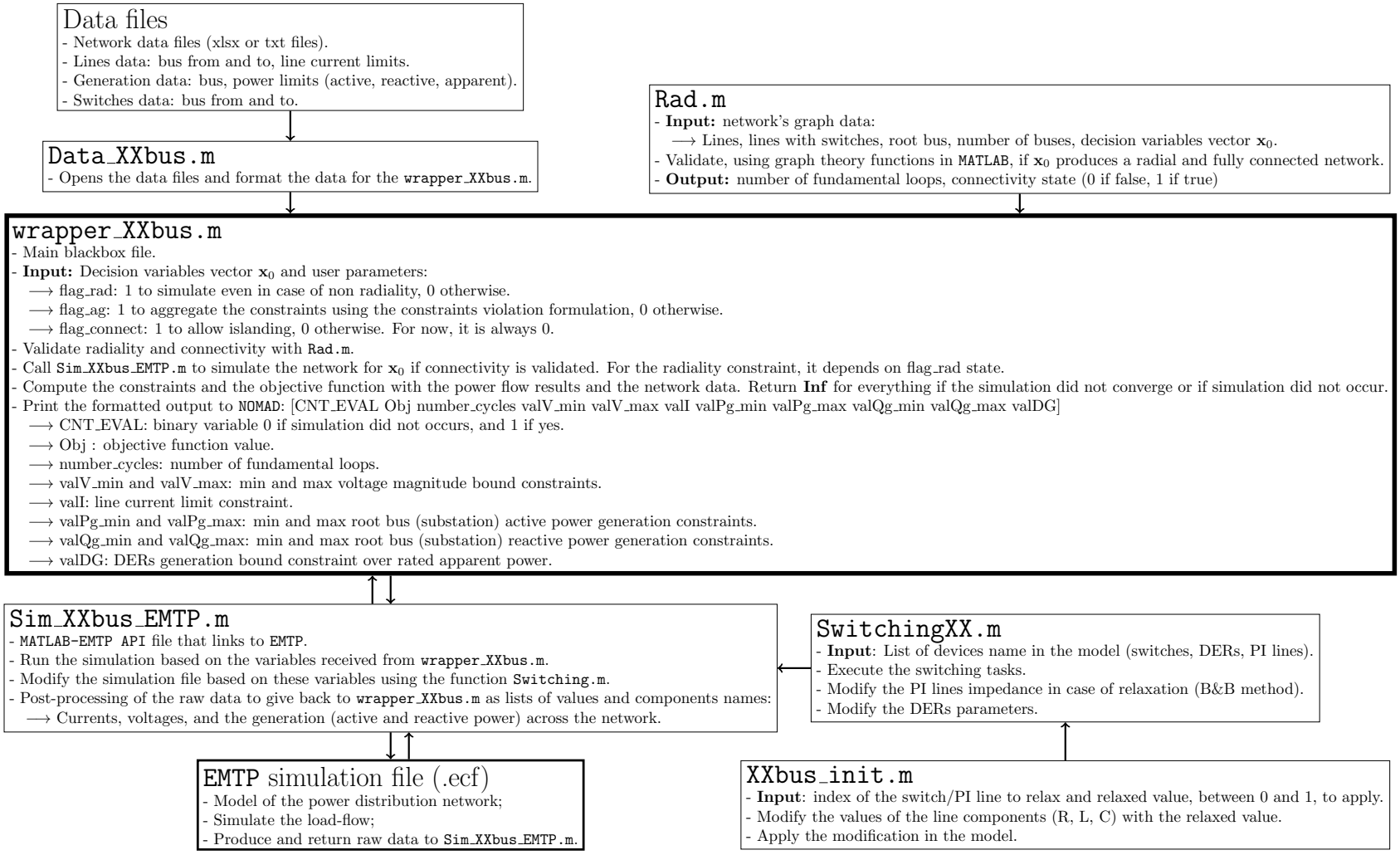

APPENDIX B IMPLEMENTATION DETAILS

This appendix provides supplementary details related to the combinatorial algorithm implementations.

In both algorithms, a BBO step is initiated using the `nomadOpt` function, which is the `NOMAD` API for `MATLAB`. A typical call to this function is:

$$[\mathbf{x}, \text{fval}, \sim, \text{runflag}, \sim] = \texttt{nomadOpt}(@\texttt{wrapper\_XXbus}, \mathbf{x}_0, \text{lb}, \text{ub}, \text{params}) \tag{B.1}$$

where `nomadOpt` execute the main blackbox file `wrapper_XXbus.m` for the initial decision variables $\mathbf{x}_0$, which is bounded by the upper bound vector **ub**, and the lower bound vector **lp**. The bounds consist in the min/max values for the continuous variables associated with the DERs, detailed in Table 4.2 and Table 4.10. Bounds for the binary variables are simply **1** for **ub**, and **0** for **lp**. The optimization parameters are defined by **params**, detailed in the sections below. The output of the function is the result of the BBO step, after the evaluation budget is reached for this node (B&B) or this iteration (VNS). It is consisted of **x**, the solution vector of the decision variables, **fval**, the value of the objective function for this solution, and **runflag**, a number indicating the status of the solution (feasible, unfeasible, or no solution).

B.1 Branch-and-Bound

Details for the Branch-and-Bound implementation are presented next.

B.1.1 `NOMAD` optimization parameters

`NOMAD` optimization parameters, named **params** in the implementation, are formatted as a `MATLAB` structure. For information on the parameters themselves, refer to `NOMAD` documentation [35]. The parameters given here as an example are for the benchmark of the 136-bus, but still apply for the other benchmarks as only the size of BB_INPUT_TYPE and FIXED_VARIABLE is specific to a test system.

- BB_OUTPUT_TYPE: (CNT_EVAL OBJ PB PB PB PB PB PB PB PB PB);
- BB_INPUT_TYPE: (R R R R R R R R R R R R R R R R R R R R R R R R R R R R R R R R R R R R R R R R R I I I);
- EVAL_OPPORTUNISTIC: true;

- DISPLAY_DEGREE: 0;
- DISPLAY_STATS: BBE (SOL) OBJ [BBO];
- FIXED_VARIABLE: (- flag_rad flag_ag flag_cont);
- MAX_BB_EVAL: N, budget of evaluations for a node;
- SEED: 0.

The user parameters, flag_rad, flag_ag, flag_cont, detailed in the workflow of Appendix A, are appended to the decision variables vector given as input to the blackbox optimization solver `NOMAD`. Next, the parameters BB_INPUT_TYPE and FIXED_VARIABLE are modified throughout the exploration of the tree, as more and more switches are fixed to a certain binary state. Moreover, as described in Algorithm 3, MAX_BB_EVAL for a node is also updated during the exploration of the tree.

B.1.2 Structure of a node of the tree

Here are listed all the fields of a node in the tree, formatted as a `MATLAB` structure.

- ID: unique identification of the node;
- solution: solution $\mathbf{x}$ for the subproblem decision variables;
- objective: value of the objective function for the solution;
- sol_init: initial $\mathbf{x}_0$ decision variables vector for the optimization, where all switch's values are binary;
- parent: ID of the direct parent node in the tree;
- fixed: index of the new fixed switch (branching variable) in this node;
- branching: index of the switch to branch on for this node;
- branching_vec: vector of indexes of all the previously branched on binary variables, so it is not repeated;
- params: `NOMAD` optimization parameters;
- status: status of the node (1: to prune from the tree, 2: leaf of the tree, full binary solution for the switches, 0: to branch on, not full binary solution);
- contour: contour (region) in which the node is currently stored in the queue $nodes_{\mathrm{q}}$.

B.1.3 Branching function `branch_CBFS.m`

Here is presented a pseudocode of the function responsible for creating a new branching from a parent node. It consists mainly in creating and initializing the two new nodes with binary branching, starting from a parent node, and updating the queue $nodes_{\mathrm{q}}$.

Algorithm 3 Function `branch_CBFS`

Input: $nodes_{\mathrm{q}}$, n_{DG}, number of DERs in the network, i, index of the parent node in the queue list, $contour_{\mathrm{c}}$, the current contour.
Output: $nodes_{\mathrm{q}}$.

$node_{\mathrm{c}} \leftarrow nodes_{\mathrm{q}}[1][i]$. ▷ Extract node to branch on.
Remove $nodes_{\mathrm{q}}[1][i]$ from $nodes_{\mathrm{q}}$.
contour $\leftarrow node_{\mathrm{c}}$.contour. ▷ Contour of the parent node.
branching $\leftarrow node_{\mathrm{c}}$.branching. ▷ Index of the switch to branch on.
Initialize newNode1 and newNode2. ▷ Two nodes produced by the binary branching.
newNode1.ID $\leftarrow 2 \times node_{\mathrm{c}}$.ID $+ 1$.
newNode2.ID $\leftarrow 2 \times node_{\mathrm{c}}$.ID $+ 2$.
newNode1.solution, newNode2.solution $\leftarrow \emptyset$.
newNode1.objective, newNode2.objective $\leftarrow \emptyset$.
newNode1.sol_init, newNode2.sol_init $\leftarrow node_{\mathrm{c}}$.sol_init.
newNode1.sol_init$[n_{\mathrm{DG}} \times 2 + \text{branching}] \leftarrow 0$. ▷ First node (left), switch fixed to 0.
newNode2.sol_init$[n_{\mathrm{DG}} \times 2 + \text{branching}] \leftarrow 1$. ▷ Second node (right), switch fixed to 1.
newNode1.parent, newNode2.parent $\leftarrow node_{\mathrm{c}}$.ID.
newNode1.fixed, newNode2.fixed $\leftarrow$ branching.
newNode1.branching, newNode2.branching $\leftarrow \emptyset$.
newNode1.branching_vec, newNode2.branching_vec $\leftarrow node_{\mathrm{c}}$.branching_vec.
newNode1.params, newNode2.params $\leftarrow node_{\mathrm{c}}$.params.
if $node_{\mathrm{c}}$.ID $==$ 1 **OR** $node_{\mathrm{c}}$.ID $==$ 2 **then** ▷ The budget for root and first tree level is bigger to quickstart the algorithm.
    Modify N, the budget for a node, to a smaller value $N_{\mathrm{local\_next}}$ for the rest of the tree.
end if
newNode1.status, newNode2.status $\leftarrow \emptyset$.
newNode1.contour, newNode2.contour $\leftarrow$ contour.
$contour_{\mathrm{index}} \leftarrow$ contour $- contour_{\mathrm{c}} + 1$.
$bound_{\mathrm{newcontour}} \leftarrow \min([nodes_{\mathrm{q}}[end].\text{contour}])$.
if contour $> bound_{\mathrm{newcontour}}$ **then** ▷ Unique contour set in $nodes_{\mathrm{q}}$ do not exist yet.
    Create new contour $nodes_{\mathrm{q}}[contour_{\mathrm{index}}]$ with newNode1, newNode2.
else if contour $== contour_{\mathrm{c}}$ **then** ▷ Contour is the current one.
    Insert newNode1, newNode2 at the top of $nodes_{\mathrm{q}}[contour_{\mathrm{index}}]$.
else if contour $> contour_{\mathrm{c}}$ **then** ▷ Contour is not the current one.
    Append newNode1, newNode2 at the end of $nodes_{\mathrm{q}}[contour_{\mathrm{index}}]$.
end if

B.2 Variable Neighbourhood Search

Details for the Variable Neighbourhood Search implementation are provided in this section.

B.2.1 NOMAD optimization parameters

NOMAD optimization parameters, named **params** in the implementation, are formatted as a MATLAB structure. For information on the parameters themselves, refer to NOMAD documentation [35]. The parameters given here as an example are for the benchmark of the 136-bus, but still apply for the other benchmarks as only the values of FIXED_VARIABLE and the size of BB_INPUT_TYPE are specific to a test system.

- BB_OUTPUT_TYPE: (CNT_EVAL OBJ PB PB PB PB PB PB PB PB PB);
- BB_INPUT_TYPE: (R R R R R R R R R R R R R R R R R R R R R R R I I I I I I I I I I I I I I I I I I I);
- EVAL_OPPORTUNISTIC: true;
- DISPLAY_DEGREE: 0;
- DISPLAY_STATS: BBE (SOL) OBJ [BBO];
- FIXED_VARIABLE: (24-42);
- MAX_BB_EVAL: N, budget of evaluations for an iteration;
- SEED: 0.

The user parameters, flag_rad, flag_ag, flag_cont, detailed in the workflow of Appendix A, are, also for the VNS, appended to the decision variables vector given as input to the blackbox optimization solver NOMAD. Next, the parameter FIXED_VARIABLE means simply that all binary variables associated to the topology are fixed throughout a blackbox optimization step. Moreover, as described in Algorithm 2, MAX_BB_EVAL is also updated during the VNS process, depending on the success, or not, of an iteration.

APPENDIX C BENCHMARKS ADDITIONAL DATA

This appendix provides the network data related to the modifications made on the original IEEE power systems.

C.1 IEEE 34-bus

Specifications for the IEEE 34-bus implementation are described next.

C.1.1 Modifications to the model

The IEEE 34-bus model is available in the `EMTP` example files, with the detailed data provided at [57]. The root or substation bus regulated voltage is lowered from 1.05 p.u, in the original `EMTP` model, to around 1.04 p.u in order to avoid frequent over-voltage situations near the main sections of the network. This model is modified in order to add three DERs and nine switches, where four of them, the tie switches, resulted in the creation of new lines, as listed in Table C.1:

Table C.1 New lines data for the IEEE 34-bus.

Tie switch	From bus	**To bus**	**PI line length (ft)**	**Configuration type**
SW_6	814	828	10565	301
SW_7	828	832	42390	301
SW_8	824	848	54570	301
SW_9	840	848	8040	301

The line length is obtained by rounding up the approximate sum of the lengths of the lines between both buses, while the configuration type aligns with that of the adjacent lines. If the buses do not share the same current line limits, the one with the largest value is chosen as the configuration type to prevent possible curtailment, while accounting for power losses in the tie line. The resulting values for the three-phase PI lines in the model are listed here for each tie line, where the resistance and the inductance matrices are in Ω and the susceptance matrix, representing the capacitive component, is in μS.

- Data for the line associated with tie switch SW_6:

$$R_{\mathbf{SW}_6} = \begin{bmatrix} 3.861827651515150 & 0.465620359848485 & 0.472023390151515 \\ 0.465620359848485 & 3.833214109848480 & 0.457816666666667 \\ 0.472023390151515 & 0.457816666666667 & 3.845619981060610 \end{bmatrix}$$

$$L_{\mathbf{SW}_6} = \begin{bmatrix} 2.82433664772727 & 1.28901003787879 & 1.13873892045455 \\ 1.28901003787879 & 2.85755236742424 & 1.04809602272727 \\ 1.13873892045455 & 1.04809602272727 & 2.84314554924242 \end{bmatrix}$$

$$B_{\mathbf{SW}_6} = \begin{bmatrix} 10.24624914772730 & -2.87416022727273 & -1.88129034090909 \\ -2.87416022727273 & 9.81564535984849 & -1.19076354166667 \\ -1.88129034090909 & -1.19076354166667 & 9.43486515151515 \end{bmatrix}.$$

- Data for the line associated with tie switch SW_7:

$$R_{\mathbf{SW}_7} = \begin{bmatrix} 19.94698863636360 & 2.40500738636364 & 2.43808011363636 \\ 2.40500738636364 & 19.79919488636360 & 2.36470000000000 \\ 2.43808011363636 & 2.36470000000000 & 19.86327329545450 \end{bmatrix}$$

$$L_{\mathbf{SW}_7} = \begin{bmatrix} 14.58817329545450 & 6.65795340909091 & 5.88177784090909 \\ 6.65795340909091 & 14.75973806818180 & 5.41359204545455 \\ 5.88177784090909 & 5.41359204545455 & 14.68532443181820 \end{bmatrix}$$

$$B_{\mathbf{SW}_7} = \begin{bmatrix} 52.92359829545460 & -14.84552045454550 & -9.71718068181818 \\ -14.84552045454550 & 50.69945738636360 & -6.15049375000000 \\ -9.71718068181818 & -6.15049375000000 & 48.73266363636360 \end{bmatrix}.$$

- Data for the line associated with tie switch SW_8:

$$R_{\mathbf{SW}_8} = \begin{bmatrix} 2.93886363636364 & 0.35433863636364 & 0.35921136363636 \\ 0.35433863636364 & 2.91708863636364 & 0.34840000000000 \\ 0.35921136363636 & 0.34840000000000 & 2.92652954545455 \end{bmatrix}$$

$$L_{\mathbf{SW}_8} = \begin{bmatrix} 2.149329545454540 & 0.980940909090909 & 0.866584090909091 \\ 0.980940909090909 & 2.174606818181820 & 0.797604545454546 \\ 0.866584090909091 & 0.797604545454546 & 2.163643181818180 \end{bmatrix}$$

$$B_{\mathbf{SW}_8} = \begin{bmatrix} 7.79742954545455 & -2.18724545454545 & -1.43166818181818 \\ -2.18724545454545 & 7.46973863636364 & -0.90617500000000 \\ -1.43166818181818 & -0.90617500000000 & 7.17996363636364 \end{bmatrix}.$$

- Data for the line associated with tie switch SW_9:

$$R_{\mathbf{SW}_9} = \begin{bmatrix} 15.49482954545450 & 1.86821079545455 & 1.89390170454545 \\ 1.86821079545455 & 15.38002329545450 & 1.83690000000000 \\ 1.89390170454545 & 1.83690000000000 & 15.42979943181820 \end{bmatrix}$$

$$L_{\mathbf{SW}_9} = \begin{bmatrix} 11.33209943181820 & 5.17190113636364 & 4.56896761363636 \\ 5.17190113636364 & 11.46537102272730 & 4.20528068181818 \\ 4.56896761363636 & 4.20528068181818 & 11.40756647727270 \end{bmatrix}$$

$$B_{\mathbf{SW}_9} = \begin{bmatrix} 41.11107443181820 & -11.53200681818180 & -7.54831022727273 \\ -11.53200681818180 & 39.38336079545450 & -4.77770625000000 \\ -7.54831022727273 & -4.77770625000000 & 37.85555454545460 \end{bmatrix}.$$

C.1.2 Model bounds

Current line limits

The original model data sort the network lines by configurations, each of them defined by a phasing and an ACSR cable type for the phases and the neutral. The current line limits are based on the ACSR cable type for the phases and taken from the specifications data-sheets of Southwire Company [67].

Table C.2 Current line limits for each line configuration in the IEEE 34-bus.

Configuration	**Phase cable type ACSR**	**Ampacity (A)**
300	1/0	242
301	2 6/1	184
302	4 6/1	140
303	4 6/1	140
304	2 6/1	184

Generation limits

In the original `EMTP` model, there are two DERs rated approximately at 660 kW, and placed at nodes 890 and 848. The actual DER generation limits presented Table 4.2, and repeated in Table C.3, are based on this and some similar applications in the literature, notably [2], [58], [68]. Also, based on the tendencies observed in the DER values, the limits are further adjusted through initial power flow testing on the modified model and following the firsts tests with BBO. As for the limits of the substation, the generation coming from the transmission network, they are based on advice from Dr. Octavio Ramos and initial power flow testing on the modified model.

Table C.3 Generation limits across the IEEE 34-bus.

Generation source (bus)	$P_{\mathbf{min}}$ **(kW)**	$P_{\mathbf{max}}$ **(kW)**	$Q_{\mathbf{min}}$ **(kVAr)**	$Q_{\mathbf{max}}$ **(kVAr)**	$S_{\mathbf{max}}$ **(kVA)**
Slack source (800)	0	3300	−190	550	3345.52
DER_1 (890)	200	900	−300	300	948.68
DER_2 (848)	200	800	−200	200	824.62
DER_3 (822)	20	200	−50	50	206.16

C.2 136-bus

Specifications for the 136-bus implementation are now discussed.

C.2.1 Modifications to the model

As this model is produced by combining four identical instances of the modified IEEE 34-bus, the model data for the latter still applies. The main difference is the root or substation bus regulated voltage that is, compared to the 34-bus implementation, lowered again to around 1.02 p.u in order to avoid frequent over-voltage situations near the main sections of the network. Also, the switches on the network are slightly different. To connect the feeders

together, four tie switches are added, resulting in the creation of new lines listed in Table C.4:

Table C.4 New lines data for the 136-bus (*FX refers to Feeder X*).

Tie switch	**From bus**	**To bus**	**PI line length (ft)**	**Configuration type**
SW_{12}	854 (F1)	824 (F2)	6830	301
SW_{13}	840 (F1)	840 (F2)	48540	301
SW_{14}	854 (F3)	824 (F4)	6830	301
SW_{15}	840 (F3)	840 (F4)	48540	301

The line length is obtained by rounding up the approximate sum of the lengths of the lines between both buses, while the configuration type aligns with that of the adjacent lines. If the buses do not share the same current line limits, the one with the largest value is chosen as the configuration type to prevent possible curtailment, while accounting for power losses in the tie line. The resulting values for the three-phase PI lines in the model are listed here for each tie line, where the resistance and the inductance matrices are in Ω and the susceptance matrix, representing the capacitive component, is in μS.

- Data for the lines associated with tie switches SW_{12} and SW_{14}:

$$R_{\mathbf{SW}_{12}} = R_{\mathbf{SW}_{14}} = \begin{bmatrix} 2.49657196969697 & 0.30101155303030 & 0.30515094696970 \\ 0.30101155303030 & 2.47807405303030 & 0.29596666666667 \\ 0.30515094696970 & 0.29596666666667 & 2.48609412878788 \end{bmatrix}$$

$$L_{\mathbf{SW}_{12}} = L_{\mathbf{SW}_{14}} = \begin{bmatrix} 1.82586079545454 & 0.83331174242424 & 0.73616534090909 \\ 5.92224772727273 & 1.84733390151515 & 0.67756704545455 \\ 5.23183977272727 & 4.81538863636364 & 1.83802026515151 \end{bmatrix}$$

$$B_{\mathbf{SW}_{12}} = B_{\mathbf{SW}_{14}} = \begin{bmatrix} 6.623935795454550 & -1.858070454545450 & -1.216205681818180 \\ -1.858070454545450 & 6.345561553030300 & -0.769797916666667 \\ -1.216205681818180 & -0.769797916666667 & 6.099396969696970 \end{bmatrix}.$$

As can be seen when looking at the inductance L for SW_{12} and SW_{14}, the matrix is not completely symmetrical. The bottom of the matrix contains incorrect values, as it should be symmetric with the top. This error occurred during model creation, and all results are obtained using the network model with this issue. While this does not affect the optimization process, given it is a BBO, it must be corrected for future work.

- Data for the lines associated with tie switches SW_{13} and SW_{15}:

$$R_{\mathbf{SW}_{13}} = R_{\mathbf{SW}_{15}} = \begin{bmatrix} 17.74284090909090 & 2.13925340909091 & 2.16867159090909 \\ 2.13925340909091 & 17.61137840909090 & 2.10340000000000 \\ 2.16867159090909 & 2.10340000000000 & 17.66837613636360 \end{bmatrix}$$

$$L_{\mathbf{SW}_{13}} = L_{\mathbf{SW}_{15}} = \begin{bmatrix} 12.97617613636360 & 5.92224772727273 & 5.23183977272727 \\ 5.92224772727273 & 13.12878295454550 & 4.81538863636364 \\ 5.23183977272727 & 4.81538863636364 & 13.06259204545450 \end{bmatrix}$$

$$B_{\mathbf{SW}_{13}} = B_{\mathbf{SW}_{15}} = \begin{bmatrix} 47.07552613636360 & -13.20508636363640 & -8.64342954545455 \\ -13.20508636363640 & 45.09715340909090 & -5.47086250000000 \\ -8.64342954545455 & -5.47086250000000 & 43.34769090909090 \end{bmatrix}.$$

C.2.2 Model bounds

The current line limits and the DER generation limits are identical to the ones for the 34-bus system. This benchmark results in a demand four times greater than that of the 34-bus. Because of this the generation limits for the substation presented in Table 4.6, and repeated in Table C.5, are doubled (quadrupled for $Q_{\min}$) to maintain dimensional consistency, as seen through initial power flow testing on the model.

Table C.5 Slack bus generation limits for the 136-bus.

Generation source (bus)	$P_{\min}$ **(kW)**	$P_{\max}$ **(kW)**	$Q_{\min}$ **(kVAr)**	$Q_{\max}$ **(kVAr)**	$S_{\max}$ **(kVA)**
Slack source (800)	0	6600	-760	1100	6691.04

C.3 IEEE 8500-bus

C.3.1 Modifications to the model

The IEEE 8500-bus is available in `EMTP` upon request, with the detailed data given at [57], [62]. The root or substation bus regulated voltage is set at 1.05 p.u. Below that level, the voltage profile exhibits even more under-voltage regions. The original model is modified to add five DERs and eight switches, where three of them are tie switches, resulting in the creation of new lines listed in Table C.6.

The line length is obtained by rounding up the approximate sum of the lengths of the lines between both buses, while the configuration type aligns with that of the adjacent lines. If the

Table C.6 New lines data for the IEEE 8500-bus.

Tie switch	From bus	To bus	PI line length (km)	Line Code
SW_6	M1069311	M1089131	1.01327246	3PH_H-2/0_ACSR2/0_ACSR2/0_ACSR2_ACSR
SW_7	L2767341	L2955081	2.39335007	3PH_H-397_ACSR397_ACSR397_ACSR2/0_ACSR
SW_8	R18241	M1026954	2.5178471	3PH_H-4_ACSR2_ACSR2_ACSR4_WPAL

buses do not share the same current line limits, the one with the largest value is chosen as the configuration type to prevent possible curtailment, while accounting for power losses in the tie line. The resulting values for the three-phase PI lines in the model are listed here for each tie line, where the resistance and the inductance matrices are in Ω and the capacitance matrix is in nF.

- Data for the line associated with tie switch SW_6:

$$R_{\mathbf{SW}_6} = \begin{bmatrix} 0.669641369 & 0.139323950 & 0.143951565 \\ 0.139323950 & 0.662679174 & 0.140356474 \\ 0.143951565 & 0.140356474 & 0.671806733 \end{bmatrix}$$

$$L_{\mathbf{SW}_6} = \begin{bmatrix} 0.881493335 & 0.393736398 & 0.370974246 \\ 0.393736398 & 0.890188226 & 0.411340994 \\ 0.370974246 & 0.411340994 & 0.671806733 \end{bmatrix}$$

$$C_{\mathbf{SW}_6} = \begin{bmatrix} 8.455961317 & -2.346749145 & -1.937944372 \\ -2.346749145 & 8.836738973 & -2.753213259 \\ -1.937944372 & -2.753213259 & 8.690544023 \end{bmatrix}.$$

- Data for the line associated with tie switch SW_7:

$$R_{\mathbf{SW}_7} = \begin{bmatrix} 0.646249992 & 0.263151233 & 0.271736180 \\ 0.263151233 & 0.633361801 & 0.265056340 \\ 0.271736180 & 0.265056340 & 0.650268426 \end{bmatrix}$$

$$L_{\mathbf{SW}_7} = \begin{bmatrix} 1.665709419 & 0.798206181 & 0.737800418 \\ 0.798206181 & 1.696236599 & 0.838292401 \\ 0.737800418 & 0.838292401 & 1.656248506 \end{bmatrix}$$

$$C_{\mathbf{SW}_7} = \begin{bmatrix} 21.865789810 & -6.384907507 & -5.209030685 \\ -6.384907507 & 23.029436610 & -7.554944553 \\ -5.209030685 & -7.554944553 & 22.574006030 \end{bmatrix}$$

- Data for the line associated with tie switch SW_8:

$$R_{\mathbf{sw}_8} = \begin{bmatrix} 4.245744846 & 0.355212833 & 0.366512931 \\ 0.355212833 & 2.840735809 & 0.357735716 \\ 0.366512931 & 0.357735716 & 2.863043934 \end{bmatrix}$$

$$L_{\mathbf{sw}_8} = \begin{bmatrix} 2.328922958 & 1.083578159 & 1.032060489 \\ 1.083578159 & 2.351077495 & 1.128461301 \\ 1.032060489 & 1.128461301 & 2.332772746 \end{bmatrix}$$

$$C_{\mathbf{sw}_8} = \begin{bmatrix} 19.211626560 & -5.158791739 & -4.289756813 \\ -5.158791739 & 20.606916710 & -6.260601628 \\ -4.289756813 & -6.260601628 & 20.316785190 \end{bmatrix}.$$

C.3.2 Model bounds

Current line limits

The original model data sort the network lines by line code, each of them defined by a phasing, and a cable type for each phases and neutral. Many cable types and standards are consulted to find the best equivalent for each line code, considering only the cable type for the phases. Table C.7 lists the phase cable types, their current limits, along with their respective source from the American Wire Group product catalogue [69]–[71].

Table C.7 Current line limits for each phases line code in the IEEE 8500-bus.

Phase line code	**Ampacity (A)**	**Source**
1/0_AXNJ_DB	217	[71]
2/0_ACSR	282	[70]
2_ACSR	188	[70]
397_ACSR	608	[70]
4_ACSR	142	[70]
1/0_ACSR	246	[70]
2_WPAL	185	[69]
4_WPAL	140	[69]
6_WPAL	105	[69]

Following early testing, it is found that current line limits of 2/0_ACSR, 4_ACSR and 4_WPAL are often violated. In order to allow more flexibility to the optimization process and to improve the network constraints, such as line congestion, voltage limits are relaxed to $\overline{v} = 1.10$ p.u and $\underline{v} = 0.90$ p.u. Regarding ACSR cable types, ACSR/AW is chosen instead,

as it consists of the same cable and standard but with an additional outer layer that enhances corrosion resistance, thus increasing current capacity.

Generation limits

In the original model, the substation bus generates an average of 12 MW of active power and 1.4 MVAr of reactive power. To provide some flexibility to the optimization process, the limits remain similar but are slightly increased compared to these values. As for the DER generation limits, they are inspired by [63]. These limits are presented in Table 4.10 and repeated in Table C.8:

Table C.8 Generation limits across the IEEE 8500-bus.

Generation source (bus)	$P_{\mathbf{min}}$ **(MW)**	$P_{\mathbf{max}}$ **(MW)**	$Q_{\mathbf{min}}$ **(MVAr)**	$Q_{\mathbf{max}}$ **(MVAr)**	$S_{\mathbf{max}}$ **(MVA)**
Slack source (SourceBus: HVMV_Sub_connector)	0	14	-4	4	14.56
DER_1 (L2692655)	0	3	−1.5	1.5	3.35
DER_2 (M1108395)	0	3	−1.5	1.5	3.35
DER_3 (L3010556)	0	3	−1.5	1.5	3.35
DER_4 (M1047507)	0	3	−1.5	1.5	3.35
DER_5 (L2673313)	0	3	−1.5	1.5	3.35

APPENDIX D MISOCP IMPLEMENTATION FOR THE IEEE 34-BUS

The proposed implementation is based on the three-phase `DistFlow` model. The 34-bus network data and the notation, apart from some exceptions, is the same as the one used for the proposed methods in this Master's Thesis. These exceptions and the model are described below.

Let $l_{ij}^{\phi} = |I_{ij}^{\phi}|^2 \in \mathbb{R}^3$ and $u_i^{\phi} = |v_i^{\phi}|^2 \in \mathbb{R}^3$ be the three-phase current flow magnitude in a line $(i,j) \in \mathcal{L}$ and the voltage magnitude at a bus $i \in \mathcal{N}$, respectively. Let $\overline{l_{ij}^{\phi}}$ be the square of the current limit on a line $(i,j) \in \mathcal{L}$. Let P_{ij}, $P_{ji} \in \mathbb{R}^3$ and Q_{ij}, $Q_{ji} \in \mathbb{R}^3$ be the active and reactive three-phase power flowing through a line for a specific direction (i,j), $(j,i) \in \mathcal{L}$. Similarly, let Let Z_{ij}, $Z_{ji} \in \{0,1\}$ be the power flow direction between buses i and j on line $(i,j) \in \mathcal{L}$. Let $r_{ij} \in \mathbb{R}^3$ and $x_{ij} \in \mathbb{R}^3$ be the three-phase resistance and reactance of line $(i,j) \in \mathcal{L}$. Finally, let $E(i)$ and $P(i)$ be the set of buses that are direct sucessors of bus i and the set of buses that are direct predecessors of bus i, respectively. The MISOCP model of the DNR problem combined with DER optimization is expressed in (D.1). The objective function (D.1a) represents the total generation on the network, (D.1b) and (D.1c) are the power flow constraints that explicitly takes into account the power losses, (D.1d)−(D.1f) represent the voltage drop along a lines without and with switches, respectively, (D.1g) are the nodal power balances, (D.1j) and (D.1k) are disjunctive constraints that model the power in the lines with switches, (D.1h)−(D.1i) and (D.1m)−(D.1n) are the power limits at each bus, (D.1h) and (D.1m) being the case specifically for buses with generation, (D.1i) being the case specifically for buses without generation, (D.1n) being the case specifically for buses with DERs, (D.1o)−(D.1q) are the thermal current limits for line with and without switches, and (D.1t)−(D.1w) are the radiality constraints. This problem is convex because of the second-order cone relaxation of constraint (D.1b) into an inequality, and the formulation of voltage and current variables in terms of their magnitudes, neglecting the angle variations. It is also mixed-integer due to constraints (D.1e), (D.1f), (D.1j), (D.1k), (D.1p), (D.1t) and (D.1w).

$$\min_{P,Q,p,q,p_{\mathrm{DER}},q_{\mathrm{DER}},l,v,Z,X} \quad \sum_{i\in\mathcal{G}}\sum_{\phi\in\{a,b,c\}} p_{\mathrm{g},i}^{\phi} \tag{D.1a}$$

s.t.

$$l_{ij}^{\phi} \geq \frac{(P_{ij}^{\phi})^2+(Q_{ij}^{\phi})^2}{u_i^{\phi}} \qquad (i,j)\in\mathcal{L}, \tag{D.1b}$$

$$P_{ij}^{\phi}+P_{ji}^{\phi}=r_{ij}^{\phi}l_{ij}^{\phi},\ Q_{ij}^{\phi}+Q_{ji}^{\phi}=x_{ij}^{\phi}l_{ij}^{\phi} \qquad (i,j)\in\mathcal{L}, \tag{D.1c}$$

$$u_j^{\phi}=u_i^{\phi}+((r_{ij}^{\phi})^2+(x_{ij}^{\phi})^2)l_{ij}^{\phi}-2(r_{ij}^{\phi}P_{ij}^{\phi}+x_{ij}^{\phi}Q_{ij}^{\phi}) \qquad (i,j)\in\mathcal{L}\backslash\mathcal{L}^{\mathrm{s}}, \tag{D.1d}$$

$$u_j^{\phi}\geq u_i^{\phi}+((r_{ij}^{\phi})^2+(x_{ij}^{\phi})^2)l_{ij}^{\phi}-2(r_{ij}^{\phi}P_{ij}^{\phi}+x_{ij}^{\phi}Q_{ij}^{\phi})-\mathcal{M}(1-X_{ij}) \qquad (i,j)\in\mathcal{L}^{\mathrm{s}}, \tag{D.1e}$$

$$u_j^{\phi}\leq u_i^{\phi}+((r_{ij}^{\phi})^2+(x_{ij}^{\phi})^2)l_{ij}^{\phi}-2(r_{ij}^{\phi}P_{ij}^{\phi}+x_{ij}^{\phi}Q_{ij}^{\phi})+\mathcal{M}(1-X_{ij}) \qquad (i,j)\in\mathcal{L}^{\mathrm{s}}, \tag{D.1f}$$

$$\sum_{j\in E(i)}P_{ij}^{\phi}+\sum_{j\in P(i)}P_{ji}^{\phi}=p_i^{\phi},\ \sum_{j\in E(i)}Q_{ij}^{\phi}+\sum_{j\in P(i)}Q_{ji}^{\phi}=q_i^{\phi} \qquad i\in\mathcal{N}, \tag{D.1g}$$

$$p_i^{\phi}=p_{\mathrm{g},i}^{\phi}-p_{\mathrm{d},i}^{\phi},\ q_i^{\phi}=q_{\mathrm{g},i}^{\phi}-q_{\mathrm{d},i}^{\phi} \qquad i\in\mathcal{G}, \tag{D.1h}$$

$$p_i^{\phi}=-p_{d,i}^{\phi},\ q_i^{\phi}=-q_{d,i}^{\phi} \qquad i\in\mathcal{N}\backslash\mathcal{G}, \tag{D.1i}$$

$$|P_{ij}^{\phi}|\leq\mathcal{M}X_{ij},\ |Q_{ij}^{\phi}|\leq\mathcal{M}X_{ij} \qquad (i,j)\in\mathcal{L}^{\mathrm{s}}, \tag{D.1j}$$

$$|P_{ji}^{\phi}|\leq\mathcal{M}X_{ij},\ |Q_{ji}^{\phi}|\leq\mathcal{M}X_{ij} \qquad (i,j)\in\mathcal{L}^{\mathrm{s}}, \tag{D.1k}$$

$$\underline{v_i^2}\leq u_i^{\phi}\leq\overline{v_i^2} \qquad i\in\mathcal{N}, \tag{D.1l}$$

$$\underline{p_{\mathrm{g},i}^{\phi}}\leq\sum_{\phi\in\{a,b,c\}}p_{\mathrm{g},i}^{\phi}\leq\overline{p_{\mathrm{g},i}^{\phi}},\ \underline{q_{\mathrm{g},i}^{\phi}}\leq\sum_{\phi\in\{a,b,c\}}q_{\mathrm{g},i}^{\phi}\leq\overline{q_{\mathrm{g},i}^{\phi}} \qquad i\in\mathcal{N}^{\mathrm{r}}, \tag{D.1m}$$

$$\underline{p_{\mathrm{DER},i}^{\phi}}\leq\sum_{\phi\in\{a,b,c\}}p_{\mathrm{DER},i}^{\phi}\leq\overline{p_{\mathrm{DER},i}^{\phi}},\ \underline{q_{\mathrm{DER},i}^{\phi}}\leq\sum_{\phi\in\{a,b,c\}}q_{\mathrm{DER},i}^{\phi}\leq\overline{q_{\mathrm{DER},i}^{\phi}} \quad i\in\mathcal{N}^{\mathrm{DER}}, \tag{D.1n}$$

$$l_{ij}^{\phi}\leq\overline{l_{ij}^{\phi}} \qquad (i,j)\in\mathcal{L}\backslash\mathcal{L}^{\mathrm{s}}, \tag{D.1o}$$

$$l_{ij}^{\phi}\leq X_{ij}\overline{l_{ij}^{\phi}} \qquad (i,j)\in\mathcal{L}^{\mathrm{s}}, \tag{D.1p}$$

$$l_{ij}^{\phi}\geq 0 \qquad (i,j)\in\mathcal{L}, \tag{D.1q}$$

$$Z_{ij}\geq 0 \qquad (i,j)\in\mathcal{L}, \tag{D.1r}$$

$$\sum_{i\in\mathcal{N}}Z_{ij}=0 \qquad j\in\mathcal{N}^{\mathrm{r}}, \tag{D.1s}$$

$$Z_{ij}+Z_{ji}=X_{ij} \qquad (i,j)\in\mathcal{L}^{\mathrm{s}}, \tag{D.1t}$$

$$Z_{ij}+Z_{ji}=1 \qquad (i,j)\in\mathcal{L}\backslash\mathcal{L}^{\mathrm{s}}, \tag{D.1u}$$

$$\sum_{j\in\mathcal{N}}Z_{ji}=1 \qquad i\in\mathcal{N}\backslash\mathcal{N}^{\mathrm{r}}, \tag{D.1v}$$

$$X_{ij}\in\{0,1\} \qquad (i,j)\in\mathcal{L}^{\mathrm{s}}, \tag{D.1w}$$

$$\phi\in\{a,b,c\}, \tag{D.1x}$$